APPLICATIONS AND CHARACTERIZATION OF A STREPTOMYCIN MOUSE MODEL FOR SHIGELLOSIS

By

Angela Daurie

Submitted in partial fulfilment of the requirements
for the degree of Master of Science

at

Dalhousie University
Halifax, Nova Scotia
May 2016

Table of Contents

List of Tables

List of Figures

Abstract

Shigella flexneri is the causative agent of dysentery. An oral murine infection model, that uses the broad-spectrum antibiotic streptomycin prior to *Shigella* infection, has been established and displays hallmarks of *Shigella* infection in humans.

I used streptomycin pretreated BALB/c mice to characterize the role of OspG during infection. *Shigella* mutant *ΔospG* causes 30% mortality accompanied by a change in the gross pathology of the cecum and colon in these mice. Mortality returned to wild type infection levels when I complemented with WT OspG but not in mice infected with the $\Delta ospG^{mut}$ that does not interact with the host E2-ubiqutin conjugate.

I infected a variety of mouse strains and found differences in susceptibility. I was able to show that host factors, bacteria effectors and facility differences play a role in disease severity to *Shigella* infection. I was successful in expanding our knowledge about the streptomycin mouse model.

List of Abbreviations Used

(Aba) Aureobasidin A

(ATP) Adenosine triphosphate

(CFU) Colony forming units

(CIP) Calf Intestinal alkaline phosphatase

(CVF) Cobra venom factor

(C3) Complement component 3

(C5) Complement component 5

(DAMPs) Danger-associated molecular patterns

(DN) Dominant negative

(DNA) Deoxyribonucleic acid

(DD) Double drop out media

(DMEM) Dulbecco's modified Eagle medium

(*E. coli*) *Escherichia coli*

(EPEC) Enteropathogenic *E. coli*

(ExoI) Exonuclease I

(FAE) Follicle-associated epithelium

(FBS) Fetal bovine serum

(GLMN) Glomulin

(H&E) Hematoxylin and eosin

(HECT) Homologous to E6-AP carboxyl terminus

(HEK) Human embryonic kidney

(HpRT) Hypoxanthine-guanine phosphoribosyltransferase

(IKK) IκB kinase

(IL) Interleukin

(IMR) Integrated Microbiome Resource

(iNOS) Inducible nitric oxide synthase

(*ipaH*s) Invasion plasmid antigen H

(LB) Luria Bertani

(Leu) Leucine

(LPS) Lipopolysaccharide

(LRR) Leucine-rich repeat region

(MALT) Mucosa-associated lymphoid follicles

(MAMPs) Microbial-associated molecular patterns

(MAPKK) Mitogen-activated protein kinase kinase

(M Cells) Microfold cells

(MET-1) Microbial ecosystem therapeutic

(MOI) Multiplicity of infection

(Mxi) Membrane expression of ipa

(NEDD) Neural precursor cell expressed developmentally down-regulated protein

(NEL) Novel E3 ligase

(NEMO) NF-kappa-B essential modulator

(NF-κB) Nuclear factor kappa-light-chain-enhancer of activated B cells

(NK) Natural killer

(NleH1) Non-LEE- encoded effectors H1

(NleH2) Non-LEE- encoded effectors H 2

(NLR) Nucleotide-binding oligomerization domain-like receptors

(OspG) Outer *Shigella* protein G

(OspI) Outer *Shigella* protein I

(OTU) Operational taxonomic unit

(PAGE) Polyacrylamide gel electrophoresis

(PBS) Phosphate buffered saline

(PCR) Polymerase chain reaction

(PEI) Polyethylenimine

(PGN) Peptidoglycan

(PIP2) Phosphatidylinositol biphosphate

(PML) Polymorphonuclear leucocyte

(PVDF) Polyvinylidene fluoride

(Q) Quadruple drop out media

(RBC) Red blood cell

(RING) Really interesting new gene

(RNA) Ribonucleic acid

(*S*. Typhimurium) *Salmonella enterica* serovar Typhimurium

(SDS) Sodium dodecyl sulfate

(SFM) Serum free DMEM

(Spa) Surface expression of ipa

(SUMO) Small ubiquitin-like modifier

(TBST) Tris buffered saline with Tween-20

(TCA) Trichloroacetic acid

(TLR2) Toll like receptor 2

(TNF) Tumor-necrosis factor

(TRAF2) TNF receptor-associated factor 2

(Trp) Tryptophan

(TSA) Trypticase soy agar

(TSB) Trypticase soy broth

(T3SS) Type three secretion system

(E1) Ubiquitin activating enzyme

(E2) Ubiquitin conjugating enzyme

(E3) Ubiquitin ligase

(Ubc) Polyubiquitin-C

(Ubl) Ubiquitin-like

(VBS) Veronal buffered saline

(X) X-alpha-gal

(WCL) Whole cell lysate

(WHO) World Health Organization

(YEPD) yeast extract peptone dextrose

(YpkA) *Yersinia* protein kinase A

ACKNOWLEDGEMENTS

I would like to thank all the members of the Rohde lab (past and present) for all their support. I have been very lucky to have worked with so many friendly and helpful people who made coming to the lab enjoyable.

Thanks to Dr. Samantha Gruenheid and her lab at McGill University and Dr. Jost Enninga and his lab at the Pasteur Institute for providing me with the opportunity to work and learn in their lab. Thank you to my committee members for providing feedback and constructive discussion about my project. Thank you to Dr. Craig McCormick, Dr. Brent Johnston and Dr. Andrew Stadnyk for their reagents, and mice.

A huge thanks to my supervisor, Dr. John Rohde. You have helped me to be a better student and scientist and have been a wonderful person to work for. You provided me with many opportunities that have allowed me to further my education and I will always be grateful that you took me on as a co-op student so many years ago and let me stick around your lab for so long.

Chapter 1: Introduction

1.1 Epidemiology of Shigellosis

Shigellae are gram-negative rod shaped bacteria that are the causative agent of bacillary dysentery, also known as shigellosis. Shigellosis is endemic in many developing countries but can also occur as epidemics that can result in significant mortalities; in 2010 it was estimated that 188 million cases of shigellosis occurre each year in the world with 64,993 deaths (Pires et al., 2015). Shigellosis is characterized by high fever, abdominal cramping, and the presence of blood and mucus in the stool. There are many serious complications associated with shigellosis including seizures, toxic megacolon, hemolytic-uremic syndrome, intestinal perforations and septicemia. These complications mainly affect young children and are more pronounced in malnourished children (Sansonetti, 2001). There are four species of *Shigella*: *S. sonnei*, *S. boydii*, *S. flexneri*, and *S. dysenteriae*, and within these four species there are many serotypes that are defined based on the composition of their outer membrane lipopolysaccharides (LPS) (Lindberg et al., 1991). All serotypes are capable of causing disease. *S. sonnei* and *S. boydii* are most often associated with mild illness, *S. flexneri* is most often associated with infection in endemic areas and *S.dysenteriae* is most commonly the cause of epidemics (WHO, 2005). The presence of Shiga toxin in type 1 *S. dysenteria*e makes this serotype the most virulent of *Shigella* species and also the leading cause of shigellosis mortality (Pires et al., 2015). *S. dysenteriae* infection is associated with large outbreaks in

overcrowded areas with poor sanitation and unsafe water sources (for example in refugee camps) (WHO, 2005).

In a study by Von Seidlein et al. (2006), it was found that the mortality associated with shigellosis has dropped in recent decades, however the incidence of infection continues to remain high. This study also investigated the rate of antibiotic resistance in *Shigella* and found high rates of cotrimoxazole resistance in all species of *Shigella*. They found 84% of *S. flexneri* strains to be resistant to ampicillin, and of the 1653 ampicillin resistant strains of *S. flexneri* cultured, 1322 were also resistant to citrimoxazole. High prevalence of ciprofloxacin resistance was also observed while nalidixic acid resistance was region-specific (von Seidlein et al., 2006). From this study we can appreciate that antibiotic resistance in *Shigella* is rising and this is troublesome since the incidence of infection (morbidity) has remained high. It is reasonable to predict that in the foreseeable future we may once again see high incidence of mortality from multi-drug resistant *Shigella* (Sansonetti, 2006).

The World Health Organization (WHO) as well as the Gates Foundation have made vaccine development for enteric diseases a priority (Gates-Foundation, 2014). Because *Shigella* is endemic mostly in developing countries in areas without access to ideal medical amenities, the hypothetical vaccine should be a thermostable, orally administered, single dose vaccine that is affordable (Levine, 2011). However, *Shigella* complicates the development of vaccines even more since all serotypes cause disease, and different endemic regions show variations in what species and serotypes are most prevalent. Moreover, infection (and presumably vaccination) with one serotype does not confer protection against other *Shigella* serotypes

(Formal et al., 1991; Levine et al., 2007). Therefore a *Shigella* vaccine would have to have common protection against all serotypes and species in order to effective (Kotloff et al., 1999).

1.2 Route of Infection

Shigella is transmitted by the fecal-oral route and gains access to the body through consumption of contaminated food or water. It colonizes the colon and is considered a human-only pathogen in the sense that the natural host for the bacteria is humans and some higher primates (WHO, 2005). Once *Shigella* reaches the lumen of the colon, the bacteria enter into host colonic tissue. *Shigella* is engulfed by Microfold cells (M Cells) that are part of the follicle-associated epithelium (FAE). The FAE is the layer of epithelium that covers the mucosa-associated lymphoid follicles (MALT), these follicles contain macrophages and other immune mediating cells that can induce a local immune response. M cells are specialized cells that are capable of sampling the luminal contents and transcytosing the sampled material across the epithelial layer into the lymphoid follicle. *Shigella* takes advantage of this M cell function to gain access to the lymphoid follicle (Sansonetti and Phalipon, 1999; Wassef et al., 1989).

Once inside the lymphoid follicle *Shigella* is internalized via phagocytosis into macrophages where it can induce a caspase-1 dependent apoptosis leading to death of the macrophage and the release and dissemination of the bacteria (Suzuki et al., 2007; Zychlinsky et al., 1992). *Shigella* then interacts with the basolateral membrane of polarized epithelial cells and induces actin rearrangement within the

host cell leading to macropinocytosis of the bacteria into the cell (High et al., 1992; Mounier et al., 1992). *Shigella* is able to quickly escape the phagocytic vacuole and polymerize host actin to propel itself in the cytoplasm of the cell. *Shigella* then use this actin-based motility to penetrate into neighboring epithelial cells, leading to the spread of bacteria (Bernardini et al., 1989). Disruption of the epithelial barrier by recruited polymorphonuclear leukocytes (PMLs) leads to further spread of the bacteria into the epithelial layer (Perdomo et al., 1994a).

1.3 *Shigella*'s Type 3 Secretion system and effectors

Invasion and spread of *Shigella* through the colonocytes of the colon is a carefully regulated process involving many bacterial proteins. These proteins are encoded on a 214 kB plasmid dubbed the virulence plasmid (Buchrieser et al., 2000; Sansonetti et al., 1982). About 50 genes on the virulence plasmid encode components of the type three secretion system (T3SS) (Hueck, 1998). The T3SS apparatus is essential for pathogenicity and structurally resembles flagella. It consists of a hollow needle-like structure attached to a basal body that anchors the system in both the inner and outer membrane of the bacteria, and a base structure termed the C-ring (Blocker et al., 2001). The basal body is made up of several membrane expression of ipa (mxi) proteins, MxiD, MxiG, MxiJ and MxiM (Blocker et al., 2001; Phalipon and Sansonetti, 2007; Schuch and Maurelli, 2001). The needle structure is composed of MxiH and is capped by a protein called IpaD, which is involved in regulating secretion timing, and is dissociated from the needle upon contact with the host cellular membrane (Menard et al., 1993). The T3SS is widely

conserved among *Shigella* species, as well as between other enteric pathogenic bacteria such as *Escherichia coli and Salmonella spp.* (Marlovits and Stebbins, 2010). Inactivation of any of the T3SS structural components will abrogate secretion.

The structural genes for the T3SS are contained in a region of the virulence plasmid that is regulated positively in response to the host temperature. At 37^0C, two transcription factors, VirB and VirF, activate transcription of the genes that encode components of the T3SS (Phalipon and Sansonetti, 2007). Substrates of the T3SS are known as "effectors" and the *Shigella* effector repertoire is thought to include ~50 proteins (Buchrieser et al., 2000). The expression of effectors is roughly divided into two "waves", with the first wave being controlled by VirF and VirB and are stored in a secretion-competent state. These effectors are maintained in a partially unfolded state through their interaction with a number of chaperones that include the multivalent chaperone IpgC (Page et al., 1999). These first-wave effectors include IpaB and IpaC that are thought to form a pore in the mammalian cell and allow transit of subsequent effectors. Once IpaB and IpaC are secreted, free IpgC serves as a co-activator with MxiE, and AraC family activator protein (Mavris et al., 2002). MxiE-dependent gene products are involved in optimizing the environment for *Shigella* and modifying the immune response (Ashida et al., 2015; Kim et al., 2005; Nataro et al., 1995). MxiE-dependent effectors will be discussed further in section 1.5 and 1.6.

1.4 The ubiquitin system

Ubiquitin is an 8.5 kD protein used as a common post-translational modification in eukaryotic cells. Ubiquitin can be covalently attached to molecules (almost always proteins) to alter their function and fate, via a process called ubiquitination (Hershko and Ciechanover, 1998). The C-terminal glycine residue of ubiquitin is attached to host proteins, usually at a lysine residue. Additional ubiquitin molecules can then be attached to the ubiquitinated protein by linkage to one of seven internal lysine residues within ubiquitin. The number and the nature of the ubiquitin linkages can have a variety of effects on the protein. The best characterized role for ubiquitination is to target proteins for degradation by the proteasome. The proteasome recognizes proteins that have acquired a polyubiquitin chain, formed through attachment of more than four ubiquitin molecules. Polyubiquitin chains formed through Lys63 of ubiquitin or those formed by end-to-end ubiquitin , known as Met-Ub or "linear" ubiquitin chains, act as scaffolds and serve to activate signaling complexes such as the NF-κB program (Hershko, 1988; Xu et al., 2009). Monoubiquitination of proteins is most often associated with the relocalization of a protein (Hicke and Dunn, 2003).

The process of ubiquitination occurs using three enzymes (Figure 1). The first enzyme in the pathway, referred to as the ubiquitin activating enzyme (E1), binds to the C-terminus of the ubiquitin molecule and activates it in an adenosine triphosphate (ATP) dependent hydrolysis event. There are two genes that encode E1 enzymes in humans. The charged ubiquitin is then passed to an active cysteine site on the ubiquitin conjugating enzyme (E2). The E2 facilitates the transfer of ubiquitin

Figure 1: The ubiquitin pathway. The ubiquitin pathway consists of three enzymes, ubiquitin activating enzyme (E1), the ubiquitin conjugating enzyme (E2) and the ubiquitin ligase (E3). The E1 bind ubiquitin in an ATP depended manner, and passes the ubiquitin to the E2. The E2 facilitates the transfer of ubiquitin to the E3 then the substrate (HECT E3), or it can pass the ubiquitin directly to the substrate which has been brought into close proximity by the E3 (RING E3). The most well characterized function of ubiquitin is targeting substrates for degradation by the proteasome.

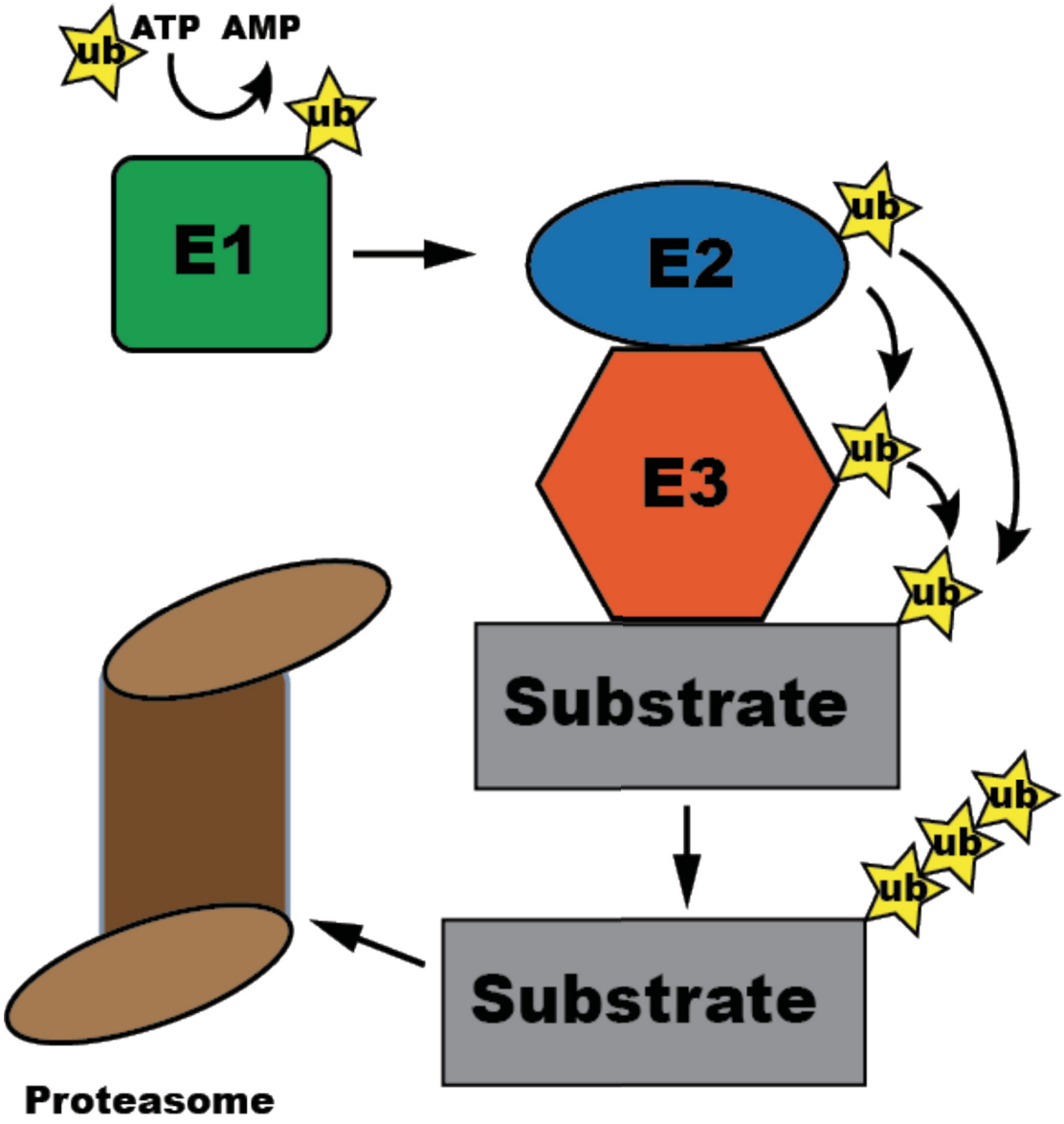
ATP
AMP
ub
ub
E1
E2
E3
ub
ub
ub
Substrate
ub
ub
ub
Substrate
Proteasome

to the target in combination with the ubiquitin ligase (E3) (Hershko and Ciechanover, 1998).This can happen in one of two ways depending on what class of E3 is being used. There are dozens of E2 genes and hundreds of E3 genes encoded by eukaryotic cells; the E3 are split into 2 classes. The homologous to E6-AP carboxyl terminus (HECT) E3 ligases that act as catalytic intermediates and accept the charged ubiquitin from the E2 on to a cysteine residue, and then transfer the ubiquitin to the target (Huang et al., 1999). The other family is the really interesting new gene (RING) E3 ligases that work more like a scaffold that brings the charged E2 and the target protein close together so that the E2 can directly transfer ubiquitin to the target (Petroski and Deshaies, 2005). Ubiquitin can be attached to a lysine, or a post translational modified cysteine or serine on the target protein. Besides ubiquitin, eukaryotes possess many "ubiquitin-like" (Ubl) post translational modification systems that transfer Ubl molecules in a manner similar to the process of ubiquitination. Small ubiquitin-like modifier (SUMO) and neural precursor cell expressed developmentally down-regulated protein (NEDD) are examples of Ubl molecules though there are other ubl molecules in the cell as well (Lima, 2007). These Ubl systems are much less well characterized than the ubiquitin system (Bradbury et al., 2014).

1.5 *Shigella* effectors that interact with the ubiquitin system

Prokaryotes lack a ubiquitin system, however *Shigella* encodes up to twelve E3 ubiquitin ligases on its virulence plasmid and in its genome (Ashida et al., 2007; Buchrieser et al., 2000). It also encodes several effector proteins that are known to

interact with the host ubiquitin system, suggesting that *Shigella* may exploit the host cell ubiquitin system to aid in its survival and spread (reviewed in Huibregtse and Rohde, 2014).

1.5.1 The IpaH family

There are 12 invasion plasmid antigen H (*ipaH*) genes encoded by *Shigella*; 6 are encoded on the chromosome and six are encoded on the virulence plasmid (Rohde et al., 2007). They are the largest class of *Shigella* proteins that are produced once contact with the host cell is made (Demers et al., 1998). These proteins are comprised of two domains: a leucine-rich repeat region (LRR) at the N-terminus and a highly conserved novel E3 ligase (NEL) domain at the C-terminal (Ashida et al., 2007; Quezada et al., 2009; Rohde et al., 2007; Singer et al., 2008). The LRR domain is unique in each of the 12 IpaHs and confers substrate specificity in the host cell (Haraga and Miller, 2006; Rohde et al., 2007). The NEL domain is required for transfer of ubiquitin to a target and is highly conserved among all *Shigella*'s IpaH proteins (Rohde et al., 2007). There are IpaH homologs in other bacteria such as the SspH1, SspH2, and SlrPs proteins in *Salmonella enterica* (Quezada et al., 2009). Mechanistically, NEL E3 ligases function similarly to HECT E3 ligases in eukaryotic cells in that they accept ubiquitin onto a cysteine residue then transfer it to a target, however they do not share any sequence or structural homology to HECT E3 or to RING E3 ligases (Rohde et al., 2007; Singer et al., 2008; Zhu et al., 2008).

Only a handful of targets have been identified for the IpaH family. IpaH0722 has been shown to target tumor-necrosis factor (TNF)-receptor-associated factor 2

(TRAF2), a RING E3 ligase, for destruction. TRAF2 is involved in the activation of NF-κB (Ashida et al., 2013). IpaH4.5 has also been shown to affect NF-κB activation by targeting the p65 subunit of the NFκB protein complex for ubiqutination (Wang et al., 2013). In a landmark study, Sasakawa and co-workers identified glomulin (GLMN) as a substrate for IpaH7.8. GLMN was shown to be ubiquitinated *in vitro* and to be degraded during *Shigella* infection. This study showed that IpaH7.8-mediated degradation of GLMN is involved in the initiation of caspase-1 dependent inflammasome formation, which *Shigella* induces to kill and escape from macrophages (Suzuki et al., 2014). The identification of GLMN, a protein previously not known to play a role in immune function, as an IpaH7.8 substrate, highlights the utility of IpaHs as probes that can identify proteins involved in combating infection.

The best characterized IpaH is IpaH9.8. The IpaHs were first described to be E3 ligases when IpaH9.8 was shown to ubiqutinate the yeast mitogen-activated protein kinase kinase (MAPKK) Ste7. In mammalian cells, IpaH9.8 has been shown to ubiquitinate NF-kappa-B essential modulator (NEMO), targeting it for destruction (Ashida et al., 2007). NEMO is a regulatory subunit for the Iκ B kinase complex that activates NF-κB. IpaH9.8 was also shown to ubiquitinate a mRNA splicing factor U2AF35, needed for the generation of several pro-inflammatory cytokines, suggesting that degradation could lead to decreased inflammation. It is also worth noting that the interaction between IpaH9.8 and U2AF35 is unusual because it is the conserved C-terminus that interacts with the splicing factor and not the LRR that normally confers binding specificity (Okuda et al., 2005).

1.5.2 OspI

Outer *Shigella* Protein I (OspI) is a deamidase and OspI homologs are encoded by other enteric pathogens such as enteropathogenic *E. coli* (Sanada et al., 2012). OspI is known to reduce IL-8 levels during *Shigella* infection. OspI targets the E2 enzyme UBC13 and renders it inactive by converting a glutamine residue in its active pocket (Gln100) on the E2 to a glutamic acid (Glu100) (Sanada et al., 2012). UBC13 is the E2 required for the E3, TRAF6 to ubiquitinate the IκB kinase (IKK). The K-63 linkages catalyzed by TRAF6-Ubc13 result in IKK activation. As a result, OspI impairs NF-κB activation and decreases the levels of pro-inflammatory cytokines (Chen, 2012).

1.5.3 OspG

Outer *Shigella* Protein G (OspG) is a protein kinase that interacts with ubiquitin- conjugated E2 enzymes in the Polyubiquitin-C (Ubc) family. The catalytic domain of OspG has a similar sequence to the catalytic domain of eukaryotic kinase Protein Kinase A. OspG has increased auto-phosphorylation capabilities when interacting with ubiquitin conjugated E2s, however, it does not phosphorylate the E2-ubiquitin conjugate suggesting that this is not the target of kinase activity by OspG (Kim et al., 2005). One member of the Ubc family, UbcH5b, is a component of a complex which promotes phospho-IκBα ubiquitination and its subsequent degradation by the proteasome. OspG prevents activation of the NF-κB pathway by preventing the degradation of phospho-IκBα following tumor necrosis factor (TNF)

treatment (Kim et al., 2005). The use of catalytically-dead variant of OspG demonstrates that the kinase activity of OspG was required for stabilization of phospho-IκBα, preventing the degradation of phospho-IκBα (Kim et al., 2005). In a rabbit ileal loop model of infection, a *ΔospG* mutant caused more destruction of tissue and increased inflammation compared to wild-type infected controls, further supporting the notion that OspG is involved in the down-regulation of the innate immune response to *Shigella* invasion (Kim et al., 2005).

OspG shares significant homology with the non-LEE-encoded effector H1 and 2(NleH1 and NleH2) from enteropathogenic *E. coli* (EPEC). NleH1 and NleH2 are also kinases and have also been shown to prevent IκB-induced NF-κB activity (Feuerbacher and Hardwidge, 2014). In a mouse model of infection, EPEC deleted for *nleH1/2* elicited increased levels of mouse KC chemokine when compared to those infected with wild type control EPEC (Royan et al., 2010). KC chemokine in mice is considered a functional homologue of human IL-8 and increased KC serum levels correlate with inflammatory conditions. Mice infected with *ΔnleH1/2* EPEC were also able to clear the bacteria faster than wild type bacteria suggesting that *NleH1/2* dampen the inflammatory response and promote survival of the pathogen (Royan et al., 2010).

Numerous other proteins from pathogenic gram negative bacteria use eukaryotic- specific factors to regulate their activity. *Pseudomonas aeruginosa* cytotoxin ExoU requires the presence of free or protein-bound ubiquitin to activate its phospholipase activity similarly to how OspG requires ubiquitin to activate its kinase activity (Anderson et al., 2011). Similarly, pathogenic *Yersinia* species use the

effector protein kinase A (YpkA) that requires interactions with host actin to become activated (Juris et al., 2000).

1.6 *Shigella* and the immune response

The intestinal epithelium has multiple surveillance systems that sense pathogens and initiate innate and adaptive immune responses that prevent pathogens from colonizing. In turn, successful pathogens have also evolved many ways to avoid detection by the immune system, and *Shigella* is no exception. *Shigella* delivers a subset of effector proteins that target immune responses to both evade immune killing and to promote bacterial spread.

1.6.1 *Shigella* mediated killing of macrophages

Shigella pass through M cells in the colon into the mucosa-associated lymphoid follicles where macrophages engulf them (Sansonetti, 2004). However, *Shigella* are not degraded by the macrophage. They escape the phagocytic vacuole via the secreted IpaB effector that is thought to form an ion channel in the vacuolar membrane, causing membrane lysis and escape of bacteria into the cytoplasm. Once in the cytoplasm the bacteria multiplies quickly (High et al., 1992). This rapid multiplication triggers cellular inflammatory pathways leading to host cell death. Intracellular bacteria shed LPS and peptidoglycan (PGN) and these bacterial components are recognized as microbial-associated molecular patterns (MAMPs) or danger-associated molecular patterns (DAMPs) by cellular signaling receptors that include the nucleotide-binding oligomerization domain-like receptors (NLR)

(Girardin et al., 2003). Activation of NLRs initiate signaling cascades that induce host immune responses to infection, including inflammasome activation and release of cytokines (Kayagaki et al., 2011; Kayagaki et al., 2013).

When *Shigella* are replicating inside macrophages they trigger a NLRP3/NLRC4 dependent program that results in the formation of a caspase-1 inflammasome and a specialized form of pro-inflammatory cell death called pyroptosis. Inflammasome activation causes the release of pro-inflammatory cytokines IL-1β and IL-18 and release of the bacteria from the macrophage as it dies (Senerovic et al., 2012; Suzuki et al., 2007). It is still unclear if the induction of pyroptosis is beneficial for *Shigella*, however *Shigella* induces the formation of the inflammasome through interactions with multiple effector proteins including Ipah7.8 (as mentioned in section 1.5.1) and IpaB, which assembles an ion channel in the cellular membrane triggering NLRC4 signaling (Senerovic et al., 2012; Suzuki et al., 2014). The release of IL-1β and IL-18 promotes the recruitment of PMLs to the site of infection as well as triggering other signals for inflammation responses leading to tissue damage that allows further invasion by *Shigella* into the epithelial layer (Phalipon and Sansonetti, 2007).

1.6.2 Epithelial infection and cell death by *Shigella*

Shigella invades epithelial cells by inducing macropinocytosis via injection of various T3SS effectors that interact with host actin, then internalized bacteria escape the phagocytic vacuole via IpaB dependent lysis of the endosomal membrane. Similar to the events that occur in macrophages, components of the bacterial cell

wall and T3SS are recognized as MAMPs and DAMPs by the epithelial cell. However *Shigella* utilizes multiple effectors to prevent epithelial cell death to create a niche favorable for replication (Ashida et al., 2014). *Shigella* prevents mitochondrial damage and activates pro-survival pathways within the epithelial cell to prevent cell death. *Shigella* also prevent epithelial cells from secreting DAMPs through the action of the effector IpgD (Puhar et al., 2013). Infected epithelial cells release ATP which is recognized as a DAMP by surrounding cells. *Shigella* counteracts this defense mechanism using IpgD, a phosphoinositide phosphatase, that blocks gap junction hemichannels from releasing ATP. When an *ΔipgD* strain of *Shigella* was used in a rabbit ileal loop model there was increased ATP released and inflammation compared to wild type infection (Puhar et al., 2013). Eventually the multiplication of, and spread of bacteria, cause extensive enough damage within the cell that the epithelial cells undergo pyroptosis (Ashida et al., 2015). Despite this epithelial cells can produce cytokines such as IL-8 and lipid mediators that function as danger signals that recruit innate immune cells including neutrophils to the site of infection (Sansonetti, 2004).

1.6.3 *Shigella* modifies the adaptive immune response

Shigella's involvement with the adaptive immune system is less well understood. One of the main reasons for this is the lack of a suitable animal model that accurately mimics the human disease. However, the adaptive immune response is important to *Shigella* resistance as it has been shown that the Rag°γ_c° mouse strain lacking T lymphocytes, B lymphocytes and natural killer (NK) cells is more

susceptible to *Shigella* infection , suggesting that T cells and NK cell are involved in clearance of the bacteria (Le-Barillec et al., 2005). Th-17 T-helper cells have also been shown to become primed during *Shigella* infection and may be important in developing lasting immunity against *Shigella* (Sellge et al., 2010).

CD8+ T cells are not primed during *Shigella* infection even though they are important in the adaptive immune response against many other cytosolic bacteria (Jehl et al., 2011). This is because *Shigella* targets the CD4+ T cell using IpgD. *Shigella* does not invade activated CD4+ T cells, but use the T3SS to deliver IpgD and impair their ability to attract CD8+ T cells to the site of infection. IpgD decreases the levels of phosphatidylinositol biphosphate (PIP2) at the plasma membrane in CD4+ T cells which leads to the inactivation of ezrin, radixin and moesin proteins, leading to the loss of chemoattractant responses in CD4+ T cells (Konradt et al., 2011; Salgado-Pabon et al., 2013).

B lymphocytes are also targeted by *Shigella* during infection. B cells secrete cytokines that contribute to the immune response to infection and are important for antibody mediated immunity. *Shigella* induces B cell death through two mechanisms. The first mechanism is by invading B cells and inducing their apoptosis (Nothelfer et al., 2014). *Shigella* also induces cell death using the T3SS needle capping protein IpaD that binds to the toll like receptor 2 (TLR2) on the surface of B-cells and triggers apoptosis via a mitochondrial dysfunction pathway. By targeting B cells, *Shigella* is able to prevent antibody mediated immune responses that would normally promote long- lasting immunity (Nothelfer et al., 2014).

1.7 Animal models for *Shigella* infection

Developing an animal model of infection for shigellosis has proven to be a difficult endeavor. This largely has to do with the problem of *Shigella* being a pathogen that only successfully infects humans and closely related higher primate species. Accurately studying the innate and adaptive immune response is essential for understanding virulence regulation and is needed for vaccine development. The ideal model should have a site of infection that resembles the conditions that *Shigella* will encounter in the human gut. The model should recapitulate the disease state, and be accessible by having an easy method for set up, and not require high levels of expertise to perform (Marteyn et al., 2012). Although several models have been developed, so far no animal model fits all of these criteria. Each model has benefits and disadvantages depending on area of research focus.

1.7.1 The rhesus monkey as a model of shigellosis

For this model, a dose of $1.5x10^{11}$ colony forming units (CFU) of bacteria, which is significantly higher thab the amount of bacteria than is needed to infect a human, is orally administered to rhesus monkeys. The monkeys are then observed and stool samples are collected are scored for the presence and amount of mucus and blood. The monkeys are euthanized at the end of the study and tissue is collected for histopathological examination (Fontaine et al., 1988).

The main advantage for the use of the rhesus monkey as a model of *Shigella* infection is that it allows for infection via the oral route, resulting in acute colitis

similar to what is observed in humans (Marteyn et al., 2012). Though this model resembles human disease closely it is not ideal because the cost and accessibility of using primate models is not feasible for most labs. Growing ethical concerns over the use of primates in research make this model increasingly less attractive for most researchers.

1.7.2 The rabbit ileal-loop model for shigellosis

Rabbits are not susceptible to oral infection with *Shigella*, however *Shigella* injected directly into the intestine it is able to elicit an inflammatory response (Etheridge et al., 1996). The rabbit ileal loop model of infection is performed using fasted anesthetized rabbits. The ileum of the small intestine is ligated into multiple 10cm compartments in a way that preserves blood flow, different strain or mutant of *Shigella* is injected at $1x10^{10}$ CFU into the compartment. The ileum is then retuned to the abdominal cavity and the rabbit is kept until the desired infection time point is reached. Then the rabbit is euthanized and the contents of each compartment are removed to be examined and a 10% formalin solution is injected into the compartment to begin preserving the organ. The tissue is then removed and preserved for histopathological examination (Perdomo et al., 1994b).

The advantages of the rabbit model of infection is that it results in a strong inflammatory response. Hallmarks of this response include the recruitment of PMLs, thickening of the muscle layer, and the destruction of the epithelial layer. This model has been used to investigate the inflammatory and invasive properties of mutant strains of *Shigella* to gain insight to effector function. The rabbit model also

has the benefit of being able to analyze multiple bacterial strains in a single animal, controlling for animal specific differences (Marteyn et al., 2012). There are several disadvantages of this model, the first being the difficulty of performing the ligations and a recovery surgery. Moreover, there is a lack of immunological tools for rabbit models (Phalipon and Sansonetti, 2007). Finally, the ileum of the small intestine differs from the the colon (the site of *Shigella* infection in humans), these two microenvironments differ in oxygen concentration, pH, nutrient availability, mucus production and microbiota diversity (Marteyn et al., 2012; Shim et al., 2007).

1.7.3 The guinea pig model of shigellosis

The guinea pig model uses young guinea pigs that are anesthetized and given an intrarectal inoculation of $1x10^9$ CFUs of *Shigella*. Their stool is observed for presence of blood and mucus and the animals develop signs of illness such as weight loss and fever. At the end of the experiment, the animals are euthanized and serum and fecal samples are collected for enzyme-linked immunosorbant assay (ELISA), colon samples can be used to extract RNA for real-time PCR, or processed for histopathological analysis (Shim et al., 2007).

The guinea pig model is advantageous because infection occurs in the colon and presents with a disease state similar to human infection. The animals develop colitis and present with fever and weight loss. They also have an appropriate immune response similar to humans with high levels of IL-8, IL-1β and NO synthase and there is PML recruitment to the site of infection and tissue destruction (Marteyn et al., 2012; Shim et al., 2007). The guinea pig model has also been used to

demonstrate that partial immunity can be induced following repeated exposure to *Shigella,* raising the possibility that guinea pigs may serve as a vaccine model of infection (Shim et al., 2007). The main disadvantages for this model are the lack of genetic and immunological tools available for guinea pigs and that it is not an oral model (Marteyn et al., 2012).

1.7.4 The neonatal mouse model of shigellosis

Unlike the adult mouse that is resistant to *Shigella* infection, a newborn mouse is colonized by *Shigella* and resulting in a lethal enteritis 4-6 hours post-infection (Phalipon and Sansonetti, 2007). 4 day old mice are given an oral infection with a dose of $5x10^9$ CFU and then kept in a warm environment for 2-6 hours. The mice are then euthanized and the jejunum of the small intestine can be removed for histopathological analysis and RNA extraction. However, mice 5-7 days old lose this susceptibility, possibly because of the development of innate immune responses such as antimicrobial peptides being secreted from Paneth cells that begin developing on day 5 (Fernandez et al., 2008). Other unknown factors are also likely to be involved in regulating the small window of time when mice are susceptible to *Shigella* infection.

The newborn mouse model has be used to investigate mechanisms on how *Shigell*a interacts with intestinal epithelium and to examine the development of factors involved in resistance (Phalipon and Sansonetti, 2007). However this is not an ideal model to investigate immune response since the bacterium is not exposed to a developed innate immune response (Marteyn et al., 2012).

1.7.5 The mouse pulmonary model of *Shigella* infection

In contrast to the neonatal mouse model of infection, the pulmonary mouse model of *Shigella* infection has been widely adopted by the *Shigella* research community to investigate the innate and adaptive immune response. Mice are given a $1x10^7$ CFU dose of *Shigella* via an intranasal mist. The mice develop an acute bronchopneumonia, have neutrophil recruitment and ulceration on the microvilli at the site of infection, and show signs of inflammation such as edema in the lung epithelial tissue. In challenge studies where mice were given intranasal doses of Immunoglobulin A (IgA) against *Shigella* LPS prior to *Shigella infection,* there was a decrease in the ulceration and a reduced bacterial burden in the lungs, and the response was serotype specific (Phalipon et al., 1995).

The pulmonary lung model of shigellosis has the advantage of being in an adult mouse so the array of immunological tools and mouse knock out strains to study the immune response is immense. Also, the ability to use this model to demonstrate a protective response makes it a candidate model for vaccine development. This model has been criticized because *Shigella* is not a respiratory pathogen and the microenvironment in the lung is different than that of the colon (Marteyn et al., 2012). Also, LPS, which is used in the adaptive studies, is highly immunogenic and would directly cause significant inflammation to the lung, which would confound the study (Phalipon et al., 1995).

1.7.6 The human colon xenograft model of *Shigella* infection

Shigella infection of human tissue can be studied in a xenograft mouse model. Human fetal intestinal tissue is transplanted into subcontaneous incisions on the of the immunodeficient (SCID) mouse, the tissue develops for 8 weeks and forms functional intestinal crypt structures (Seydel et al., 1997). *Shigella* are then injected at a 3- $5x10^7$ CFU directly into the lumen of the xenograft. Once infected, the tissue develops features of shigellosis including epithelial damage and neutrophil recruitment. This model has been used to investigate innate immune response to *Shigella* by examining cytokine production and neutrophil recruitment and the roles that these factors play in the intestinal damage (Zhang et al., 2001). This model has been particularly useful for transcription profiling of the innate immune response to *Shigella* infection.

The advantage of this model is that the interaction between the epithelial lining and bacteria can be observed in a host species-specific context. The disadvantages of this model is that it is very complex and requires surgical expertise. Also the mice need to be severely immune comprised for the transplant to be accepted, limiting the scope of possible immunological studies (Marteyn et al., 2012).

1.7.7 The BALB/c streptomycin model of shigellosis

This mouse model for shigellosis uses the broad-spectrum antibiotic streptomycin prior to infection with *Shigella*. The antibiotic clears a niche for

Shigella to colonize in the intestinal epithelium of the mouse (Martino et al., 2005). The mice are given 5g/L of streptomycin in their drinking water ad libitum for three days prior to infection, followed by an oral dose of $1x10^8$ CFU of *Shigella,* and the bacterial burden is monitored for the duration of the infection. When the experimental endpoint or time course for the infection is reached the mice are euthanized and serum and organs are removed. Harvested tissues can be used to examine bacterial burden or can be preserved in 10% formalin and stained for histopathological analysis. In this model, the *Shigella* are found most densely around the colonic lymphoid follicles. Between 24 and 72 hours post infection there is increased expression of mRNA for the pro-inflammatory cytokines IL-12, IFN-γ, IL-1β, IL-6 and TNF from cells in the lymphoid tissue(Martino et al., 2005). By 120 hours post infection there is expansion of the follicle and evidence of cellular apoptosis(Martino et al., 2005). Taken together these observations suggest the route of entry in this model causes disease in a manner that is representative of what occurs in humans. In contrast to what is observed in human infection, the model lacks a robust neutrophil recruitment to the site of infection and tissue destruction in the gut is minor (Martino et al., 2005).

The streptomycin-treated mouse model is advantageous because infection occurs in the colon, the natural site of infection in humans. Another strength is that this oral model is directly comparable with the route of infection in humans. The main disadvantage for this model is that the microbiome is altered significantly because of the antibiotic treatment and there is a lack of neutrophil recruitment to the gut, a hallmark of *Shigella* infection in humans.

The *Shigella* streptomycin treated mouse model was adapted from the streptomycin treated *Salmonella enterica* serovar Typhimurium (*S.* Typhimurium) model of colitis. Mice infected with *S.* Typhimurium, intraparotoneally, develop a systemic infection that resembles typhoid fever whereas humans develop an enterocolitis when infected with *S.* Typhimurium. The lack of a gastrointestinal model for *Salmonella* infection has been problematic for investigating the disease. It was discovered that mice pretreated with 20mg of streptomycin 24 hours prior to oral infection with *S*. Typhimurium developed an enterocolitis illness without systemic disease (Barthel et al., 2003). Deitric-Hardt and coworkers found that the infection elicited a similar inflammatory response as seen in human enterocolitis from *S*. Typhimurium, including edema and ulceration in the epithelium and submucosa of the intestine tissue, and massive infiltration of PMLs (Barthel et al., 2003).

1.8 The microbiome and intestinal pathogens

A microbiome is a microbial community that consists of non-pathogen bacteria, viruses, phage, archaea and eukaryotic microorganisms that colonize a specific niche, such as segments of our intestinal tract. The diversity and abundance of microbes varies immensely between niches. Approximately 10^{14} microbes colonize the adult body (Lawley and Walker, 2013). These microbes interact with one another and with the host to shape the environment that they live in. In the mammalian intestine the microbiome begins to establish itself at birth and continues to increase in diversity with age (Lawley and Walker, 2013). The

microbiome alters the physiological development of the intestine through nutrient absorption and training of the immune system. The microbiome also prevents pathogen invasion in a phenomenon known as “colonization resistance” (Lawley and Walker, 2013). Bacteria have been the main focus of studies involving the microbiome and we often refer to the bacteria naturally present in the gut as commensal bacteria. Disruption of the host microbiota is called dyisbiosis and can leave the host more vulnerable to infection. Pathogens can take advantage of antibiotic use or secrete virulence effectors that help them overcome colonization resistance and invade host cells (Lawley and Walker, 2013).

In a report by Gordon and coworkers, (Hsiao et al., 2014) bacterial taxa associated with recovery of from *Vibrio cholera* infection were collected from the stool of convalescing adults. Various bacteria were cultured and then pooled together to create a community called a consortium. This consortium was administered to mice that were simultaneously challenged by co-infection with *Vibrio.* They observed significantly lower bacterial burden of *V. cholera* in treated mice compared to mice that did not receive the consortium. They characterized one isolate, *Ruminococcus obeum*, and found it to be involved in restricting the colonization of *V. cholera* by interfering with the pathogen’s quorum-sensing mechanisms (Hsiao et al., 2014). This work demonstrates the protective properties that even low-abundance commensal bacteria can provide.

Another example of the protective capability of commensal bacteria is the use of a consortium of 33 bacterial strains, isolated from human stool, that has previously been used to cure patients with recurrent *Clostridium difficile* infection.

This consortium is referred to as Microbial Ecosystem Therapeutic (MET-1) (Martz et al., 2015). Martz *et al.* investigated if this protective community could prevent infections in the context of the streptomycin treated model of *S.* Typhimurium. C57BL/6 mice were pretreated with streptomycin then given the MET-1 community of commensals. The researchers observed that the MET-1 treated mice had a reduced immune response to infection despite similar bacterial load to the group of mice that did not receive MET-1. They observed that tight junctions were preserved at the intestinal epithelial barrier, preventing dissemination of the bacteria to the spleen (Martz et al., 2015).

1.9 Research described in this thesis

The streptomycin-treated mouse model of *Salmonella* infection has provided a means for genetic analysis of salmonellosis in both the host and the pathogen. My goal was to characterize a *Shigella*-adapted mouse model and determine if a similar genetic analysis was possible. This thesis research was undertaken to expand the knowledge of the streptomycin mouse model for *Shigella* infection. As yet, no single model accurately reflects all of the symptoms of shigellosis in humans. The mouse remains the best animal model option because of the large number of tools and depth of understanding of this species in terms of host resistance. Mice are normally resistant to *Shigella,* making their use as an animal model for shigellosis difficult, however the model described by Martino et al. displays several hallmarks of human shigellosis. To date, this model has only been used in the BALB/c mouse strain, and it remains unknown whether this model can be applied to other strains of mice. It is

also unknown whether the streptomycin treated mouse model may be used to assess virulence of different *Shigella* strains. **I hypothesize that genetic factors in mice play a role in susceptibility to *Shigella* infection. I also hypothesize that the streptomycin mouse model can be used to assess specific virulence factors for *Shigella*. Overall, my hypothesis is that the streptomycin-treated model of infection for *Shigella* may be a tool for understanding the genetic basis for shigellosis in both the pathogen and host.**

I infected several strains of mice with wild type *Shigella* and characterized their relative susceptibility. BALB/c mice were used to characterize the role of the *Shigella* effector OspG during infection. I also characterized the microbiome of mice throughout the course of infection in this model. My results show that the streptomycin treated mouse model may be used to identify the genetic basis of shigellosis with the genetics of the pathogen and the host both playing a role in the severity of disease.

Chapter 2: Methods and Materials

2.1 Bacterial strains and growth conditions

All strains used were from the streptomycin resistant *Shigella flexneri* stereotype 5a, M90T Sm (Allaoui et al., 1993). Any mutant knock-out strains of *Shigella* used (Table 1) were generated using lambda red recombination as described elsewhere (Sidik et al., 2014). Cultures were maintained on solid medium consisting of 30 g/L trypticase soy broth (TSB) with 20 g/L agar and 0.01% Congo red, to induce the T3SS. Working cultures were grown overnight at 37°C and stored at 4°C for up to a month. To grow *Shigella* in liquid cultures, a single colony from a Congo red plate was grown overnight at 37°C with agitation in 30 mg/mL TSB. Antibiotic selection, if needed, was added to the medium at a concentration of: ampicillin 100 μg/mL, tetracycline 5 μg/mL, streptomycin 100 μg/mL or spectinomycin 100 μg/mL**.**

Escherichia coli (*E. coli*) strains DH5α and S17 λpir were used for propagation of plasmids and for genetic manipulations of Deoxyribonucleic acid (DNA). Cultures were maintained on Luria Bertani (LB) agar (10 mg/mL tryptone, 5mg/mL yeast extract and 10 mg/mL sodium chloride 20 mg/mL agar) The bacteria were grown overnight at 37°C and placed at 4°C for up to a month. These two strains were grown in LB broth (10 mg/mL tryptone, 5mg/mL yeast extract and 10 mg/mL sodium chloride) at 37°C with agitation. Antibiotic selection, if needed, was added to the medium at a concentration of: ampicillin 100 μg/mL, tetracycline 5 μg/mL, streptomycin 100 μg/mL or spectinomycin 100 μg/mL**.**

Table 1: Bacterial strains used in this thesis.

Strain name	description
M90T	Streptomycin resistant *Shigella flexneri* stereotype 5a
ΔmxiD	Streptomycin resistant *Shigella flexneri* stereotype 5a containing a deletion of *mxiD*
ΔospG	Streptomycin resistant *Shigella flexneri* stereotype 5a containing a deletion of *ospG*
$\Delta ospG^{wt}$	Streptomycin resistant *Shigella flexneri* stereotype 5a containing a deletion of *ospG*. With WT *ospG* complemented into the virulence plasmid
$\Delta ospG^{mut}$	Streptomycin resistant *Shigella flexneri* stereotype 5a containing a deletion of *ospG*. With a mutant *ospG* complemented into the virulence plasmid that can not bind to host E2-ubiquitin conjugate
$\Delta ospG^{CD}$	Streptomycin resistant *Shigella flexneri* stereotype 5a containing a deletion of *ospG*. With a catalytically dead *ospG* complemented into the virulence plasmid
DH5α	Lab strain of *E.coli* used for propagating plasmids
S17 λpir	Strain of conjugating *E.coli* used to mate plasmids into *Shigella flexneri*
M90T-dsRed	*S. flexneri* serotype 5s (M90T parent) with pdsRed (Ampicillin) and pafaE (Spectinomycin)
ΔospG-dsRed	*S. flexneri* serotype 5s (M90T parent) with *ΔospG:: tet* with pDsRed (Ampicillin) and pafaE (Spectinomycin)

Frozen stocks for all bacterial strains were created by adding 15% glycerol to overnight liquid cultures grown at 37°C and placed at -80°C for long-term storage.

2.2 Streptomycin mouse model of infection

All experimentation involving mice was approved by the University Committee on Laboratory Animals. See Table 2 for a list of all mouse strains used. *Shigella* infections were performed in mice according to the methods of Martino et al. (2005). Mice were given 5g/L streptomycin in their drinking water starting 2 days prior to infection and continued throughout the experiment. Were fasted six hours before oral infection. The night before oral infections, a single *Shigella* colony was picked from a Congo red plate, inoculated into 5mL of TSB, and grown overnight at 37°C. The culture was subcultured 1:100 into 9.9 mL of fresh TSB to a total final volume of 10mL. The subculture was grown for approximately 3 hours at 37°C. Following the incubation, the OD_{600} of each culture was measured and recorded. A 50μL sample of the subculture was removed and serially diluted 1:10 in sterile PBS and plated on a Congo Red TSA plate containing 100μg/mL streptomycin to confirm inoculation amounts. The remaining 10mL culture was centrifuged at 3,200g for 10 minutes. The supernatant was discarded and the pellet was resuspended in 1mL of sterile PBS. Resuspended bacteria was given to each mouse by oral gavage (0.1mL) resulting in a dose of approximately $1x10^8$ bacteria. The mice were monitored 3 times a day (approximately 8 hours apart) for the duration of the infection with assessments of the severity of clinical illness and daily collection of fecal samples to

Table 2: Mouse strains used in this thesis.

Mouse strain	Background	Origin	*Shigella* strain used to infect
BALB/c	BALB/c	Charles River Laboratories (Saint Constant Quebec)	WT, *ΔmxiD* ,*ΔospG* and *ΔospG* complemented strains
C57BL/6	C57BL/6	Jackson Laboratories (Bar Harbor, Maine)	WT and *ΔmxiD*
Properdin -/-	C57BL/6	Stadnyk lab breeding colony	WT
IL-10 -/-	C57BL/6	Stadnyk lab breeding colony	WT
C5aR-/-	BALB/c	Stadnyk lab breeding colony	WT
FVB	FVB	Gruenheid lab breeding colony	WT
A/J	A/J	Gruenheid lab breeding colony	WT
C3H OUJ	C3H OUJ	Gruenheid lab breeding colony	WT
C3H OUJ.BL/6J	C3H OUJ	Gruenheid lab breeding colony	WT
AKR/J Dalhousie	AKR/J	Jackson Laboratories (Bar Harbor, Maine)	WT
AKR/J McGill colony	AKR/J	Gruenheid lab breeding colony	WT
AKR/J McGill Jax	AKR/J	Jackson Laboratories (Bar Harbor, Maine)	WT

Table 3: Clinical scoring parameters for monitoring mouse health. Each parameter is assessed on a scale of 0-3, with 3 being the worst. Mice that reach a total score of 12 are monitored every 2 hours until their condition either improves or worsens. Mice with a score >14 are euthanized.

Parameter	Observation	Score
Appearance	Normal	0
	Lack of grooming	1
	Rough hair coat	2
	Very rough coat	3
Food intake	Normal	0
	Reduced appetite	1
	Not eating since last checkpoint	2
	Not eating for last 2 checkpoints	3
Hydration	Normal	0
	Mildly dehydrated (<l sec skin tent)	1
	Moderately dehydrated (l-2 sec skin tent)	2
	Severely dehydrated (>2sec skin tent)	3
Temperature	Normal (as measured by pre-infection temperature)	0
	±1°C change from pre-infection temperature	1
	±2°C change from pre-infection temperature	2
	±3°C change from pre-infection temperature	3
Behavior	Normal	0
	Somewhat reduced/minor changes in behavior	1
	Above plus change in respiratory rate or effort	2
	Moves only when stimulated	3
Posture	Normal	0
	Sitting in hunched position	1
	Hunched posture, head resting on floor	2
	Lying prone on cage floor/unable to maintain upright posture	3
Weight-loss	Normal (<5% change from pre-infection weight)	0
	<l0% weight loss from pre-infection weight	1
	10-l5% weight loss from pre-infection weight	2
	15-19% weight loss from pre-infection weight	3

determine bacterial burden. Clinical illness was scored based on appearance, behavior, appetite, hydration, temperature and weight loss (Table 3).

On the last day of the experiment the mice were anesthetized to a surgical plane using inhaled isoflurane gas or intraperitoneal injected of 0.1mL ketamine solution (1mL saline, 0.75mL zylazine, 0.75mL ketamine), and euthanized by exsanguination via cardiac puncture followed by cervical dislocation. The blood was left at room temperature to coagulate then was centrifuged at 17000g for five minutes. The serum was collected and frozen. The colon, cecum, liver and spleen were removed from each mouse during necropsy and were processed as described in sections 2.3 and 2.4.

2.3 Determining bacterial burden from organ tissue and fecal pellets

Fecal samples were collected from each mouse at the midday check over the duration of the infection. Each sample was weighed and diluted 1:10 w/w in sterile phosphate buffered saline (PBS) and homogenized. Seven serial dilutions of 1:10 were then made, and 25µL of the final six dilutions were spot plated on MacConkey agar (peptone 20g; lactose 10g; bile salts 5g; sodium chloride 5g; neutral red 0.075g in 1L dH2O) containing 100 mg/mL streptomycin and incubated at 37°C overnight. The bacterial colonies that grew on the plates were counted from a dilution containing between 20-150 colonies and recorded so that the colony forming units per gram of feces could be determine.

A portion of the liver and spleen were weighed and diluted 1:10 w/w in sterile PBS, then homogenized using Pyrex homogenizer, serially diluted 1:10, and

plated on MacConkey agar containing 100 mg/mL streptomycin and incubated at 37°C overnight. The bacterial colonies that grew on the plates were counted from a dilution containing between 20-150 colonies if possible, or as many as were present in the lowest dilution, and recorded so that the colony forming units per gram of tissue could be determined.

2.4 Processing of mouse intestinal tissue for histology

The colon and cecum were removed during necropsy and were flushed with ice cold PBS. The colon was cut open along the marginal artery, then cut longitudinally again to create two halves. Half of the colon was Swiss rolled from the proximal end to the distal end and fixed in a histology cassette overnight with 10% formalin, along with half the spleen and the cecum. The histology samples were then transferred to 70% ethanol and sent to the pathology lab at the IWK hospital to be embedded in paraffin wax, cut, and stained with hematoxylin and eosin (H&E). The slides were viewed and assessed for signs of inflammation and destruction of mucosal epithelium (Table 4). The other half of the colon was used for cytokine detection from overnight cultured tissue explants as described elsewhere (Jain et al., 2015). Briefly, the length of colon was cut into 1cm sections and was placed in a tissue culture dish with 1mL Dulbecco's Modified Eagle Medium (DMEM ,Thermo Fisher) containing 0.5% Fetal Bovine Serum (FBS, Thermo Fisher), 100mM HEPES (Thermo Fisher), 50mg/mL of gentamycin, and 100mg/mL of ampicillin. The tissue culture samples were placed overnight at 37°C with 5% CO_2. Following the

Table 4. Histopathology Scores used to rank level inflammation of the colon. Designed for DSS mouse model (Stillie and Stadnyk, 2009).

Score	Infiltrate	Crypt Damage	Ulceration	Edema
0	No infiltrate	None	None	Absent
1	Occasional cell limited to submucosa	Some crypt damage, spaces between crypts	Small, focal ulcers	Present
2	Significant presence of inflammatory cells in submucosa, limited to focal areas	Larger spaces between crypts, loss of goblet cells, some shortening of crypts	Frequent, small ulcers	
3	Infiltrate present in both submucosa and lamina propria, limited to focal areas	Large areas without crypts, surrounded by normal crypts	Large areas lacking surface epithelium	
4	Large amount of infiltrate in submucosa, lamina propria and surrounding blood vessels, covering large areas of mucosa	No crypts		
5	Transmural inflammation (mucosa to muscularis0			

incubation, the media was centrifuged at 13,000 g for one minute and the supernatant was collected and frozen.

2.5 Tissue culture cell maintenance

HEK293T, HeLa and Phoenix cell lines were a gift from Dr. Craig McCormick and were all maintained in the following manner. Cells were subcultured at 80% confluency, approximatly every 3-4 days. To subculture cells, media was removed from the flask, cells were briefly rinsed with PBS and then treated with trypsin (0.05% trypsin with 0.5 M EDTA, Thermo Fisher) for 10 minutes at 37°C. Following incubation, cells were resuspended in media and reseeded into new flasks at a 1:10 dilution. The media used was Dulbecco's Modified Eagle Medium (DMEM, Thermo Fisher) supplemented with 10% FBS (Thermo Fisher) and 100 mM HEPES (Thermo Fisher). Cells were grown in an incubator at 37°C and 5% CO_2.

2.6 *In vitro* gentamycin protection assay

Two days prior to infection, HeLa cells were seeded at $1X10^6$ cells per well into a six well tissue culture plate. The night before infection, single *Shigella* colonies were picked from a Congo red plate, grown overnight at 37°C in TSB, subcultured 1:100 into 5ml of fresh TSB, and grown to an OD_{600} of 0.3. During this time, fresh media (DMEM with 10%FBS) was added to each well of the tissue culture plate. Once the bacteria cultures reached the desired $OD_{600,}$ one well of HeLa cells was treated with trypsin (0.05% trypsin with 0.5 M EDTA) for 10 minutes at 37°C, then collected and counted using a hemocytometer to calculate the number of cells per

well. Bacteria were then added to the remaining wells at a multiplicity of infection (MOI) of 10. The plate was centrifuged at 1,250g for ten minutes at room temperature and transferred to a 37°C incubator with 5 % CO_2 for one hour. After one hour the media was removed from each well of the tissue culture plate and 1mL of DMEM containing 50 µg/mL of gentamycin was added to kill extracellular bacteria without being able to penetrating mammalian cells. The plate was returned to 37°C for 30 minutes. The wells were washed in PBS and the cells were lysed using 500µL NP-40 lysis buffer (0.1% NP-40, 50mM Tris-HCl pH 7.5, 5mM EDTA, 10% glycerol, 100mM sodium chloride). Seven serial dilutions of 1:10 were made for each sample and 25µL of each dilution was plated onto a Congo red TSA plate. The Congo red plates were placed at 37°C overnight. Colonies were counted on a dilution containing between 20-150 CFU to determine the CFU/mL.

2.7 Creation of point mutation in OspG using site directed mutagenesis

Three point mutations were made in *ospG*, one variant contained two point mutations to inhibit the ability of OspG to bind to the host E2-ubiquitin conjugate and one variant had a mutation to create a catalytically-dead OspG that lacked kinase activity. The positions for the E2-Ub binding mutant were chosen based on the crystal structure of OspG (Pruneda et al., 2014) and the kinase-dead variant was previously described (Kim et al., 2005). The protocol for creating the point mutations was adapted from (Zheng et al., 2004). Oligonucleotides (Table 5) were purchased from Sigma-Aldrich, diluted to 100 µM stock concentrations and 10 µM

Table 5. Primers used to create point mutations in OspG.

Primer name and function	Forward primer sequence 5'-3'	Reverse primer sequence 5'-3'
OspG_K53M (conversion to create catalytically dead OspG)	GAATGATTCATCTGCT TTGTATATGAAGTATG ATCTTATTGGCAAC	GTTGCCAATAAGATCA TACTTCATATACAAAG CAGATGAATCATTC
OspG_G81R (conversion to create OspG that does not bind to host E2)	GAGCTTTTTAATGCT TTTTATCGCGATGAA GCATCCGTTG	CAACGGATGCTTCA TCGCGATAAAAAGC ATTAAAAAGCTC
OspG_C127R (conversion to create OspG that can not bind to Ubiquitin)	GCCTTTATCTACAGTT GATACGTAAATTGAA TGAGTTGAG	CTCAACTCATTCAAT TTACGTATCAACTGT AGATAAAGGC

working stocks, and stored at -20°C. these OspG mutants were then digested with Bam HI and Xho1 restriction enzymes and ligated into a pBluescript KS+ plasmid.

2.8 Plasmid preparation from bacteria

An overnight culture of DH5α containing the desired OspG cloned plasmids was grown overnight in 3mL of LB broth. The bacterial culture was pelleted at 17,000g for 1 minute, then resuspended in 100μL of resuspension buffer (1% ethylene glycol, 1 mM sodium azide, 10 mM Tris-HCl pH 8.0). Cells were incubated for 4 minutes on ice with 150μL of lysis buffer (2% sodium dodecyl sulfate, 0.15 M sodium hydroxide, 0.025 M sodium iodate, 10 mM EDTA). The lysis was then neutralized by the addition of 200μL of acid iodide precipitate (2.5 M cesium chloride, 0.25 M tartaric acid, 0.25 M sodium iodide). The solution was then centrifuged at 17,000g for 1 minute, and the supernatant was transferred to a new tube containing 200μL of PEG- ethanolamine (37% polyethylene glycol, 4 M monoethanolamine). This mixture was incubated on ice for 10 minutes. Following the incubation DNA was pelleted at 17,000g for 5 minutes. The supernatant was discarded, and the pellet was washed three times with 80% isopropanol and air dried. Once dry the pellet was resuspended in 50μL of water. DNA were stored at -20°C until use.

2.9 Creation of $CaCl_2$ competent bacterial cells

Shigella or *E.coli* cultures were grown overnight at 37°C, in TSB with appropriate antibiotic selection. The next day, cultures were diluted 1:100 and

grown to mid-log phase (OD_{600} 0.4-0.6). The cells were placed on ice to arrest growth and centrifuged at 3,200g for 15 minutes at 4°C. Supernatant was discarded and pelleted cells were resuspended in ice-cold 100mM $CaCl_2$. The cells were centrifuged again at 3,200g for 15 minutes and resuspended again in ice-cold 100mM $CaCl_2$. Following the second wash the cells were incubated for 20 minute on ice. Cell suspension was centrifuged at 3,200g and resuspended in 100mM $CaCl_2$ supplemented with 15% glycerol at 1/100 of the original culture volume.

One microliter of plasmid DNA was used for each transformation and DNA was incubated for one-hour with 100uL competent cells before heat shock. Cells with plasmid DNA were heat shocked at 42°C for 90 seconds, incubated on ice for one minute and one milliliter of TSB was added to the cells. The heat shocked cell suspension was plated on TSA containing selectable markers for plasmid DNA and plates were grown at 37 °C overnight. To confirm the presence of a plasmid, colonies were grown overnight in TSB and minipreped (described in section 2.8), digested with the restriction enzymes Bam HI and Xho1 and run on a 1% agarose gel to confirm insert and plasmid presence.

2.10 Complementation of the *ospG* mutant

Previous members of the Rohde lab created an *ospG::tetRA* mutant *(ΔospG*). *OspG* was deleted in M90T using lambda red recombination as described in (Sidik et al., 2014). For complementation studies, $OspG^{wt}$ or $OspG^{mut}$ (G81R, C127R) or $OspG^{CD}$ (K53M) were introduced into the pWR100 virulence plasmid under control of the constitutive *lac* promoter using the pJQ200 suicide integration vector (Quandt

and Hynes, 1993). To do this, a fragment of the M90T virulence plasmid corresponding to bp 71414 to 71913 ("site C") was amplified with a *PvuI* cut site on each end. This region of pWR100 contains no coding regions so insertion of the integration vector will not disrupt other genes (Buchrieser et al., 2000). The fragment was restriction digested and ligated into a *PvuI* in pJQ200 outside of the multiple cloning site. $OspG^{wt}$ or $ospG^{mut}$ or $OspG^{CD}$ were created as described in section 2.7 and were restriction digested out of pBluescript using the *BamHI* and *XhoI* restriction enzymes and ligated into the multiple cloning site of pJQ200.

The modified pJQ200 plasmids were transformed into a $CaCl_2$ competent *E. coli* strain S17-1λ pir. *ΔospG Shigella* was mixed with S17-1λ pir containing pJQ200 variants in approximately a 1:1 ratio and spotted on TSB and allowed to incubate at 37° C for five hours. The mix of bacteria was then plated on TSB plates with tetracycline and gentamycin (to select for *Shigella* containing pJQ200-*ospG* variants) and incubated at 37° C overnight. Colonies were struck onto TSB Congo red plates containing tetracycline and gentamycin. Integration of was confirmed using oligos specific to *ospG* and to site C (OspG forward check 5'- atgaaaataacatctaccat-3' and site C reverse check 5'-gatttcaggcgttgggtgtg-3'). An overview of the complementation procedure is shown in Figure 2.

2.11 *Shigella* secretion assay

Single colonies were picked from a Congo red plate, grown overnight in 3mL of TBS, and 500µL was used to inoculate 50mL of TBS. Cultures were grown at 37°C for 4 hours. From this culture three types of samples were taken, a bacterial pellet

Figure 2. Methods for creating OspG complemented bacteria by integration into the virulence plasmid using a suicide vector. OspG constructs were created using point mutation PCR and cloned into the multiple cloning cite in the pJQ200 suicide vector under the control of the LacZ promoter. Site C was amplified from the virulence plasmids of *Shigella* with *PvuI* cut site on each end, it was the cloned into a *PvuI* site outside of the multiple cloning cite on pJQ200. The plasmid was mated into *ΔospG Shigella* where it intergraded into the virulence plasmid.

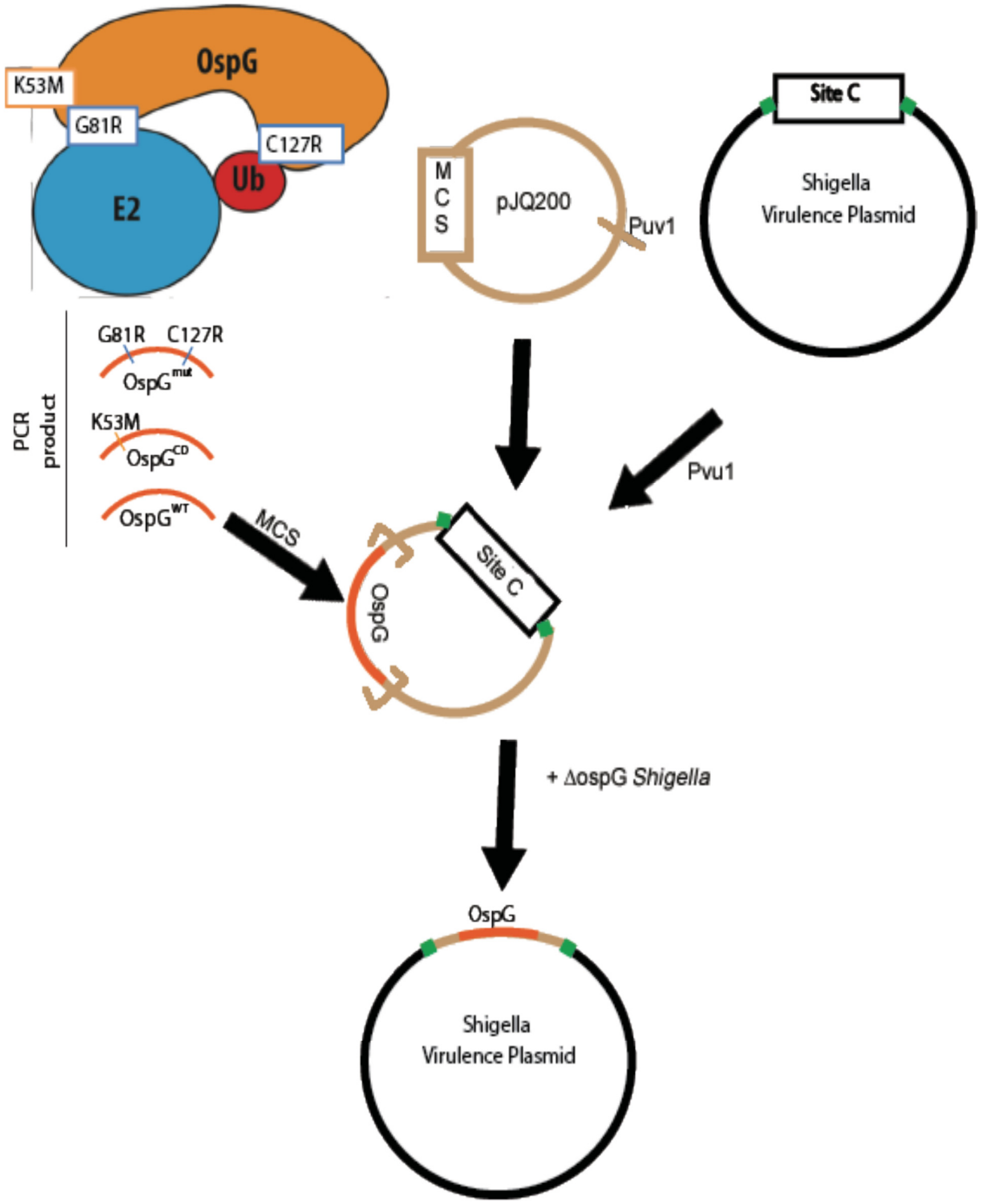
OspG
K53M
G81R
C127R
Ub
E2
M
C
S
pJQ200
Puv1
Site C
Shigella
Virulence Plasmid
PCR
product
G81R C127R
OspG^mut
K53M
OspG^CD
OspG^WT
MCS
Pvu1
OspG
Site C
+ ΔospG Shigella
OspG
Shigella
Virulence Plasmid

protein sample, a supernatant protein sample and a Congo red induced protein sample.

To obtain bacterial pellet protein samples, 1mL of culture was centrifuged at 17,000g for 1 minute and resuspended in 200μL of NP-40 lysis buffer (0.1% NP-40, 50 mM Tris-HCl pH 7.5, 5 mM EDTA, 10% glycerol, 100 mM sodium chloride) and boiled for 10 minutes. Supernatant protein samples were prepared by first centrifuging 25mL of culture for 10 minutes at 3,200g. The supernatant was collected and 2.5mL of 100% Trichloroacetic acid (TCA) was added to it. The solution was then placed on ice for 20 minutes followed by centrifugation at 17,000g for 20 minutes. The supernatant was then discarded and the pellet was resuspended in 200μL of NP-40 lysis buffer and boiled for 10 minutes.

For Congo red induced protein secretion samples, 25mL of culture was centrifuged at 3,200g for 10 minutes. The supernatant was discarded and the pellet was resuspended in 2.5 mL of PBS with 7.5 mg/mL of Congo red to induce T3SS secretion (Parsot et al., 1995). The cells were incubated for 30 minutes at 37°C. Following incubation, 1.5 mL of the culture was centrifuged at 17,000g for 2 minutes. The supernatant was collected and 150 μL of 100% TCA was added to each sample and placed on ice for 20 minutes and then centrifuged at 17,000g for 10 minutes. The pellet was resuspended in 200 μL NP-40 lysis buffer and boiled for 10 minutes. Protein samples were separated on a 10% polyacrylamide gels and silver stained using a BioRad silver staining kit. All steps were performed according to the manufacture's instructions.

2.12 Retroviral stable cell lines

Human embryonic kidney 293T (HEK 293T) stable cell lines expressing codon-optimized OspG and OspG^{mut} were created using retroviral transduction. Human codon-optimized *ospG* was purchased from Genewiz. Using site directed mutagenesis as described in section 2.7, two point mutations were made converting G81R and C127R. The codon optimized OspG and OspG^{mut} were created with a myc-tag and cloned into the pBMN-IRES-PURO (here on referred to as pBMN) vector using restriction digestion enzymes *BamHI* and *XhoI* (NEB) and ligated into pBMN using T4 DNA ligase (NEB) (pBMN vector was a gift from Dr. Craig McCormick).

Empty pBMN, pBMN- OspG and pBMN-OspG^{mut} were transfected into Phoenix cells using polyethylenimine (PEI, Sigma). To do this Phoenix cells were seeded at 70% confluency (4 x 10^6 cell/well) in a 6 well plate. Plasmid DNA was prepared from Qiagen Midi prep kit (Qiagen) and diluted to a final concentration of 500 µg/mL. For each well of a 6 well plate, 1 µg of DNA was mixed with Opti-MEM (Thermo fisher) to a total volume of 100 µL and 3 µg of PEI (1 mg/mL) was mixed with Opti-MEM to a total volume of 100 µL. The two mixtures were incubated at room temperature for 5 minutes and then the PEI mixture was added to the DNA mixture, mixed and incubated for another 15 minutes at room temperature. Phoenix cells were washed twice with serum free DMEM (SFM) and then 1 mL of SFM was left in each well. Transfection mixture was added to the well drop wise and the cells were incubated with the transfection mixture for 4-6 hours at 37°C with 5% CO_2.

Following incubation, the media was removed and replaced with 2mL of DMEM containing 10%FBS and 100mM HEPES. The cells were incubated at 37°C with 5% CO_2 for 2 days. Supernatants from the Phoenix cells containing packaged virus were collected and filtered through 0.45 μm filters and polybrene was added to a final concentration of 8 μg/mL. The supernatants were then added to the media of HEK293T cells and left for 2 days at 37°C and 5% CO_2. Following incubation with viral supernatants, media was removed, cells were rinsed with PBS and fresh media was added. Cells were given one day of recovery before selection for cells containing pBMN plasmids by adding puromycin to the media. Cell lines were maintained by subculturing every 3-4 days, when 80% confluent and were grown in DMEM with 10% FBS and 100mM HEPES supplemented with puromycin at 37°C and 5% CO2.

2.13 Protein extraction from mammalian cell lines

HEK 293T cells stably expressing empty pBMN, pBMN- OspG and pBMN-$OspG^{mut}$ were used to create lysates to confirm expression in mammalian cells. Cells were seeded into 6 wells plates at a density of ($4x10^6$ cell/well) and grown for 2 days. DMEM was removed and cells were washed twice with PBS, and lysed by addition of RIPA buffer (10% NP40, 1% SDS, 0.5 M Tris-HCl pH7.4, 1.5 M NaCl, 5% sodium deoxycholate, 0.01 M EDTA, 10mM DTT dH2O). Cell lysates were collected into tubes and cellular debris was pelleted by spinning samples at 17,000g for 2 minutes. The supernatants were saved, 1x the volume PBS was added and samples were boiled for 5 minutes. Cell lysates were stored at -20°C for immunoblotting.

2.14 Immunoblotting

protein samples extracted from stable cell lines or produced in bacterial secretion assays were leaded into a 10% polyacrylamide gels and run at 120V for approximately 2 hours. Proteins were transferred at either 0.5 A overnight or 1.5 A for two hours, to polyvinylidene fluoride (PVDF) via wet transfer system. Immunoblots were performed at room temperature with rocking unless otherwise stated. Membranes were blocked with 5% skim milk powder in Tris buffered saline with Tween-20 (TBST, 145 mM sodium chloride, 5 mM Tris-HCl pH 7.5, 0.1% Tween-20) between one hour to overnight at 4°C. Primary antibodies (anti-myc tag diluted 1:1000, Cell Signaling. Anti-HA tag diluted 1:1000, Cell Signaling. Anti-actin diluted 1:1000, Cell Signaling) diluted in 5% skim milk powder in TBST were applied to the membranes and incubated for an hour. Membranes were then washed 3x for 10 minutes each time in TBST and incubated in secondary antibodies (Anti-rabbit diluted 1:2000, Cell Signaling) conjugated to horseradish peroxidase for one hour. Membranes were again washed 3x for 10 minutes in TBST, then developed using ECL+ development reagent (GE Healthcare). The development reagent interacts with horseradish peroxidases to produce a fluorescent substance that was imaged using a ChemDoc imaging system from BioRad.

2.15 Yeast two-hybrid screen

The yeast two-hybrid screen was performed according to directions by the Matchmakers Gold System (Clontech). The bait was created using the $OspG^{CD}$ variant (described in section 2.10) and was ligated into the multiple cloning site of

pGBKT7 DNA-BD Cloning Vector in frame with the Gal4 DNA binding domain. The bait plasmid was transformed in Y2HGold yeast cells and tested for auto-activity by plating it on selective media that was deficient in Tryptophan (yeast nitrogen base without amino acids 6.7g/L, glucose 20g/L, amino acid mix without tryptophan 2g/L, agar 20g/L) that contained x-alpha-gal and Aureobasidin A, to confirm that growth of the bait alone in the presence of x-alpha-gal and Aureobasidin A was not possible.

To perform the screen the pGBKT7 DNA-BD- $OspG^{CD}$ (bait) was grown overnight at 30°C with agitation in 50mL of SD –Trp until an OD_{600} of 0.8 was reached. The culture was then spun at 1000g for 5 minutes to pellet the cells, and resuspended at $1X10^8$ cell/mL in fresh SD-Trp media and combined with 1mL of the Normalized human GADT7-AD library (prey library) (a gift from Dr. Roy Duncan). The bait and prey library were added to a 2L flask containing 50mL of 2x yeast extract peptone dextrose (YEPD) (Peptone 40g/L, Yeast extract 20g/L, glucose 40g/L) and were incubated at 30°C with slow agitation (30-50 rpm) for approximately 24 hours until budding zygote yeast was present. The yeast was then spun at 1000g for 10 minutes to pellet cells and resuspended in 10 mL 0.5x YEPD (Peptone 10g/L, Yeast extract 5g/L, glucose 10g/L). To determine mating efficiency, 100μL of the cells were removed and 4 serial diluteions of 1:10 were made and plated on SD-Trp, SD-Leu and SD –Trp-Leu to select for number of bait cells, number of prey cells and number of zygotes respectively. The rest of the cells were plated in 200μL volumes onto SD-Tryptophan/-Leucine/X-α-Gal/Aureobasidin A. All plates were incubated at 30°C for 3-5 days. Colonies that grew and were blue in colour

were then transferred to more selective media containing SD/-Adenine /-Histidine /-Leucine/-Trptophan/ X-α-Gal /Aureobasidin A. Colonies that successfully grew on the SD/-Adenine /-Histidine /-Leucine/-Trptophan/ X-α-Gal /Aureobasidin A media were amplified and sent for sequencing to identify the interacting prey.

To identify the prey that interacted with the bait, colony PCR was performed. To create a template, colonies were resuspended in 30μl of 0.2% SDS in water and vortexed at max speed for 15 seconds. The sample was incubated at 90°C for 5 minutes and pelleted at 17,000g for 1 minute. The supernatants were collected and used for PCR amplification using primers specific for the prey site (pGADT7 amplimer forward 5'- ctattcgatgatgaagataccccaccaaaccc-3', pGADT7 amplimer reverse 5'- gtgaacttgcggggtttttcagtatctacgat-3'). PCR product (10μl) was run on a 1% agarose gel to look for amplification. Any samples with amplification were treated with 2μL of calf intestinal alkaline phosphatase (CIP, NEB) and 1μL of exonuclease I (ExoI, NEB) at 37°C for 45 minutes to destroy primers from the PCR reaction. Samples were heated to 80°C to inactivate ExoI and CIP and the PCR products were sent for sequencing using a service procived by Genewiz and were sequenced using a T7 primers.

2.16 Co-immunopercipitations

HEK293T cells stably expressing empty pBMN, pBMN- OspG and pBMN-OspG^{mut} were transfected with GFP-Rab11WT (Adgene plasmid #12674) or GFP-Rab11DN (Adgene plasmid #12678) plasmid DNA. Plasmid DNA was prepared using a Qiagen midi prep kit and transfected using the PEI transfection method described

in chapter 2.12. Transfected cells were grown for 24-48 hours and treated with trypsin (0.05% trypsin containing 0.5 M EDTA, Invitrogen) for 10 minutes at 37°C then collected into a 1.5mL tube and pelleted at 500g for 2 minutes. The cells were washed twice with PBS and pelleted. The supernatant was removed and the cells were frozen at -80°C overnight. Cells were removed from the freezer, placed on ice, and then 1mL RIPA buffer (10% NP40, 1% SDS, 0.5M Tris-HCl pH7.4, 1.5M NaCl, 5% sodium deoxycholate, 0.01M EDTA, 10mM DTT dH_2O) containing protease inhibitor (1 tablet per 10mL) (Pierce) was added. Following incubation at 4°C with agitation cells were sheared by passing the suspension through a 21G needle five times. The cell lysates were then centrifuged at 17,000g for 2 minutes at 4°C to pellet the cellular debris. Myc-Tag (Cell Signaling) primary antibody was added to the collected supernatants at a 1:100 dilution and incubated overnight at 4°C. 100µL of AG antibody resin beads (Thermo Fisher) were then added and the slurry was incubated at room temperature for 2 hours. The beads were then centrifuged at 500g for 2 minutes and washed once in Co-immunopercipitations wash buffer 1 (25mM tris, 150mM NaCl, 1mM EDTA, 0.5%NP40 pH 7), once in Co-immunopercipitations wash buffer 2 (50mM tris, 100mM NaCl, 0.5mM EDTA, 5mM NaF, pH 7) and once in Co-immunopercipitations wash buffer 3 (50mM tris, 100mM NaCl, 5mM EDTA, 0.01%NP40, 5mM NaF, 10% glycerol, pH 7), with beads pelleted at 500g for 2 minutes between each wash. Proteins were eluted off the beads by incubating for 5 minutes at room temperature using an elution buffer (0.1M glycine pH 5.8) then pelleting the beads for 2 minutes at 500g. The supernatants were collected and analyzed by immunoblotting with antibodies specific for proteins of

interest.

2.17 Live-cell fluorescent imaging

This technique was used to examine the possible interaction between OspG and Rab11a. HeLa cells were seed in at a density of 10000 cells/well into a 96 well plate. Ells were transfected with a plasmid containing GFP-rab11a (provided by Dr. Jost Enninga at the institut pasteur) using X-tremeGENE 9 reagent (Roche) for 24 or 48 hr, according to the manufacturer's instructions. The cells were then infected with either M90T-dsRed or *ΔospG*-dsRed *Shigella* (Table 1) and imaged using a wide field fluorescent microscope. Each well was imaged at the same position each minute for an hour to create a time-lapse video. The cells were observed for deficiency or change in time of Rab11 recruitment to the site of bacterial entry.

2.18 RTq-PCR for colon tissue preparations

2.18.1 Trizol extraction of RNA from colon tissue and generation of cDNA

Trizol (1mL) (Invitrogen) was added to each 50-100mg colon tissue sample and homogenized for 1 minute using a Pyrex homogenizer. Samples were centrifuged at 17,000g for 10 minutes at 4°C and supernatant collected. chloroform (200μL) (Bioshop) was added and the samples were shaken vigorously for 15 seconds, then incubated at room temperature for 3 minutes before spinning at 17000 g for 15 minutes at 4°C. The aqueous phase was collected and 0.5x volumes of 100% ethanol was added to the samples and the samples were inverted 10 times. The RNA was collected and eluted using a Qiagen RNeasy mini kit. (Qiagen). cDNA

was then made from the RNA template using SuperScript one-step RT-PCR with Platinum *Taq* (Invitrogen) in accordance with the manufacturer's manual.

2.18.2 Creating standards for qPCR

All standards were created using activated dendritic cell RNA (cells were obtained from Dr. Brent Johnston). RNA was converted to cDNA using reverse Transcrption PCR. CDNA was diluted 1:2 seven times and run in triplicate to determine efficiency of primers. Primers were specific to mice and were previously published (Cersini et al., 2003) and are listed in Table 6. All primers were confirmed using a Basic Local Alignment Search Tool. A housekeeping gene was also used for reference, Hypoxanthine Phosphoribosyltransferase (HPTR), and the primers were previously published (Su et al., 2004).

cDNA generated from the kit was used directly as a template for qPCR. Samples for qPCR were set up as follows: 12.5µl SYBR Green (Quanta Biosciences), 0.1µl of 10mM forward primer, 0.1µl of 10mM reverse primer, 0.5µl MgCl, 1µl cDNA and 10.8µl dH_2O. The MxPro software and MX3000 was used to collect qPCR data. Primers were confirmed to have equal efficacy (between 90%-110%) analysis of the data was preformed using double delta Ct analysis comparing each gene CT value to the housekeeping gene HPTR.

Table 6. list of primer sets used for qPCR

Primer	Sequence 5'-3'
IL-1β I	TCATGGGATGATGATGATAACCTGCT
IL-1β II	CCCATACTTTAGGAAGACACGGATT
IL-6 I	CTGGTGACAACCACGGCCTTCCCTA
IL-6 II	ATGCTTAGGCATAACGCACTAGGTT
IL-12 I	CGTGCTCATGGCTGGTGCAAAG
IL-12 II	CTTCATCTGCAAGTTCTTGGGC
TNF I	GGCAGGTCTACTTTGGAGTCATTGC
TNF II	ACATTCGAGGCTCCAGTGAATTCGG
iNOS I	ACGCTTGGGTCTTGTTCACT
iNOS II	GTCTCTGGGTCCTCTGGTCA
HPRT I	AAGGACCTCTCGAAGTGTTGGATA
HPRT II	CATTTAAAAGGAACTGTTGACAACG

2.19 Preparation of samples for 16S rRNA sequencing

All samples for 16s sequencing were extracted from fecal pellets of mice and processed for total DNA using a PowerSoil kit (MoBio Labs). Total DNA was extracted according to the manufacture's instructions. 16S rRNA sequencing was performed by Dr. Andre Comeau at the Integrated Microbiome Resource (IMR) Facility at Dalhousie University. Approximately 12,400 reads per sample were produced.

2.20 Cobra venom factor pretreatment for the streptomycin BALB/c mouse model of shigellosis

To deplete complement in the streptomycin BALB/c mouse model, mice were administered streptomycin following the procedure described in section 2.2. One day prior to oral infection with *Shigella* mice are given a 10unit/mouse dose of cobra venom factor (CVF) by intraperitoneal injection. The mice were then infected according to the described infection model. At the endpoint of the experiment, serum that had been collected by cardiac puncture tested for hemolytic activity.

2.21 Hemolytic activity assay

This assay was used to determine hemolytic activity of mouse serum in response to cobra venom-induced depletion of complement. Sheep red blood cells (4mL) (RBCs, VWR) and 6ml of veronal ubffered saline (VBS), were combined and mixed by inversion. The solution was centrifuged at 600g for 5 minutes, the supernatant was discarded, and the RBCs were washed 2 more times in VBS. After

the final wash, the cells were centrifuge at 900g for 5 minutes to pack the cells and then resuspended the cells in sufficient VBS to prepare a 10% solution (0.5ml of packed cells are resuspended in 5 ml of VBS buffer). Haemolysin (rabbit anti-sheep red blood cell antibody) was diluted 1:50 and added dropwise to the cells. The solution was incubated at 30°C for 30 minutes with mixing by inversion every 15 minutes to sensitize the cells. Using the mouse serum, two-fold serial dilution in VBS were made (five total) for each dilution, 200μL of serum and 200μL of suspended sensitized RBC were mixed. As a blank to measure background lysis of RBC, 200μL of sensitized RBC and 200μL of VBS were mixed together. To measure total lysis, 200μL of sensitized RBC were mixed with 200μL distilled water. All tubes were mixed by inversion and incubated at 37°C for 30 minutes with mixing after 15 minutes. The samples were centrifuged at 1,500g for 5 minutes to sediment the RBCs, 100μL of supernatant from each tube was transferred to a well in a 96 well plate. 100μL of distilled water was added to each well and the absorbance of the samples at 540nm using a plate spectrophotometer. To calculate percent lysis, the A_{540} of the background lysis was subtracted from the A_{540} of both the samples and the total lysis control. Then the corrected sample value was divided by the corrected total lysis value and multiplied by 100 to get percent lysis (Costabile, 2010).

2.22 Statistical tests

All statistical analyses were preformed using Microsoft Excel and Graph Pad Prism. A non-parametric Kruskal-Wallis test was used for statistical analysis of bacterial counts in feces and organs comparing more then two groups, followed by a

Dunn's multiple comparison post-test (Sellge et al., 2010). A Mann-Whitney U test was used to compare bacterial counts between only two groups. Survival curves were analyzed using a Log-rank (Mantel-Cox) test. Significance was set at a p value <0.05.

Chapter 3: Results

3.1 The type 3 secretion system is required for disease in the streptomycin mouse model of shigellosis

The streptomycin treated mouse model of *Salmonella* infection has been adapted to *Shigella* (Barthel et al., 2003; Martino et al., 2005). Characteristics of shigellosis were observed when BALB/c mice were infected with wild type *Shigella,* but not when the virulence plasmid-cured strain BS176 was used (Martino et al., 2005). This demonstrated that the virulence plasmid was required for pathogenicity, however the plasmid-encoded factor(s) required for disease were not determined. To investigate whether the T3SS is needed for the induction of disease symptoms, C57BL/6 mice (Figure 3A) and BALB/c mice (Figure 3B) were infected with M90T (WT) or T3SS deficient strains (*ΔmxiD*) of *Shigella*. Two experiments were performed on each mouse strain one lasting 3 days post infection and one lasting 5 days post infection. Two BALB/c mice infected with WT *Shigella* reached experimental endpoints and were euthanized early (marked with black circles on their weight loss graph in Figure 3B). When C57BL/6 mice were used for the infections, I observed less average weight loss for mice infected with WT *Shigella* when compared to BALB/c mice: 6% for C57BL/6 compared to 8.2% for BALB/c mice as compared three days post-infection, this difference was not significant. When infected with Δ*mxiD Shigella* both mouse strains gained weight over the course of the experiment (Figure 3). The bacterial burden from feces for the C57BL/6 and BALB/c mice infected with WT or Δ*mxiD* were compared. No significant differences were observed on day 3 or day 5 between the two mouse

Figure 3. Weight loss observed in the BALB/c and C57BL/6 mice infected with WT *Shigella*. BALB/c mice infected with WT *Shigella* exibited greater weight loss than seen in C57BL/6 mice infected with WT *Shigella*. A) The percent of total body weight lost over the course of a five- day infection of BALB/c mice. B) The percent of total body weight lost over the course of a five- day infection of C57BL/6 mice. C) Average weight loss for each infection group. Statistical analysis was preformed using a Mann-Whitney U test significance set at $p<0.05$ on the average weightloss at day 3 (point of greatest difference) and the difference was not significant.

A)

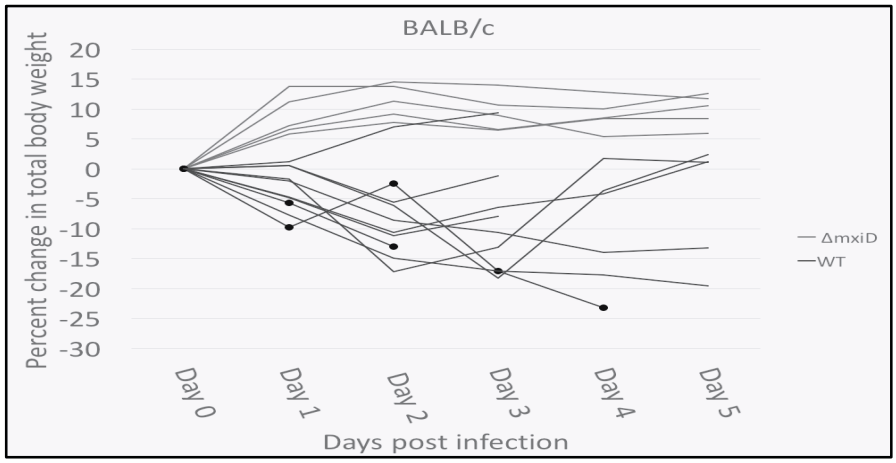
BALB/c
Percent change in total body weight
20
15
10
5
0
-5
-10
-15
-20
-25
-30
Day 0
Day 1
Day 2
Day 3
Day 4
Day 5
Days post infection
ΔmxiD
WT

B)

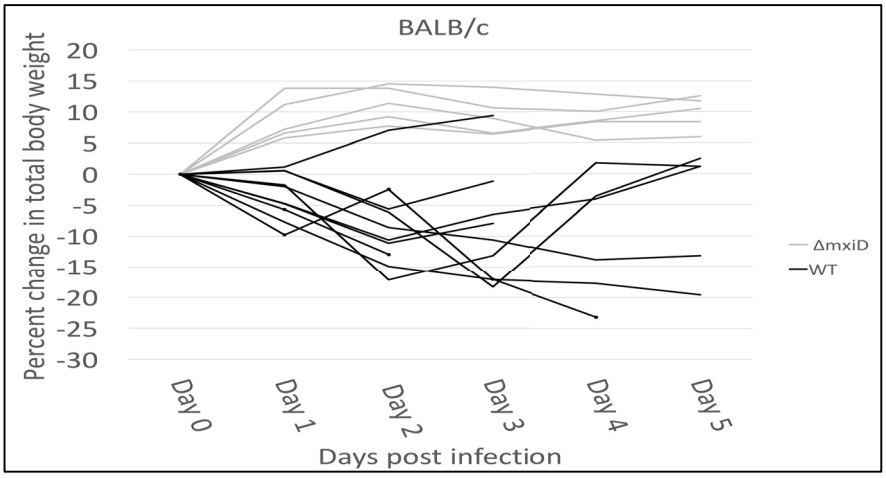
BALB/c
Percent change in total body weight
20
15
10
5
0
-5
-10
-15
-20
-25
-30
Day 0
Day 1
Day 2
Day 3
Day 4
Day 5
Days post infection
ΔmxiD
WT

C)

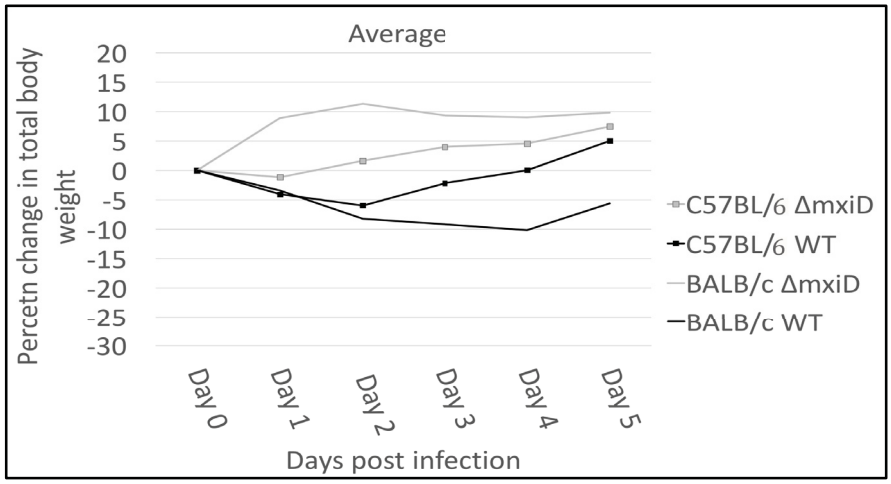
Average
Percetn change in total body weight
20
15
10
5
0
-5
-10
-15
-20
-25
-30
Day 0
Day 1
Day 2
Day 3
Day 4
Day 5
Days post infection
C57BL/6 ΔmxiD
C57BL/6 WT
BALB/c ΔmxiD
BALB/c WT

strains in either infection condition(figure 4A). The spleen and liver of mice in the three-day infection experiment were homogenized and bacterial burden was measured. There was a significant increase in WT bacteria in the liver and the spleen in the BALB/c mice when compared to the C57BL/6 mice (Figure 4B).

Histological samples of the colon were examined for signs of inflammation including edema, ulceration, crypt loss and cellular infiltrate (Figure 4C). There was evidence of hyperplasia and damage of crypts in sections of the colon for each sample and evidence of minor cellular infiltrate as determined by the parameters outlined in Table 4. Overall, no major pathology, such as ulceration, was observed in tissues infected with WT or Δ*mxiD Shigella*. Figure 4C shows representative pictures from each infection group, crypt destruction can be seen in both the Δ*mxiD* infected C57BL/6 mice and in the WT infected BALB/c mice. Hyperplasia can been seen in both the Δ*mxiD* infected mouse samples of both strains and small infiltrates can been seen in both WT infected mouse samples. However these characteristics were seen in all infection groups though not in every sample. Taken together these data show that *Shigella*-induced weight loss in BALB/c mice is dependent on a T3SS. These data also show that C57BL/6 mice do not experience significant weight loss upon *Shigella* infection, despite being colonized to a similar level as BALB/c mice.

Figure 4. Comparing bacterial burdens and pathology of C57BL/6 mice and BALB/c mice. (A) Comparison of bacterial burden from feces on day 3 and day 5. (B) Comparing bacterial dissemination between WT infected strains of mice in the liver (p value of 0.0013) and the spleen (p value of 0.0025) statistical analysis was preformed using a Mann-Whitney U test significance set at $p<0.05$ compared to C57BL/6. (C) Comparison of H&E stain colon Swiss rolls, all images are at 100x.

A)

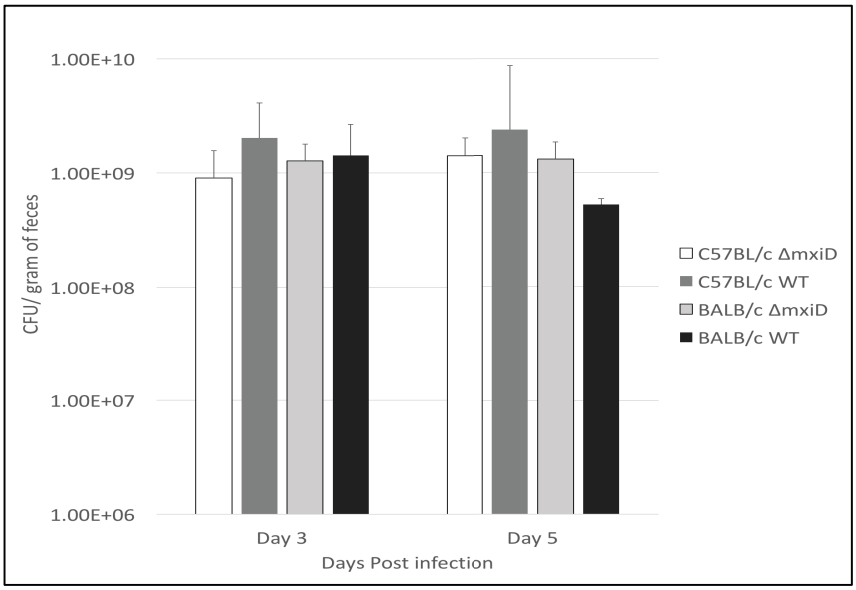
1.00E+10
1.00E+09
1.00E+08
1.00E+07
1.00E+06
CFU/ gram of feces
Day 3
Day 5
Days Post infection
C57BL/c ΔmxiD
C57BL/c WT
BALB/c ΔmxiD
BALB/c WT

B)

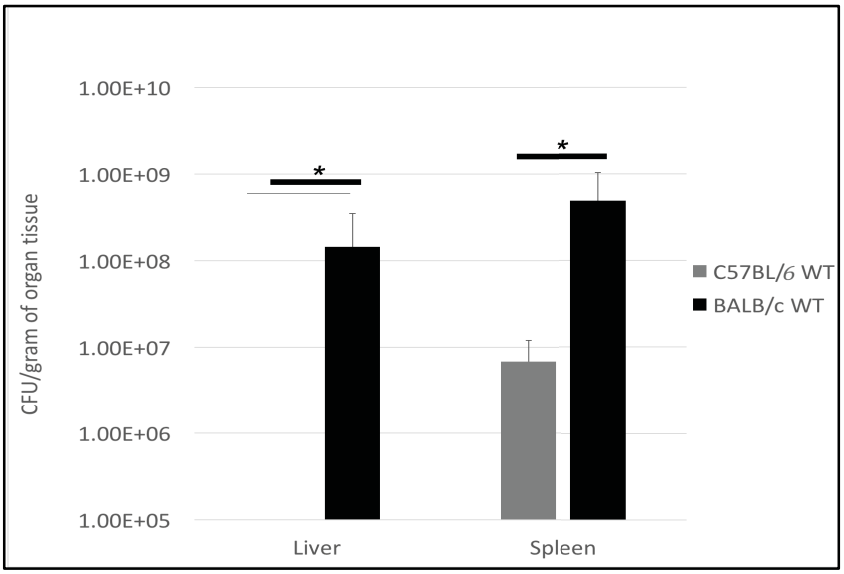
1.00E+10
1.00E+09
1.00E+08
1.00E+07
1.00E+06
1.00E+05
CFU/gram of organ tissue
*
*
Liver
Spleen
C57BL/6 WT
BALB/c WT

C)

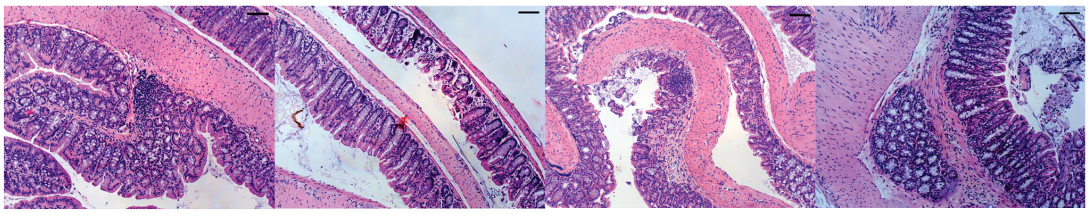
WT
ΔmxiD
WT
ΔmxiD
C57BL/6
BALB/c

3.2 The bacterial effector OspG plays a major role in disease susceptibility in the BALB/c streptomycin treated mouse model of shigellosis

The established streptomycin treated mouse model of shigellosis only examined WT or virulence plasmid-cured strains of *Shigella (Martino et al., 2005).* An open question was whether this model could be used to investigate the role of bacterial effector proteins. To address this, I directly compared wild-type and *ΔospG* mutant *Shigella* in the streptomycin treated mouse model of shigellosis using BALB/c mice. One reason that OspG was chosen was that this would allow for comparison to another animal model of *Shigella* infection: previously, it was shown that an *ospG* mutant elicited a more severe inflammatory response than WT *Shigella* in a rabbit ileal loop model of infection (Kim et al., 2005).

3.2.1 Characterization of *ΔospG in vitro* and creation of stable cell lines

To determine whether *ΔospG* and WT *Shigella* were internalized by epithelial cells to a similar extent, a gentamycin protection assay was performed on HeLa cells. Gentamycin is a broad spectrum antibiotic that can kill extracellular bacteria, however used at the concentration in this assay it does not penetrate mammalian cells. Mammalian cells can then be washed and lysed to release intracellular bacteria that can be plated and enumerated. This assay provides a quantitative measure for the ability of bacteria to enter cultured epithelial cells. When HeLa cells were infected with WT or *ΔospG* mutant *Shigella* no noticeable difference in invasion was

Figure 5: *In vitro* characterization of *ospG* mutants. (A) Bacterial burden following infection of HeLa cells in a gentamycin protection assay. The indicated strains were used to infect confluent HeLa cells for one hour. Gentamycin was added to kill extracellular bacteria, HeLa cells were lysed and internalized bacteria were plated and cultured. The infection was performed in duplicate then the two CFU/mL were averaged and plotted. (B) 1% agarose gel showing PCR confirmation of OspG variants being integrated successfully into the *Shigella* virulence plasmid. (C) Silver staining showing secretion profiles of ospG mutant and complemented strains. The indicated strains were grown in TSB at 37^{o}C to mid-log and concentrated. Cells were resuspended in PBS and and T3SS activity was induced with Congo red. The cell-free supernatant was collected and loaded onto 10% SDS polyacrylamide gels. Gels were stained with silver stain to visualize proteins. (D) Western blot against the myc tag epitope showing expression of codon optimized OspG variants in stable cell lines. The indicated cell lines were lysed and protein samples were separated by SDS PAGE and transferred to PVDF membrane. The membrane was subjected to immunoblotting using an anti- Myc antibody (diluted 1:1000, Cell signaling). Blot is a representative of N=3.

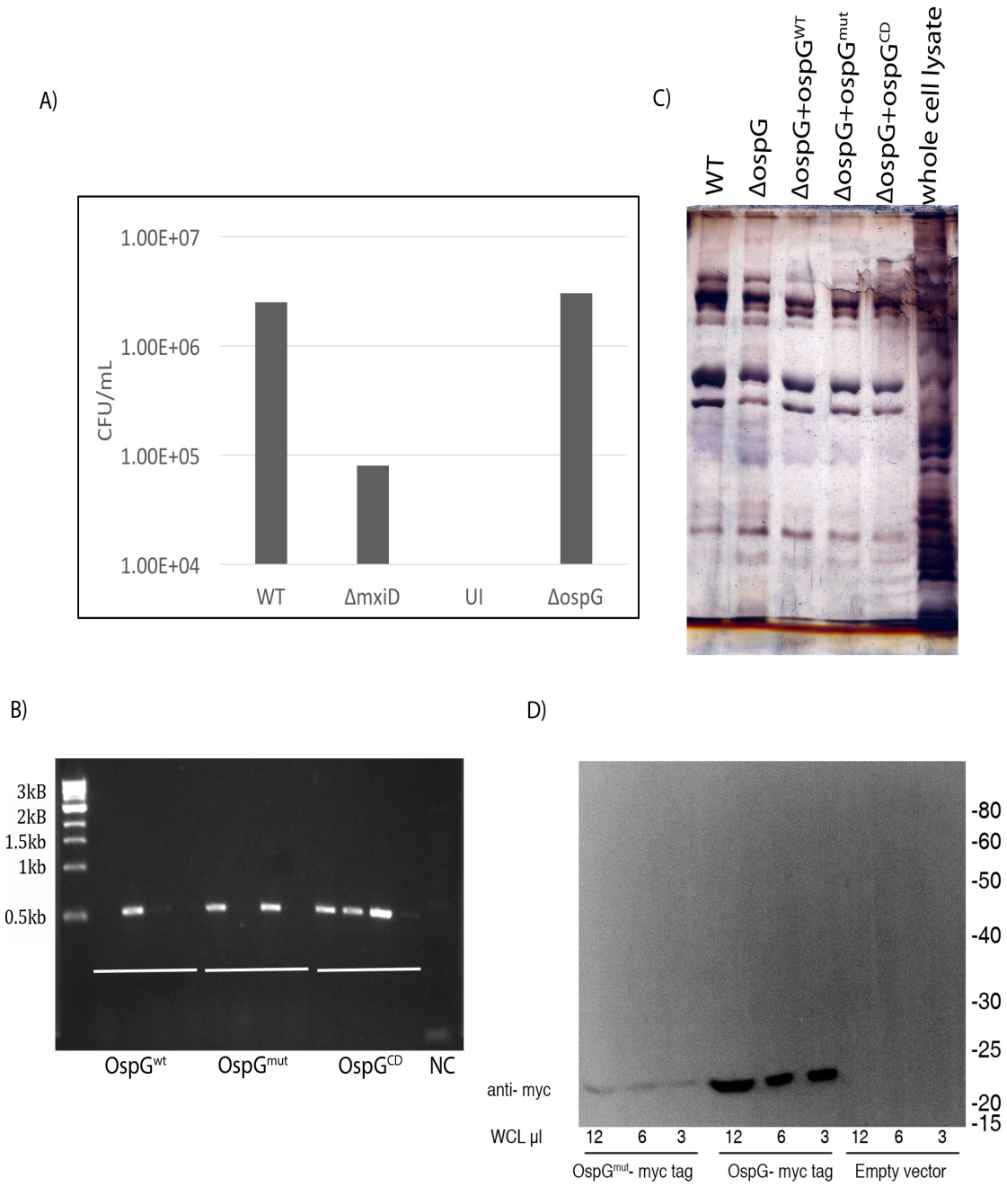
A)
1.00E+07
1.00E+06
1.00E+05
1.00E+04
CFU/mL
WT
ΔmxiD
UI
ΔospG
C)
WT
ΔospG
ΔospG+ospG^WT
ΔospG+ospG^mut
ΔospG+ospG^CD
whole cell lysate
B)
3kB
2kB
1.5kb
1kb
0.5kb
OspG^wt
OspG^mut
OspG^CD
NC
D)
anti- myc
WCL µl
12 6 3 12 6 3 12 6 3
OspG^mut- myc tag
OspG- myc tag
Empty vector
-80
-60
-50
-40
-30
-25
-20
-15

observed between the two strains (Figure 5A). These data demonstrate that loss of OspG does not affect the ability for *Shigella* to invade epithelial cells. In contrast the the T3SS deficient mutant *ΔmxiD* which has decreased invasion capability compared to WT or *ΔospG.*

Several variants of OspG ($OspG^{wt}$, $OspG^{mut}$, $OspG^{CD)}$ were complemented into the virulence plasmid of the *ΔospG* mutant as described in section 2.10. These specific variants were constructed based on the site determined in the crystal structure of OspG bound to a Eukaryotic E2-ubituitin conjugate (Pruneda et al., 2014). The integration of these variants was confirmed using colony PCR using a primer specific for *ospG* and a primer specific for the targeted integration site. Production of a PCR product indicated the correct integration (Figure 5B). Four colonies were selected for screening for each of the OspG variants, one $\Delta ospG^{wt}$ colony had integration, two colonies from the $\Delta ospG^{mut}$ had integration and three $\Delta ospG^{CD}$ colonies had integration. To further characterize the complemented strains, an effector secretion assay was performed. Secreted proteins were separated on 10% polyacrylamide gels and silver stained. Figure 5C shows that the secretion profile for the complemented OspG strains is comparable to that of WT *Shigella*. These data demonstrate that the mutant *ΔospG* does not have an increased ability to infect epithelial cells and that complementation of the *ΔospG* mutant does not alter T3SS function. These *in vitro* data provide proof of principle that these strains, in a streptomycin mouse model for infection, should be directly comparable with WT *Shigella*.

HEK 293T cells expressing codon optimized OspG^{mut}-myc tag or OspG-myc were established by retroviral transduction. Cells were harvested and assessed for expression of OspG and OspG^{mut} by western blotting against the myc epitope. Both cell lines expressed myc-tagged proteins that were appropriately sized for OspG. WT OspG had stronger expression than the mutant OspG (Figure 5D). Both constructs were able to be expressed in mammalian cells. These cell lines can be used as a tool to further study OspG function *in vitro*.

3.2.2. *In vivo* characterization of *ΔospG*

After *in vitro* characterization, the constructed strains were used to infect streptomycin treated BALB/c mice. Infection with the *ΔospG* strain resulted in 30% mortality at day 3, while mortlality was <10% with WT *Shigella* (Figure 6A). This increase in mortality was reversed when wild-type OspG was complemented into the virulence plasmid *(ΔospG^{wt})*. In contrast, when *ΔospG^{mut}* was used to infect BALB/c mice there was no reduction in mortality. Finally, when the catalytically dead variant of OspG (*ΔospG^{CD}*) was used to infect mice, I observed an intermediate phenotype (Figure 6A). Upon necropsy, it was observed that mice that reached an experimental endpoint due to weight loss following infection with *ΔospG had* accompanying changes in the gross morphology of the cecum and colon. These mice had discolored colons, filled with gas and devoid of fecal pellets. This phenotype was also observed in mice infected with *ΔospG^{mut}* and partially in mice infected with *ΔospG^{CD}*. The change in the cecum and colon was not observed in the WT or *ΔospG^{wt}* infected mice (Figure 6B). This suggests that OspG is important in preventing

Figure 6. *ΔospG* infection causes increased mortality and a change in gross morphology of the colon. (A) Oral infection with $1x10^8$ CFU of *ΔospG* mutant *Shigella flexneri* causes a 30% increase in mortality in BALB/c mice over BALB/c miceinfected with wildtype (WT) *Shigella* . This mortality was alleviated by introducing *ospG* back into the *ΔospG* mutant (*ΔospG+ospG*^{wt}). OspG variants that cannot bind to the host E2 did not alleviate the mutant phenotype (*ΔospG+ospG*^{mut}). An OspG mutant that lacks kinase activity reduced the mortality, but not to WT levels (*ΔospG+ospG*^{CD}*)*. (*n* = 10–25 per group). Survival curves were analyzed using a Log-rank (Mantel-Cox) test. Significance was set at a p value <0.05. A significant difference was determined. (B) Cecum and colon from the mouse infection groups exhibited difference in colour and fecal content. *ΔospG* and *ΔospG*^{mut} are representative of mice who died due to infection (C) Bacterial burden recovered from homogenized liver and from cecal contents, on day 3 of infection. No significant difference observed between groups. *ΔospG* n was 5, *WT* n was 5, *ΔospG+OspG*^{WT} n was 14, *ΔospG+OspG*^{mut} n was 10. (D) H&E strained colon Swiss roles comparing uninfected, wildtype infect and *ΔospG..* This data was published in (Pruneda et al., 2014).

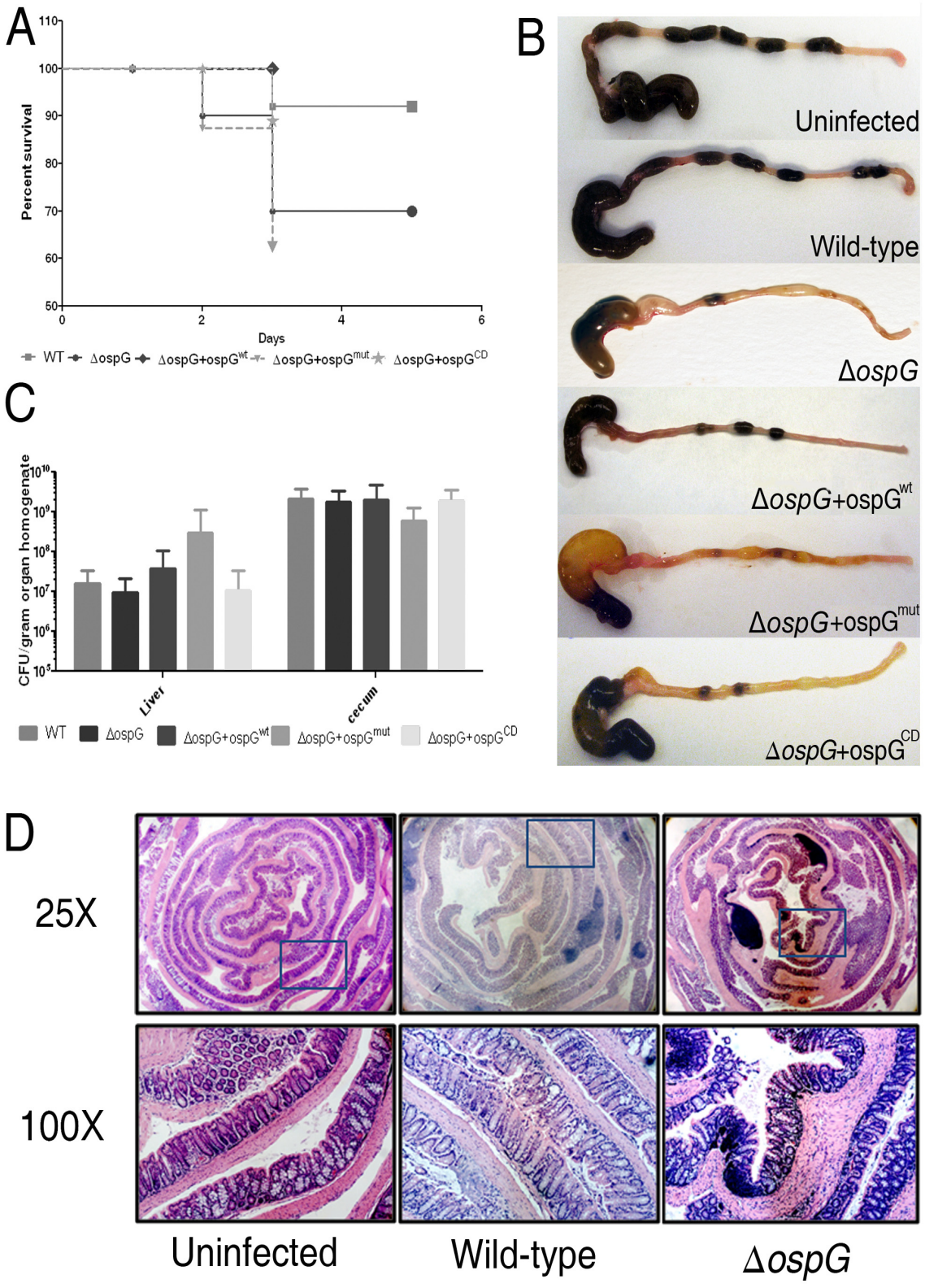
A
Percent survival
Days
WT
ΔospG
ΔospG+ospG^wt
ΔospG+ospG^mut
ΔospG+ospG^CD
B
Uninfected
Wild-type
ΔospG
ΔospG+ospG^wt
ΔospG+ospG^mut
ΔospG+ospG^CD
C
CFU/gram organ homogenate
Liver
cecum
D
25X
100X
Uninfected
Wild-type
ΔospG

mortality in the streptomycin treated BALB/c mouse model, and that the interaction with host systems is involved. I considered the possibility that the increased mortality may be due to an increased dissemination of the bacteria to deeper organs, or an alteration in the infection site. Homogenates of liver and cecum were prepared and examined for bacterial burden. No significant differences in bacterial burdens were observed between any *Shigella* strains used in the mouse infections (Figure 6C). Swiss rolls of the colon were examined for histopathological differences. There was no ulceration or massive infiltrate observed in any of the infected animals (Figure 6D). These data demonstrate that the increase in mortality is not caused by an increased dissemination of the*ΔospG* bacteria or an increased colonization in the cecum. The increase in mortality does not appear to be caused by massive damage or ulceration in the colon in the *ΔospG* infection.

3.3 Investigating potential kinase targets for OspG

Infections with the $\Delta ospG^{CD}$ strain demonstrated that the kinase-dead variant of OspG was not capable of fully complementing the phenotype observed in the defecient mutant. These data suggests that a potential kinase target exist in the mouse that may play a role in susceptibility. To date there are no known targets for OspG kinase activity. To investigate potential human targets, a yeast two-hybrid screen was performed using a normalized human prey library and the catalytically dead OspG as bait. Since OspG is known to interact with the host ubiquitin system, the catalytically dead variant was used to prevent possible degradation of the target by the proteasome. A list of potential targets was generated (Table 7) and two were

picked for confirmation using co-immunoprecipitation of Rab11a and COPS3. I was unable to validate a OspG-COPS3 interaction via co-immunoprecipitation (data not shown). The co-immunoprecipitation for Rab11 was performed in HEK293T cell lines expressing WT OspG-myc tag or $OspG^{mut}$-myc tag. Two variants of Rab11 were used, a WT and a dominant negative variant, and an empty vector served as the negative control. Immunoprecipitation using the Myc epitope and subsequent immunoblotting for Rab11 showed that both the WT and dominant negative variants of Rab11 could be detected in anti-Myc immunocomplexes (Figure 7). These data suggest that Rab11 and OspG interact in mammalian cells. In both cell lines, the WT Rab11 had slightly higher concentrations of transfected Rab11 expression compared to the dominant negative. The OspG- E2 interaction did not appear to have a large effect on Rab11 binding (Figure 7).

Rab11 had previously been implicated in *Shigella* entry into epithelial cells (Mellouk et al., 2014). WT and *ΔospG Shigella* were transformed with a plasmid expressing a red fluorescent protein (dsRed) so that the recruitment of Rab11 to the site of entry could be investigated using live cell fluorescent imaging (experiments were performed by me at the Institute Pasteur in the lab of Dr. Jost Enninga) . HeLa cells transfected with GFP-Rab11 were infected at a multiplicity of infection (MOI) of 50, and recruitment of Rab11 was observed over the course of a 1 hour infection with imaging every 60 seconds (Figure 8). No invasion events were observed in HeLa cells that cultured with WT *Shigella*, but there was invasion with the *ΔospG*

Table 7: Potential targets for OspG identified from a yeast 2-hybrid screen

Yeast Two-Hybrid Identification	Number of times recovered from screen
Homo sapiens cDNA FLJ78105 complete cds, highly similar to Homo sapiens pleiotrophin (heparin binding growth factor 8, neurite growth-promoting factor 1) (PTN)	9
Homo sapiens COP9 signalosome subunit 3 (COPS3)	4
Homo sapiens CCR4-NOT transcription complex, subunit 8 (CNOT8)	3
Homo sapiens coiled-coil domain containing 113 (CCDC113)	3
Homo sapiens dual specificity phosphatase 22 (DUSP22)	3
Homo sapiens ferritin, light polypeptide	2
Homo sapiens matrix Gla protein	2
Homo sapiens RAB11A, member RAS oncogene family (RAB11A)	2
Homo sapiens proline-rich coiled-coil 1	2
Homo sapiens zinc finger, DHHC-type containing 9 (ZDHHC9)	2
Homo sapiens WD repeat domain 72 (WDR72)	2
Homo sapiens prolyl endopeptidase-like (PREPL)	1
Homo sapiens transcriptional regulating factor 1 (TRERF1)	1
Homo sapiens fibulin 5 (FBLN5)	1
PREDICTED: Homo sapiens uncharacterized LOC285423 (LOC285423)	1
Homo sapiens SEC22 vesicle trafficking protein homolog B (S. cerevisiae) (gene/pseudogene) (SEC22B)	1
Homo sapiens importin 5 (IPO5)	1
Homo sapiens neurofilament, light polypeptide (NEFL)	1
Human DNA sequence from clone RP11-460H15 on chromosome 1	1

Yeast Two-Hybrid Identification	Number of times recovered from screen
Homo sapiens CGG triplet repeat binding protein 1 (CGGBP1)	1
Homo sapiens death-domain associated protein (DAXX)	1
Homo sapiens presenilins-associated rhomboid-like protein, mitochondrial-like (LOC100131471) pseudogene on chromosome 6	1
Homo sapiens PAC clone RP5-1007F24 from 7	1
Homo sapiens La ribonucleoprotein domain family, member 1	1
Homo sapiens protein phosphatase 3, catalytic subunit, beta isozyme (PPP3CB)	1
Homo sapiens host cell factor C1 (VP16-accessory protein), with apparent retained intron	1
Homo sapiens ribosomal L24 domain containing 1	1
Homo sapiens phosphatidylinositol glycan anchor biosynthesis, class K (PIGK)	1
Homo sapiens serine/threonine protein kinase 26 (STK26)	1
Homo sapiens transmembrane protein 260 (TMEM260)	1

Figure 7. Confirming OspG-Rab11 interactions via co-immunoprecipitation. (A) Western blots against Ha tagged Rab11 in whole cell lysate (WCL) showing total Rab11. (B) Western blots against actin in the WCL showing protein levels loaded. (C) Western blots against Ha tagged Rab11 that was and co-immunoprecipitated following myc tag OspG pull down. Blots are representative of N=2-5 blots.

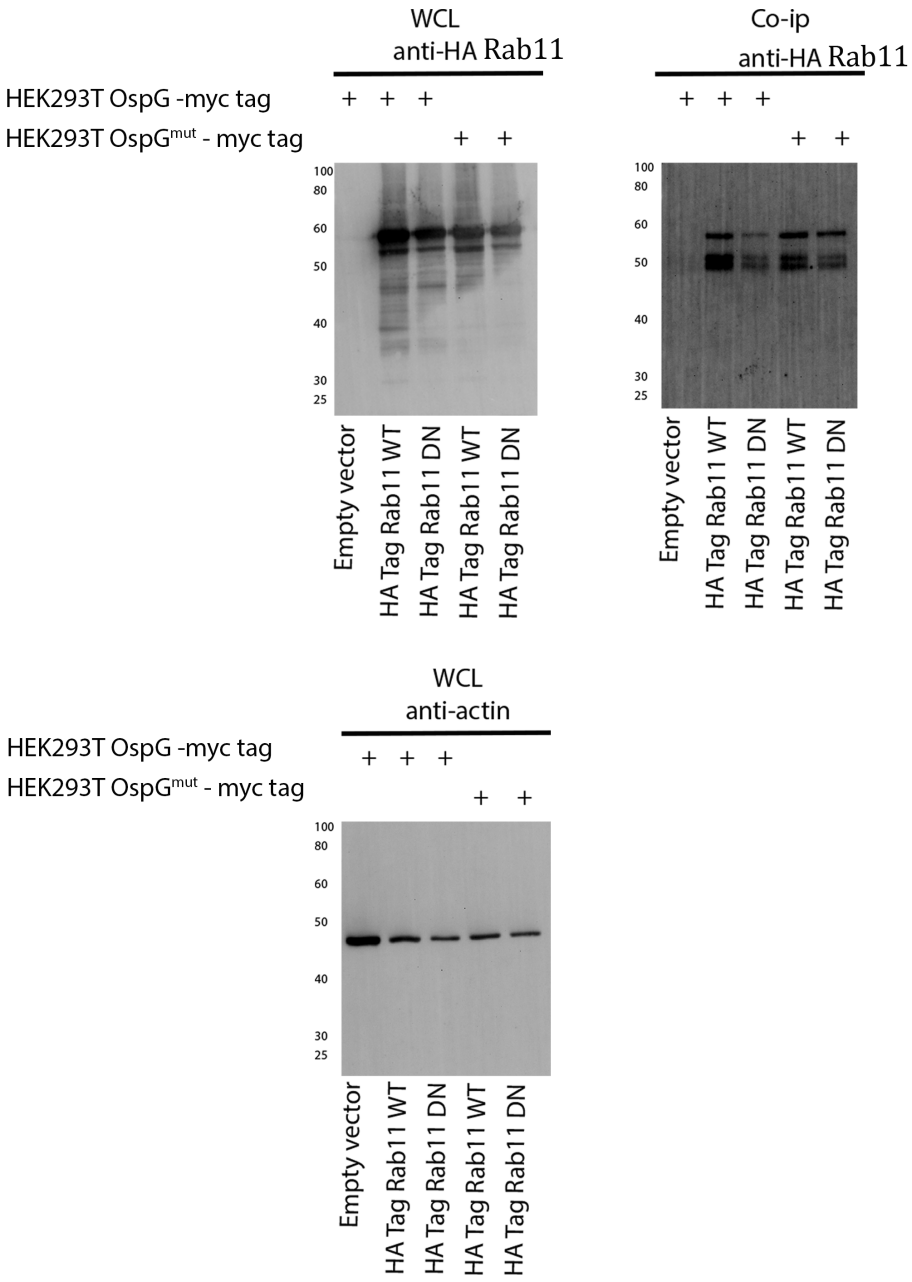
WCL
anti-HA Rab11
Co-ip
anti-HA Rab11
HEK293T OspG -myc tag
HEK293T OspG^mut - myc tag
+ + +
+ +
100
80
60
50
40
30
25
Empty vector
HA Tag Rab11 WT
HA Tag Rab11 DN
HA Tag Rab11 WT
HA Tag Rab11 DN
WCL
anti-actin
HEK293T OspG -myc tag
HEK293T OspG^mut - myc tag
+ + +
+ +
100
80
60
50
40
30
25
Empty vector
HA Tag Rab11 WT
HA Tag Rab11 DN
HA Tag Rab11 WT
HA Tag Rab11 DN

Figure 8. Time lapse images showing live cell infection with *Shigella*. Red fluorescent protein (dsRed) expression plasmids were transformed into WT or ΔospG strains of *Shigella*. These bacteria were used to infect HeLa cells expressing Rab11-GFP and were imaged once a minute for one hours post infection. These images show ΔospG infecting a cell and recruiting Rab11 containing vesicles to the site of infection. Times points are 23 minutes, 32 minutes and 40mins post inoculation. Magnification is 400x.

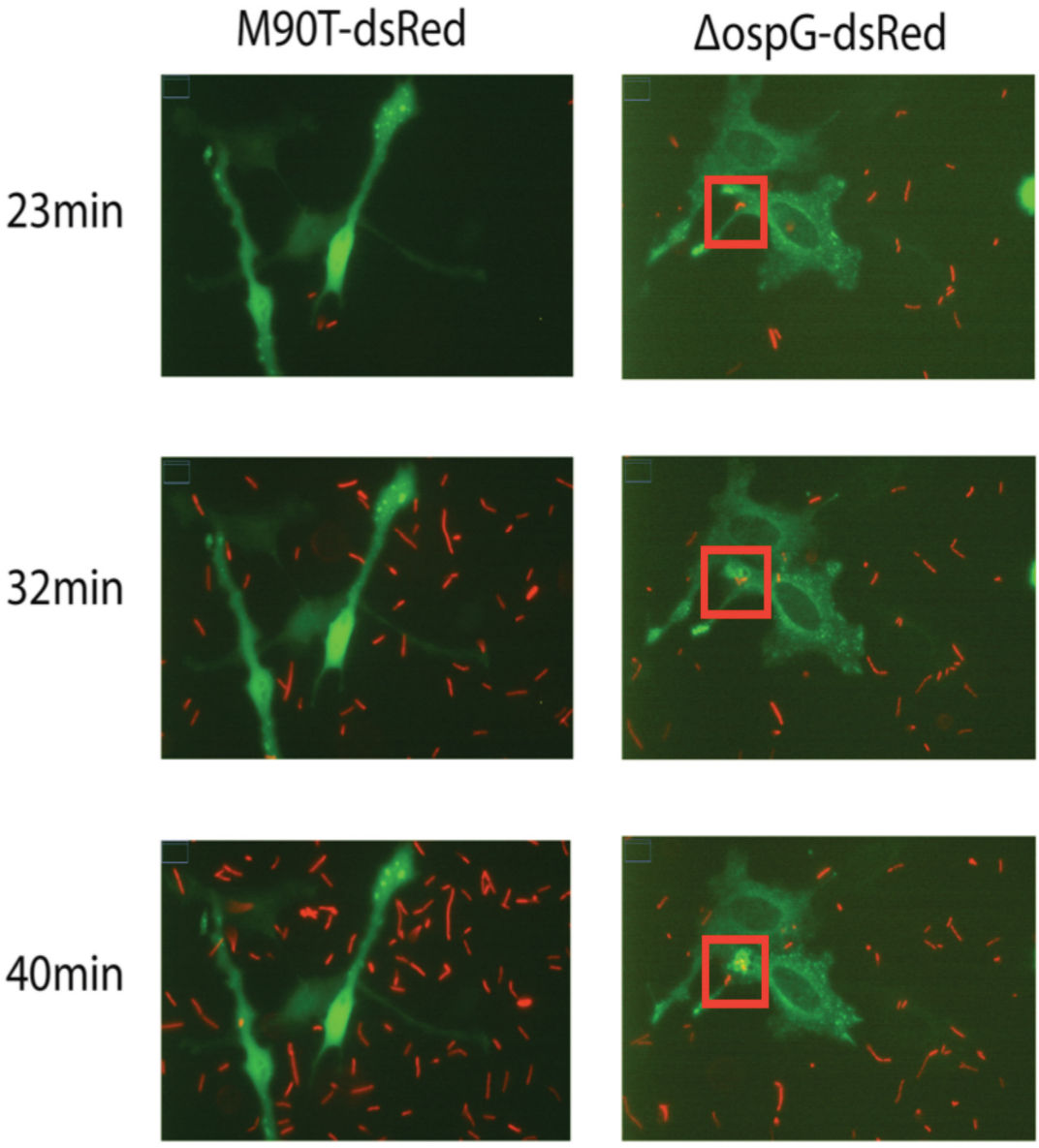
M90T-dsRed
ΔospG-dsRed
23min
32min
40min

Shigella. However, there was not obstruction in the Rab11 recruitment to the site of *Shigella* entry in the *ΔospG* mutant *Shigella* infection as colocalization of GFP and dsRed were observed. Alternative approach will be needed to further characterize the interaction between OspG and Rab11.

3.4 Mouse strain-specific differences in susceptibility to wild type *Shigella* infection

While the streptomycin treated mouse model (Martino et al., 2005) displays several hallmarks of human shigellosis it has been described exclusively in the BALB/c mouse strain. When the C57BL/6 strain of mice were infected they became colonized but lacked signs of clinical illness, indicating variability in the severity of disease depending on the strain of mouse used. To further investigate this, several lab strains of mice, congenic strains, and genetic knock-out mice were infected with wild type *Shigella* using the streptomycin oral infection model. A range of disease was observed, from severe with incidence of mortality, to colonization with no signs of clinical illness or mortality (Figure 9). This range in disease severity suggests that host factors or differences in the colon micro-environment may alter the susceptibility to *Shigella* infection. There was no significant difference in survival between BALB/c and C57bL/6 (Figure 9A).

The Cri locus in mice is involved in susceptibility to *Citrobacter rodentium* infection (Diez et al., 2011). To determine if this locus was involved with *Shigella* susceptibility, the C3HOUJ strain that is highly susceptible to *Citrobacter,*

Figure 9. Percent survival of mice infected with wild-type *Shigella flexneri* varies depending on murine strain. Percent survival of *Shigella flexneri* susceptible mouse strains compared to various resistant mouse strains, following oral infection with $1x10^8$ CFU of wild-type *Shigella flexneri*. Number of mice that succumbed to *Shigella* infection out of total number infected is depicted in the legend. Significant differences seen between strain in Figured 9D (p value< 0.0001)

A)

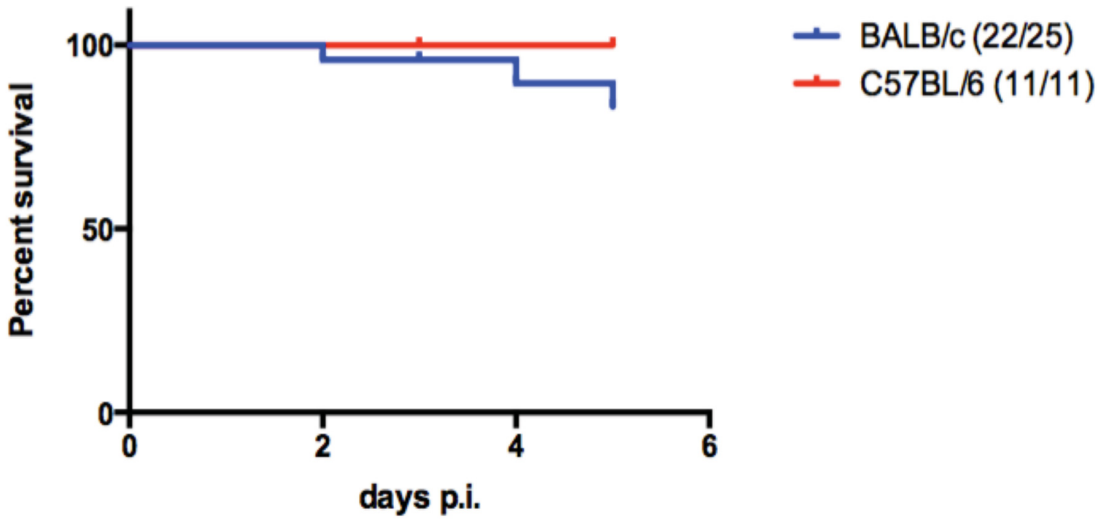
Percent survival
100
50
0
0
2
4
6
days p.i.
BALB/c (22/25)
C57BL/6 (11/11)

B)

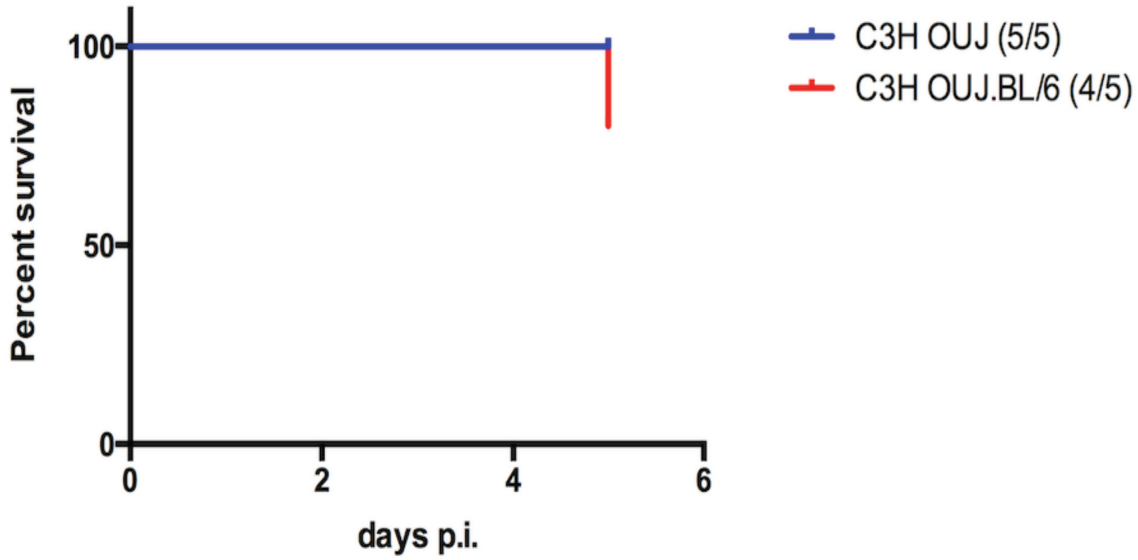
Percent survival
100
50
0
0
2
4
6
days p.i.
C3H OUJ (5/5)
C3H OUJ.BL/6 (4/5)

C)

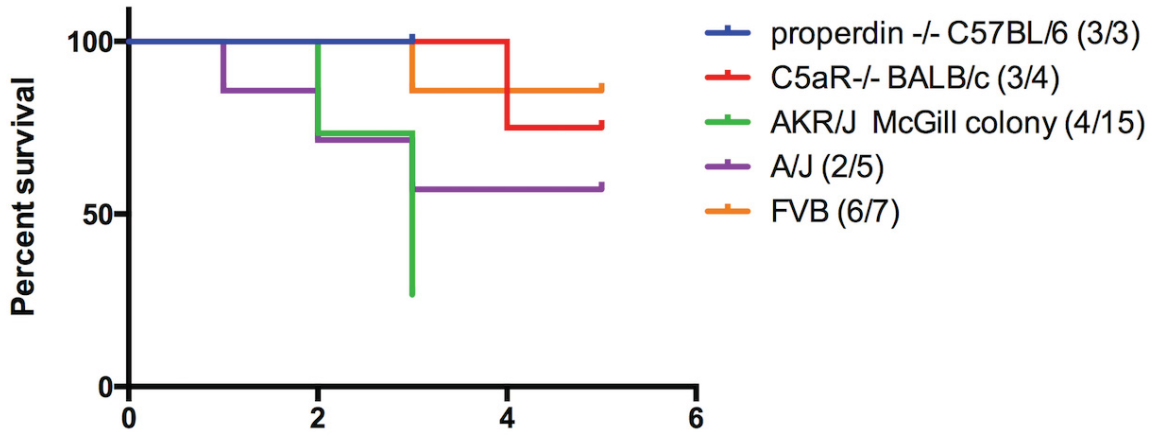
Percent survival
100
50
0
0
2
4
6
properdin -/- C57BL/6 (3/3)
C5aR-/- BALB/c (3/4)
AKR/J McGill colony (4/15)
A/J (2/5)
FVB (6/7)

D)

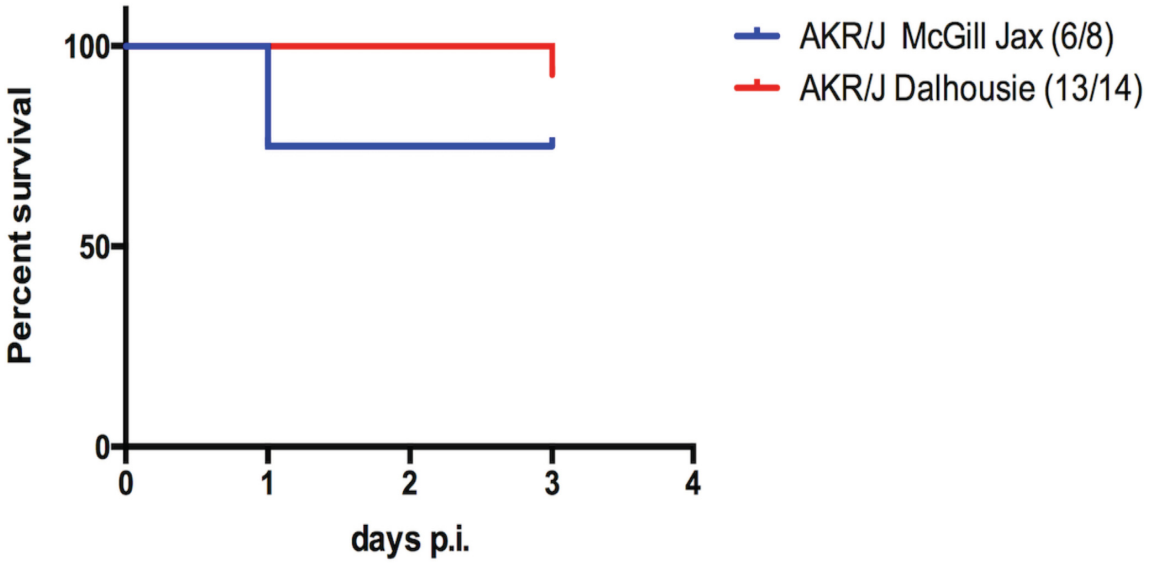
Percent survival
100
50
0
0
1
2
3
4
days p.i.
AKR/J McGill Jax (6/8)
AKR/J Dalhousie (13/14)

and congenic C3HOUJ-BL/6 strain that has the Cri1 locus of the non susceptible C57BL/6 strain, were infected with WT *Shigella* at the lab of Dr. Samantha Gruenheid (McGill University). The strains had not exhibited a significant difference in mortality (Figure 9B).

During my work term in the Gruenheid lab, the AKR/J McGill colony of mice were found to have increased mortality following *Shigella* infection compared to the BALB/c model (Figure 9C). This group of mice were part of an in house breeding colony at the McGill animal facility. In the first set of infection experiment 11 of 15 mice reach an experimental endpoint by day three, either by weight loss greater than 20% or from a combined clinical illness score that was greater than 14 (Figure 9C). AKR/J mice have a deficiency in the complement component C5 (Ooi and Colten, 1979). At Dalhousie I infected several complement deficient knock out strains which were gifts from Dr. Andrew Stadnyk. such as properdin -/- mice that are deficient in the alternative pathway for complement, and C5aR-/- mice which lack the receptor for complement component C5a. Two inbreed lab strains that were also deficient in complement component C5 (A/J and FVB) were infected with wild-type *Shigella* at McGill. There was variability in the severity of disease between these groups. With some strains of mice having increased mortality compared to BALB/c or C57BL/6 mice when infected with WT *Shigella*. However many of these groups where small sample sizes and will need further investigation (Figure 9C).

I decided to further investigate the AKR/J mice which had the most pronounced mortality. When The AKR.J mice were infected with WT *Shigella* at Dalhousie using the same conditions (brand of food, housing, age and sex) but using

AKR/J mice ordered directly from Jackson laboratories, the increased mortality phenotype was not observed and only 1 of 14 mice reached an experimental endpoint early (Figure 9D). When new AKR/J mice were ordered into the McGill facility from Jackson laboratories and infected with WT *Shigella* the increased mortality phenotype was again absent (Figure 9D). These data suggested that either a difference in the gut microenvironment or a genetic mutation present in the breeding colony was responsible for increase in mortality in these mice.

I examined the possibility that a difference in the immune environment of the colon in response to proinflammatory cytokines was responsible for the differences seen between the susceptible AKR/J groups at McGill and the non susceptible AKR/J mice at Dalhousie. RT-qPCR was used to measure mRNA levels for several common proinflammatory cytokines and immune modulating cytokines: interleukin-1β (IL-1β), interleukin -6 (IL-6), interlukin-12 (IL-12), TNF-α and inducible nitric oxide synthase (iNOS) in colonic tissue of Shigella infected AKR/J mice. These were chosen to detect changes in the immune or inflammatory environment in the tissue. Expression of a control "housekeeping gene" was also measured: Hypoxanthine-Guanine Phosphoribosyltransferase (HPRT). When total RNA was obtained from infected colonic tissue of the susceptible McGill colony of AKR/J mice and compared to the infected Dalhousie AKR/J mice using RT-qPCR it was found that the McGill mice had 13.5 fold higher expression of iNOS compared to the Dalhousie mice (Figure 10A). Other cytokine mRNA levels were analyzed but no differences were observed. Representative data for IL-6 and IL-1β are shown(Figure 10B-C). However quantities detected were at a high cycle threshold suggesting the amounts

Figure 10. Differences in expression of inflammatory mediators in McGill and Jackson AKR/J mice. (A) Fold change in iNOS mRNA normalized to HPRT. (B) Fold change in IL-6 mRNA normalized to HpRT. (C) Fold change in IL-1β mRNA normalized to HpRT. Q-RT-PCR was performed on mRNA isolated from colon tissue of AKR/J mice treated with streptomycin and infected with wild type *Shigella* at the McGill animal facility or at the Dalhousie animal Facility. Each value represent average of 3-5 mice.

(A)

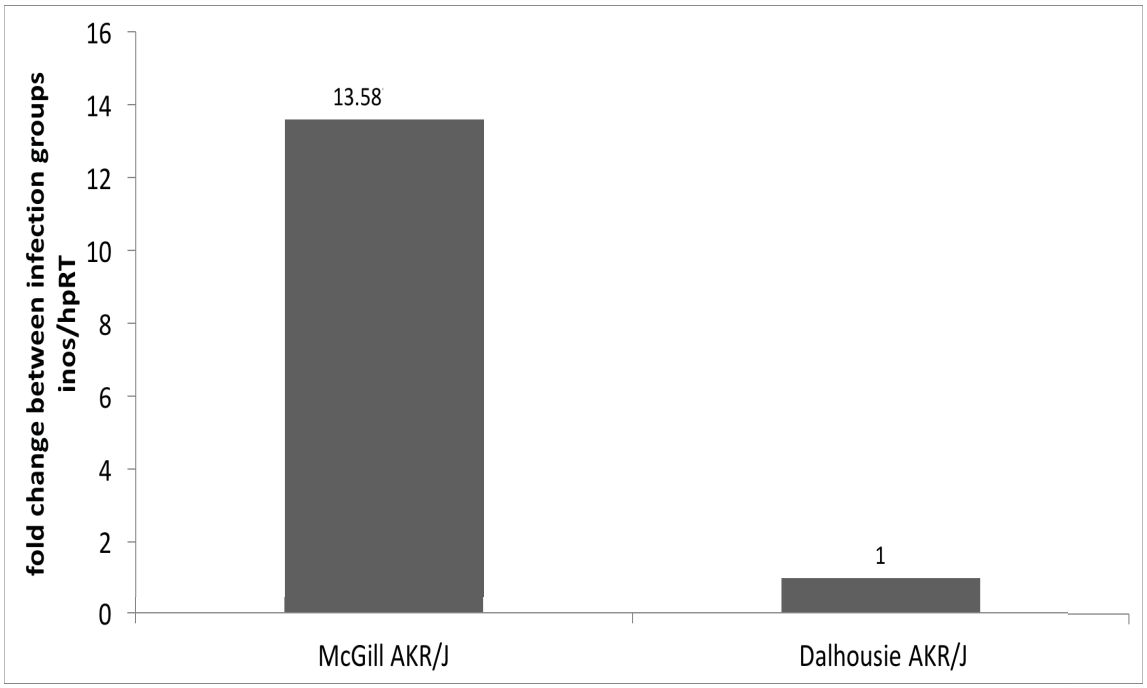
fold change between infection groups inos/hpRT
16
14
12
10
8
6
4
2
0
13.58
1
McGill AKR/J
Dalhousie AKR/J

(B)

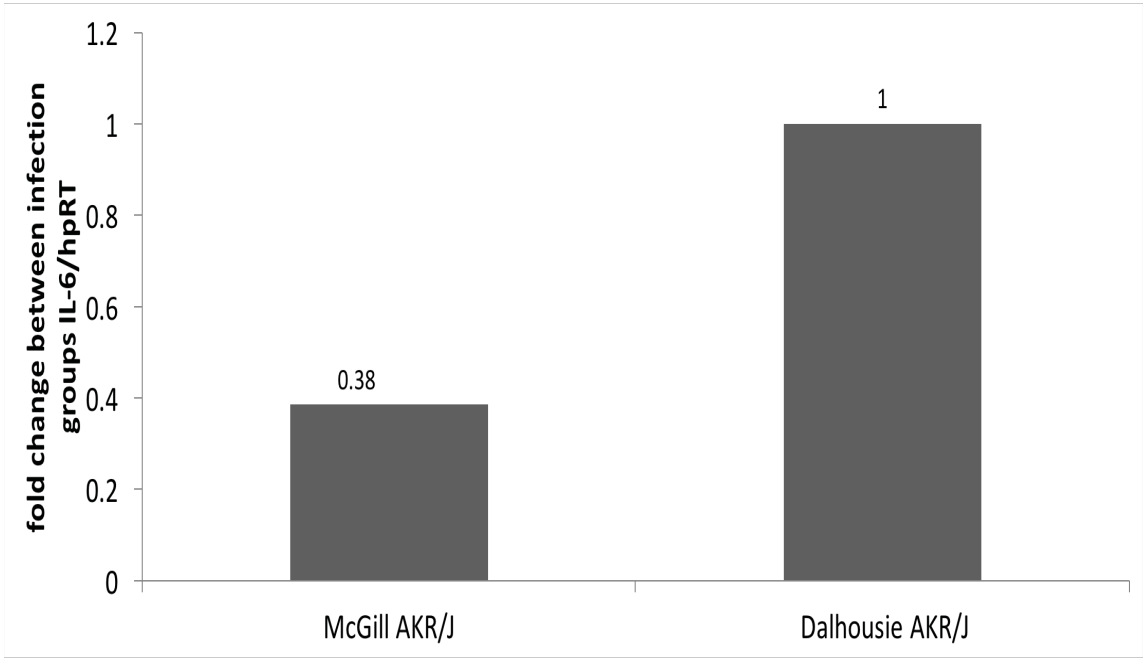
fold change between infection groups IL-6/hpRT
1.2
1
0.8
0.6
0.4
0.2
0
0.38
1
McGill AKR/J
Dalhousie AKR/J

(C)

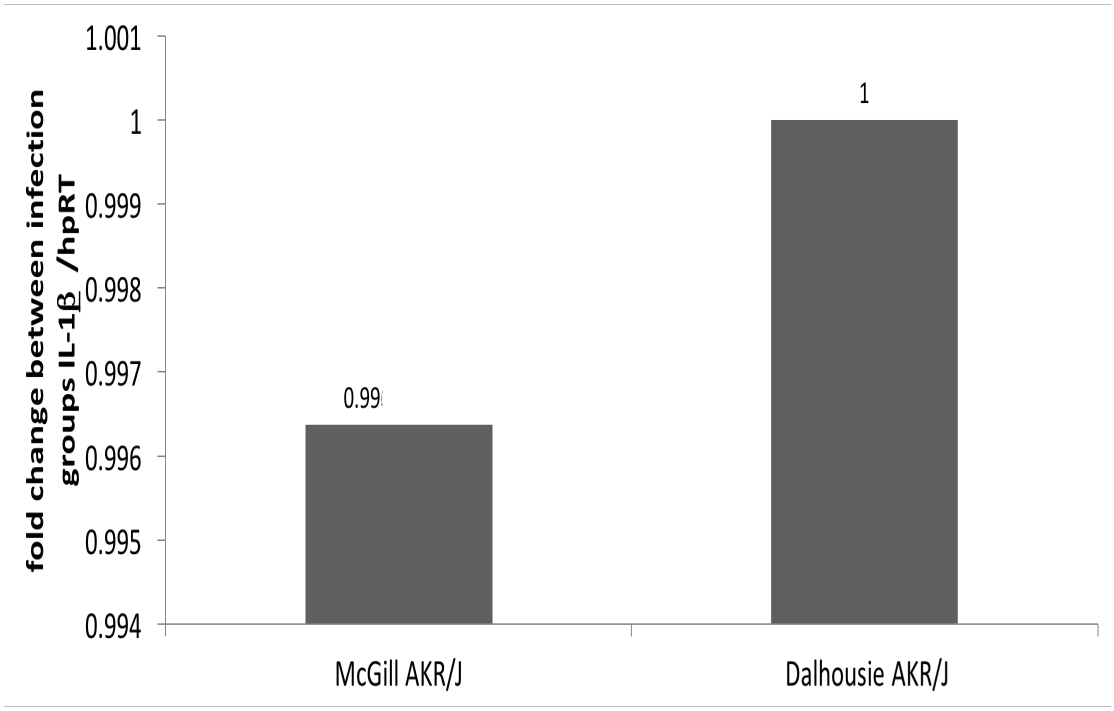
fold change between infection groups IL-1β /hpRT
1.001
1
0.999
0.998
0.997
0.996
0.995
0.994
0.99
1
McGill AKR/J
Dalhousie AKR/J

are near the limit of detection and not likely to be accurate, and IL-12 and TNF were detected at similar levels to Il-6 and IL-1β (Data not shown).

3.5 Changes in the microbiome in the streptomycin mouse model of *Shigella* infection.

Another possible reason for the differences in susceptibility of McGill AKR/J mice could be differences in the microbiome. The microbiome has been shown to play protective role against enteric infection as described in Chapter 1.8. Potentially, differences in the microbiome between the McGill and Jackson Labs AKR/J strains could be responsible for the differences in *Shigella*-induced mortality. DNA was extracted from homogenates obtained of fecal pellets from a cage of five mice. Samples were collected from the McGill AKR/J that were bred in house, from the McGill AKR/J that were ordered from Jackson laboratories and the Dalhousie AKR/J mice ordered from Jackson Laboratories. The samples were sent for 16S analysis using the Integrated Microbiome Resource (IMR) Facility at Dalhousie University. The community of bacteria were compared at the genus level, except when the 16S could not be identified to the genus level it was grouped as an unknown family or order (Figure 11). The 3 groups of AKR/J mice shared many of the same genus and families but in varying proportions. There were some genera unique to each group such as the *Akkermansia* and *Allobaculum,* which were only found in the McGill breeding colony, however these unique genera were a low proportion of the total reads, suggesting a low abundance in the community. It is also not known if these bacteria are able to persist during streptomycin treatment.

Figure 11: 16S profiles of AKR/J mice before streptomycin treatment. Stacked bar graph showing proportions of total operational taxonomic unit (OTU) reads detected by 16S rRNA sequencing from fecal samples collected from AKR/J mice prior to any treatment. McGill Jax mice were ordered from Jackson laboratories housed at McGill, McGill colony mice were bred in house for multiple generations at the McGill facility, and Dalhousie AKR/J mice were ordered from Jackson laboratories and housed 3 weeks prior to sample collection. Each group is the combination of fecal pellets from a cage of 5 mice. The Illumina MiSeq was used to obtain an output of approximately 12422 reads.

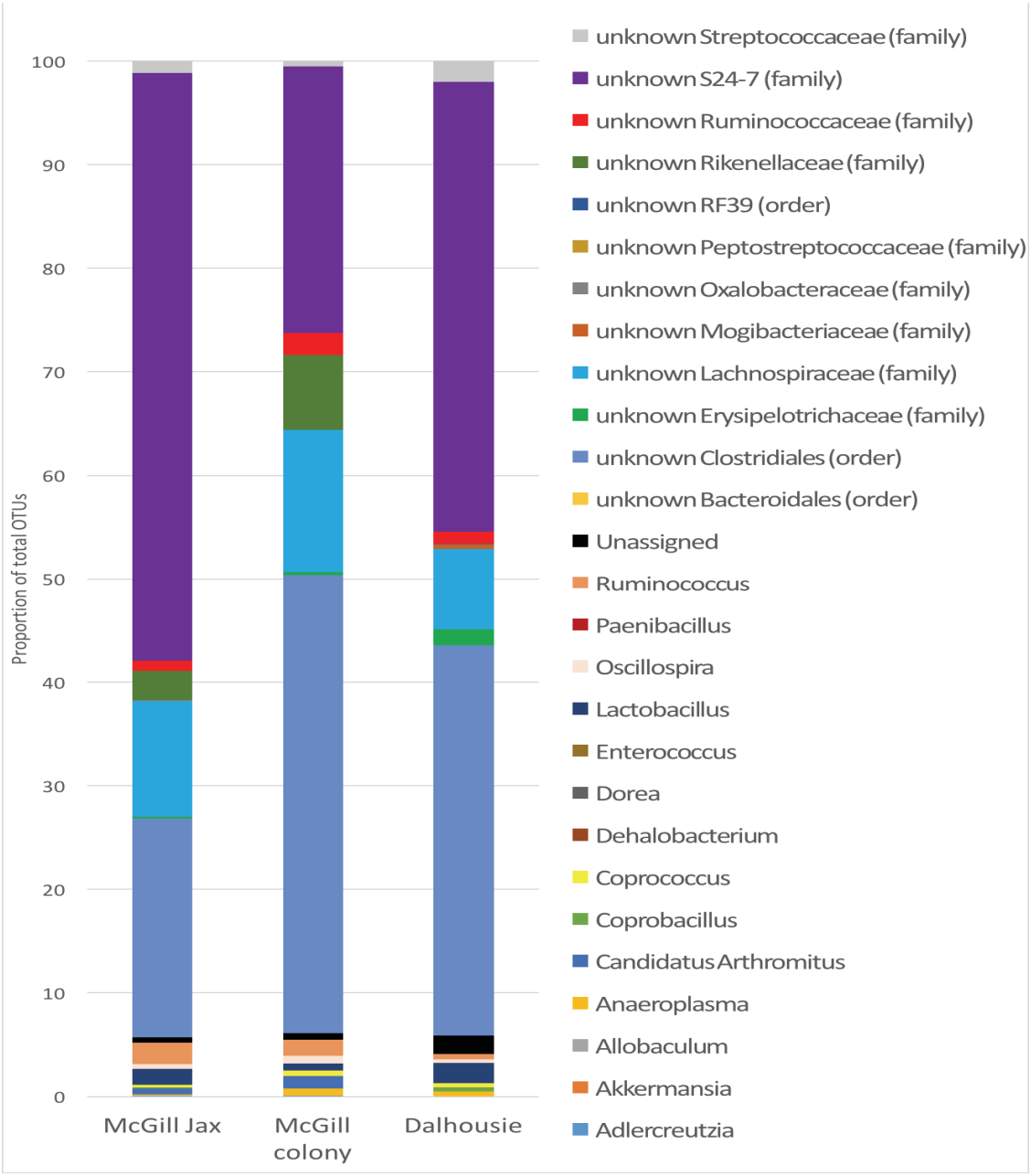
Proportion of total OTUs
100
90
80
70
60
50
40
30
20
10
0
McGill Jax
McGill colony
Dalhousie
unknown Streptococcaceae (family)
unknown S24-7 (family)
unknown Ruminococcaceae (family)
unknown Rikenellaceae (family)
unknown RF39 (order)
unknown Peptostreptococcaceae (family)
unknown Oxalobacteraceae (family)
unknown Mogibacteriaceae (family)
unknown Lachnospiraceae (family)
unknown Erysipelotrichaceae (family)
unknown Clostridiales (order)
unknown Bacteroidales (order)
Unassigned
Ruminococcus
Paenibacillus
Oscillospira
Lactobacillus
Enterococcus
Dorea
Dehalobacterium
Coprococcus
Coprobacillus
Candidatus Arthromitus
Anaeroplasma
Allobaculum
Akkermansia
Adlercreutzia

The next consideration was how the AKR/J microbiome changes over the course of infection. To examine this, fecal samples were collected from the same group of five mice before treatment with streptomycin, post treatment with streptomycin, and post infection with WT *Shigella* (Figure 12). Unfortunately, time course samples for the McGill in house breeding colony that had increased susceptibility were not collected before the breeding colony had new AKR/J mice from Jackson Labs introduced for breeding. Comparisons between the McGill and Dalhousie AKR/J mice ordered from Jackson Labs revealed similar genera present in the fecal samples but at varying abundance (Figure 12), again there were facility specific differences seen as well but their genera were at low abundance. After streptomycin treatment, the abundance of bacteria in the fecal pellets decreased dramatically. In fact, the average DNA recovered from in the AKR/J sample from the Dalhousie mice was too low to sequence. The McGill AKR/J had similar species present as the pretreated mouse (Figure 12). After mice were infected with *Shigella,* over 99% of the community was *Shigella*.

I conducted similar experiments to monitor microbiome changes in BALB/c mice in the streptomycin model. Streptomycin treatment of BALB/c mice resulted in significant microbiome changes with dissapperance of prominent genera and emergence of low abundance species (Figure 13). Once the BALB/c mice were infected with *Shigella,* a large proportion of the 16S reads were *Shigella* (around 85%) but some of the species that became abundant after streptomycin treatment are still present. One example was *Paenibacillus*, which made up less then 1% of the fecal community in untreated mice, but increased to a~12% after treatment with

Figure 12:16S profiles of AKR/J mice at different time points in the streptomycin model pf shigellosis. Stacked bar graph showing proportions of total operational taxonomic unit (OTU) reads detected by 16S rRNA sequencing from fecal samples collected from AKR/J mice from over the course of infection. McGill Jax mice from Jackson laboratories were housed at McGill for 3 weeks prior to infection. Dalhousie were AKR/J mice were housed at Dalhousie 3 weeks prior to infection. Fecal samples were collected before treatment, post streptomycin treatment (Dalhousie sample abundance was too low to amplify), and following *Shigella* infection. each group is the combination of fecal pellets from a cage of 4-5 mice. The Illumina MiSeq was used to obtain an output of approximately 12422 reads.

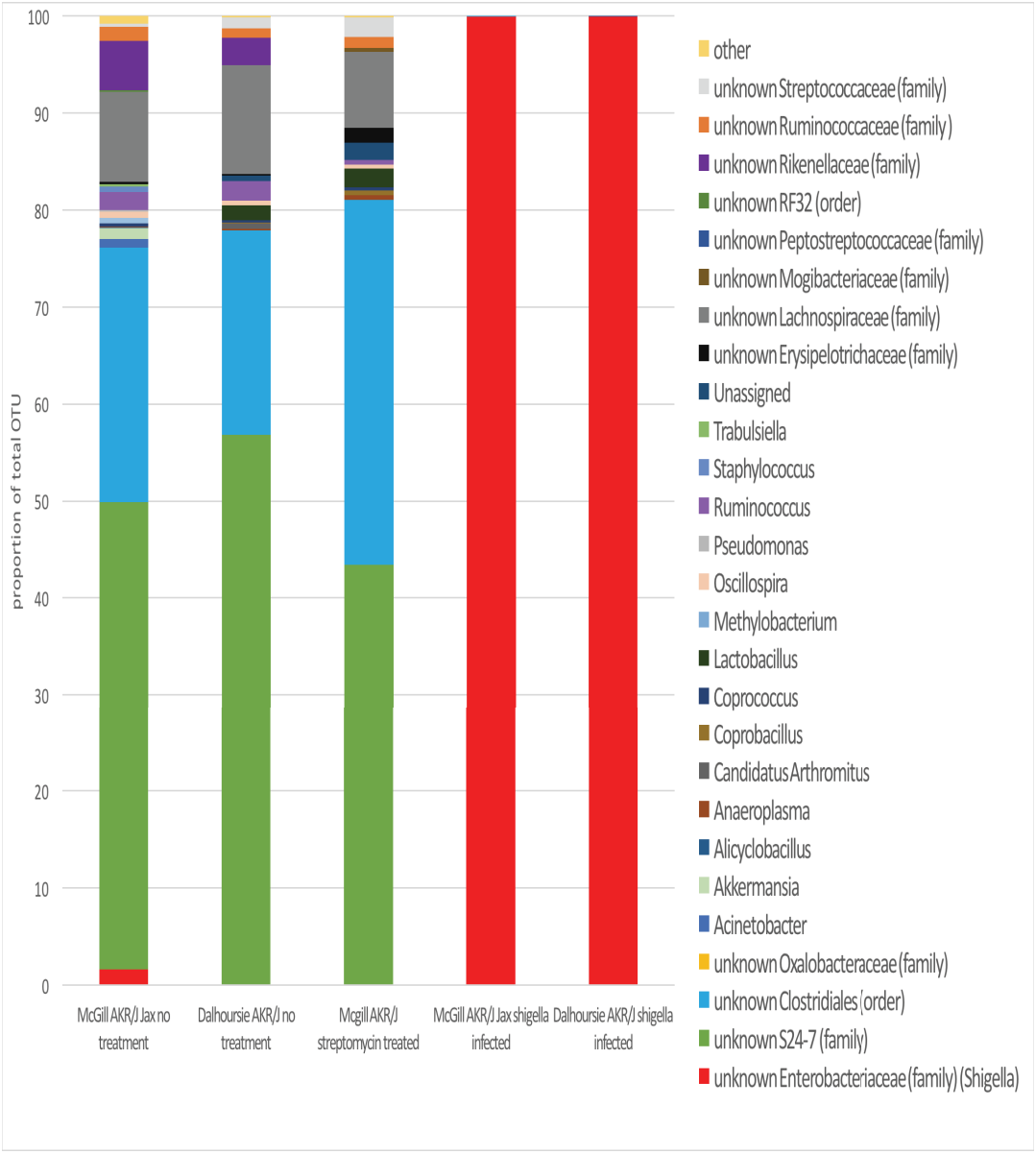
100
90
80
70
60
50
40
30
20
10
0
proportion of total OTU
McGill AKR/J Jax no treatment
Dalhoursie AKR/J no treatment
Mcgill AKR/J streptomycin treated
McGill AKR/J Jax shigella infected
Dalhoursie AKR/J shigella infected
other
unknown Streptococcaceae (family)
unknown Ruminococcaceae (family)
unknown Rikenellaceae (family)
unknown RF32 (order)
unknown Peptostreptococcaceae (family)
unknown Mogibacteriaceae (family)
unknown Lachnospiraceae (family)
unknown Erysipelotrichaceae (family)
Unassigned
Trabulsiella
Staphylococcus
Ruminococcus
Pseudomonas
Oscillospira
Methylobacterium
Lactobacillus
Coprococcus
Coprobacillus
Candidatus Arthromitus
Anaeroplasma
Alicyclobacillus
Akkermansia
Acinetobacter
unknown Oxalobacteraceae (family)
unknown Clostridiales (order)
unknown S24-7 (family)
unknown Enterobacteriaceae (family) (Shigella)

Figure 13 **:** 16S profiles of BALB/c mice at different time points in the streptomycin model pf shigellosis Stacked bar graph showing proportions of total operational taxonomic unit (OTU) reads detected by 16S rRNA sequencing from fecal samples collected from BALB/c mice over the course of streptomycin treatment and *Shigella* infection. BALB/c mice were ordered from Jackson Laboratories and housed in the Dalhousie animal facility 1 week prior to infection. Fecal samples were collected before treatment, post streptomycin treatment, and following *Shigella* infection. Each group represents the combination of fecal pellets from a cage of 5 mice. The Illumina MiSeq was used to obtain an output of approximately 12422 reads.

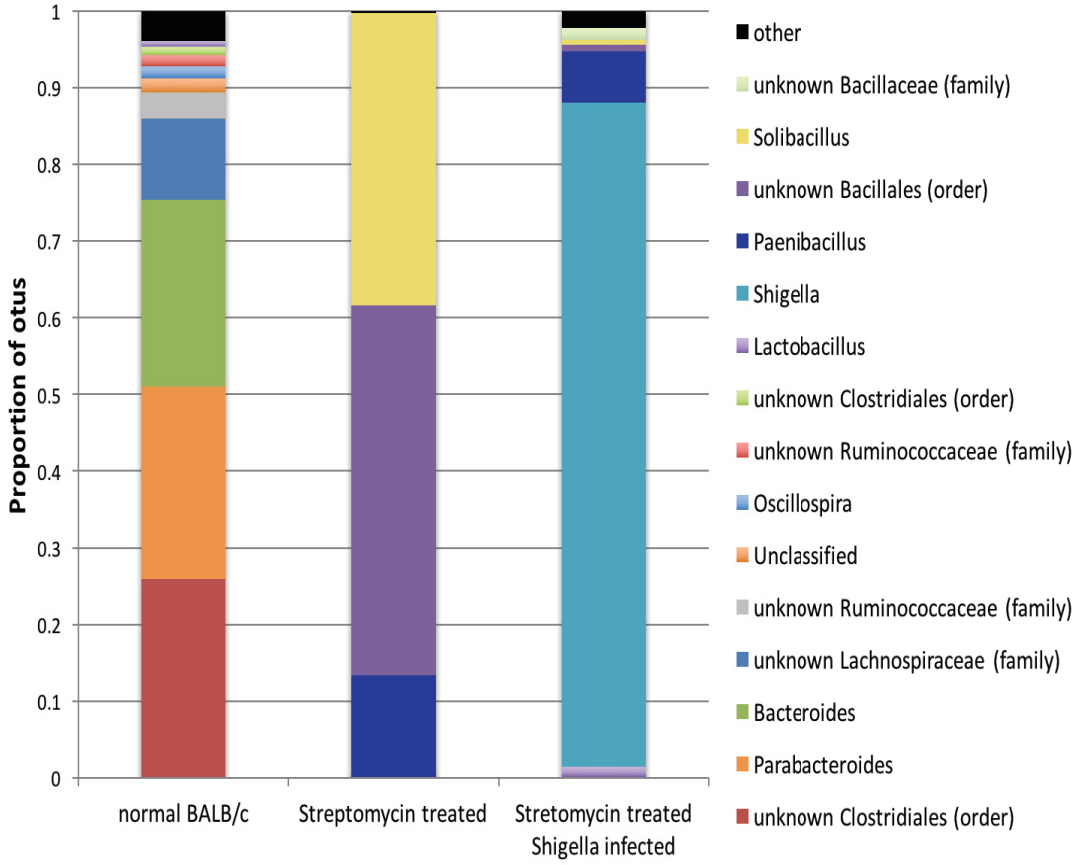
Proportion of otus
1
0.9
0.8
0.7
0.6
0.5
0.4
0.3
0.2
0.1
0
normal BALB/c
Streptomycin treated
Stretomycin treated Shigella infected
other
unknown Bacillaceae (family)
Solibacillus
unknown Bacillales (order)
Paenibacillus
Shigella
Lactobacillus
unknown Clostridiales (order)
unknown Ruminococcaceae (family)
Oscillospira
Unclassified
unknown Ruminococcaceae (family)
unknown Lachnospiraceae (family)
Bacteroides
Parabacteroides
unknown Clostridiales (order)

streptomycin, and then was reduced to around 8% once *Shigella* was introduced. These data suggest that the microbiome in each strain of mice are different and that they will be altered differently over the course of infection. In both cases, *Shigella* is the dominant genus after infection but it colonizes to a greater extent in the AKR/J mice compared to BALB/c mice. Although this suggests that the microbiome may not play a major role in the susceptibility to *Shigella* of the streptomycin mouse model, there are low abundance species that may influence the susceptibility in some form.

3.6 Investigation of complement as a host factor involved in the susceptibility to *Shigella* infection.

One well-characterized difference that the mouse strains more susceptible to *Shigella* infection had in common was a defect in the complement component. C5. A/J, AKR/J and FVB mice all are C5 deficient and C5aR-/- knock out mice lack the receptor for C5a. Host factors can influence susceptibility, so the role of complement during *Shigella* infection was further characterized by pretreating with Cobra venom factor (CVF) to deplete complement(Shapiro et al., 2002). CVF has been shown to hyper-activate complement in the mouse resulting in depletion (Shapiro et al., 2002).

Mice were given an intraperitoneal dose of 10 units of CVF one day prior to *Shigella* infection. Complement activation was monitored using a hemolysis activity assay, where at the end of the experiment serum from the mouse was mixed with sheep red blood cells. Complement factors present in the serum will lyse the sheep RBC causing the release of heme.. The release of heme can be read using a plate

reader. BALB/c mice were pretreated with CVF or vehicle then infected with WT *Shigella.* There was a 60% increase in mortality in mice pretreated with CVF compared to vehicle treated BALB/c mice infected with WT *Shigella* (Figure 14A). When the seras were tested for hemolytic activity, the CVF treated mice exhibited lower hemolysis capability (Figure 14B). These data indicate that the complement was depleted by the CVF, suggests that the complement system may play a protective role during *Shigella* infection. However additional experiments are needed to be done to confirm this finding.

Figure 14: Depletion of complement before *Shigella* infection leads to increased mortality. (A) Percent survival of BALB/c mice treated with or without an intraperitoneal injection of Cobra Venom Factor (CVF), Followed by oral infection with $1x10^8$ CFU of wild-type *Shigella flexneri*. (B) Relative hemolysis of Sheep red blood cells by mouse serum following CVF treatment.

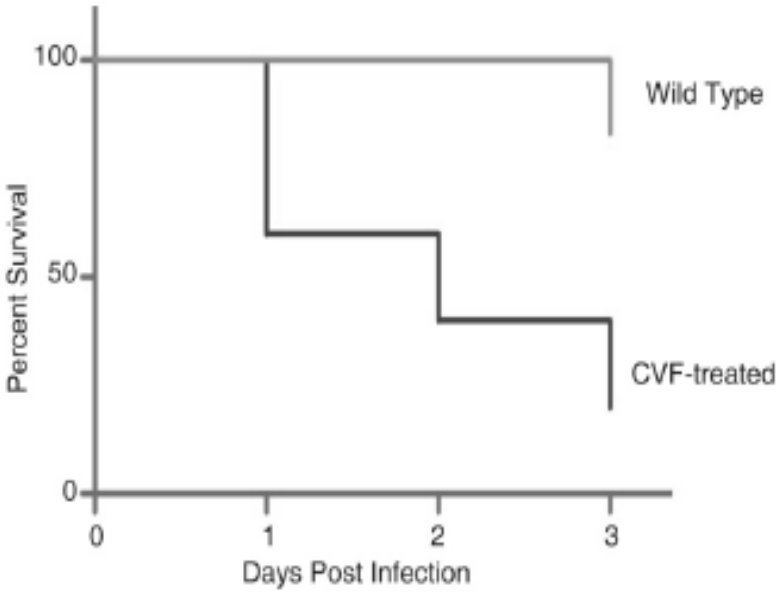
100
50
0
Percent Survival
Wild Type
CVF-treated
0
1
2
3
Days Post Infection

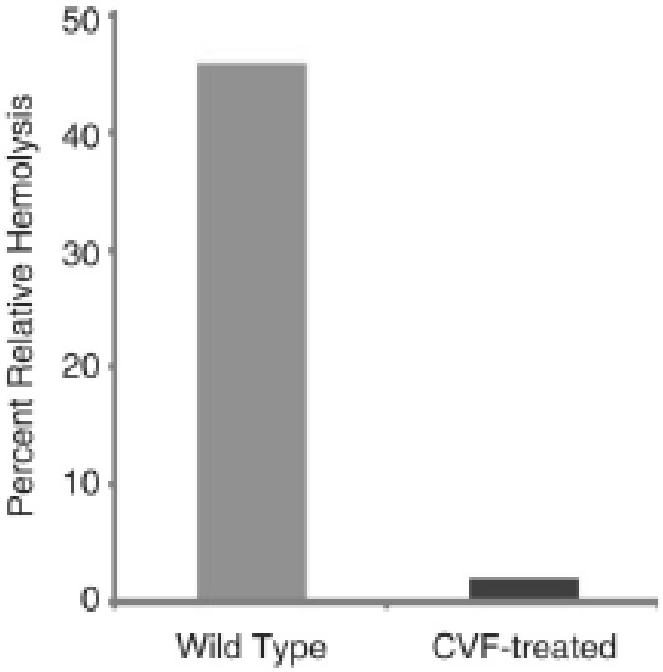
50
40
30
20
10
0
Percent Relative Hemolysis
Wild Type
CVF-treated

Chapter 4: Discussion

4.1 *Shigella* effectors influence susceptibility in the streptomycin mouse of shigellosis.

4.1.1 The Type three secretion system is important for pathogenicity in the streptomycin mouse model.

The invasive phenotype of *Shigella* requires expression of the T3SS that allows for translocation of effectors into host cells. The T3SS is required for localized changes in the epithelium leading to cell invasion and more systemic effects through massive increase in inflammation and recruitment of immune cells (Phalipon and Sansonetti, 2007). In the published streptomycin mouse model, the necessity for a functional T3SS was not tested (Martino et al., 2005). I infected BALB/c mice with Wild type and a T3SS mutant *Shigella* and found that without the T3SS there were no signs of clinical illness. Weight loss was similar to what was observed upon infection with the virulence plasmid-cured strain of *Shigella*. This is the first demonstration that a specific virulence determinant in the case of the T3SS, required for disease in humans is also required for disease in the streptomycin treated mouse model.

4.1.2 The role of OspG in infection

OspG is a protein kinase that interacts with ubiquitin- conjugated E2 enzymes in the Ubc family. OspG has been shown to prevent phospho-IκBα ubiquitination and its subsequent degradation by the proteasome (Kim et al., 2005). In a rabbit model of infection, *ospG* mutant *Shigella* elicit more severe damage in infected tissues. Taken together, these data had implicated OspG in regulating the immune response

during infection. What was not known was how OspG interacts with E2-ub directly reduces the inflammatory response. (Kim et al., 2005; Zhou et al., 2013).

Our collaborators, led by the laboratory of Dr. Peter Brzovick, solved the co-crystal structure of OspG bound to UbcH5c-Ub (Pruneda et al., 2014). The structure and their in vitro biochemical experiments suggested that OspG kinase activity is activated by the host ubiquitin conjugation machinery. They provided evidence that upon binding to the E2-Ub conjugate, OspG undergoes a conformational change that leads to a more open structure that increases kinase activity. At the same time this interaction causes the host E2-Ub conjugate to assume a less favorable conformation, reducing its ability to pass ubiquitin from the E2 to the E3 proteins. These biochemical studies provided molecular insight into microbial virulence factor regulation of the host response, and provided an example of how host factors regulate bacterial effector activity, and provided a mechanism for the functional increase in OspG kinase activity.

The role of OspG-E2-Ub binding in the context of infection was an open question. I infected streptomycin-treated BALB/c mice with an *ΔospG* strain and observed that there was more severe disease in these mice when compared to those infected with wild-type *Shigella*. In fact, infection with the *ΔospG* strain reliably resulted in 30% mortality (Figure 6), demonstrating the first example of a lethal infection of adult mice using an oral route of *Shigella* infection. These data were congruent with the previous studies in rabbits that demonstrated an increase in virulence when *ΔospG* was used to infect the ileal loop (Kim et al., 2005). When I complemented the *ΔospG* strain with wild-type *ospG*, the lethal infection phenotype

was abolished. When I complemented *ΔospG* strain with *ospG* variants that that could not bind to the host E2-Ub conjugate, the lethal infection phenotype was still observed, demonstrating that the OspG-host E2 interaction was required for the mortality phenotype. By contrast, an intermediate mortality phenotype was seen when the kinase-dead OspG was used to complement *ΔospG* (Pruneda et al., 2014).

The mortality was also accompanied by an increase in inflammation in the cecum and the colon of the mice. The most severely sick *ΔospG* infected mice that reached an experimental endpoint displayed cecums and colons that were discolored, gas filled, and void of fecal pellets. Notably, these gross pathologies were not accompanied by ulceration nor increased cellular infiltrate, increased bacterial burden in the feces, or any increase in dissemination of the bacteria into deeper tissues. At this time the mechanism for the increased mortality and change in gross morphology of the cecum and colon is not known and require further examination. Since the E2-Ub interaction is necessary it suggests that OspGs kinase activity may play a part in reducing the mortality, A target for OspG kinase activity would have to be identified before a mechanism could be determined. Taken together, my results demonstrate that the ubiquitin conjugation system in mammals is required for OspG function during infection. It is notable that my findings are consistent with those obtained in a rabbit model of infection (Kim et al., 2005).

After the publication of our paper, (Pruneda et al., 2014) another group published similar findings and concluded that the E2-ub interaction increased OspG kinase activity and decreased the capability of the E2 to transfer ubiquitin to the E3 (Grishin et al., 2014). They also demonstrated that OspG was degraded more quickly

by the proteasome when it was not bound to the E2-Ub conjugate (Grishin et al., 2014). This discovery, that the OspG^{mut} may be less stable in mammalian cells, likely explains why in stable cell lines I constructed, the variant that cannot interact with the E2-Ub conjugate was expressed to a lower level than WT OspG (figure 5). It also may explain why my *ΔospG^{mut}* infected mice behaved more similarly to *Δosp infectionG* than the *ΔospG^{CD}*, infection because the OspG^{mut} infection protein may have been degraded in the infected cells. My results suggest however, that the kinase target of OspG is involved in the mortality and that OspG is involved in suppressing the host immune response. These findings also demonstrate that the streptomycin mouse model can be used to investigate effector functions *in vivo*.

4.2 Potential kinase targets for OspG

To try to identify a kinase target for OspG a yeast two-hybrid screenwas performed. One potential concern was that no E2 enzymes were identified as targets for OspG, even though E2-ubiqutin conjugates in a yeast two-hybrid screen (Kim et al., 2005). However, it is likely that the kinase-dead variant used in my screen may adopt a different conformation that would result in different opportunities for protein-protein interactions. I was able to confirm biochemically, an interaction between OspG and one of my interactors, Rab11. Rab11 is a small GTPase that was chosen to investigate further, because Rab11 has previously been shown to be altered during *Shigella* infection (Mellouk et al., 2014). Rabs are enzymes that bind GTP and play an important role in vesicle transport. Rab11 is involved in coordinating endosomal recycling (Stenmark, 2009). Rab11 is recruited to the site of

Shigella entry of before *Shigella* escapes into the cytoplasm of the cell(Mellouk et al., 2014). Without Rab11, there is a decrease in vacuole rupture and *Shigella* escape. The *Shigella* protein IpgD was identified to be responsible for the recruitment of Rab11 (Mellouk et al., 2014).

Rab11 is also involved in receptor recycling to the cell surface. The *Shigella* effector IpaB causes Golgi fragmentation and reorganization of the recycling compartments, leading to reduced expression of cell surface receptors, causing the disruption of the epithelial cell barrier (Mounier et al., 2012). Since Rab11 had been shown to interact with multiple *Shigella* effectors and the disruption of Rab11 containing vesicles is important for multiple features of *Shigella* infection, it was an attractive target to investigate further. Using live cell imaging I investigated whether OspG was required for the recruitment of Rab11 to the site of bacterial entry during *Shigella* infection; however, I did not observe a defect in Rab11 recruitment in cells infected with the *ospG* mutant bacteria. OspG may play a role in Rab11 function during *Shigella* infection, however, my results indicate that if this is the case the effect is likely to be subtle.

It might be interesting to investigate if OspG is involved in reorganization of the recycling endosomes, since this is linked to disruption of the epithelial layer, an important feature of infection (Mounier et al., 2012). To investigate this, a fluorescent transferrin receptor could be examined as a marker for receptor recycling, using live cell imaging. This would determine whether there is an increase in receptor recycling in the ΔospG infected cells in comparison to wild type cells.

4.3 Mouse strains have variable susceptibility to *Shigella* infection

During my research, I have observed that the severity of disease caused by *Shigella* infection varies dependeing on the strain of mouse used. This variation ranges from high mortality in some strains to colonization without clinical symptoms in other strains. It has been shown using other pathogens that the genetic background of the mouse strain can affect disease severity (Vallance et al., 2003). *Citrobacter rodentium* is a mouse pathogen that displays similar disease to enteropathogenic *Escherichia coli* in humans. Since enteropathogenic *Escherichia coli* is unable to infect mice *Citrobacter rodentium* is often used as a surrogate model of infection. Upon infection with *Citrobacter rodentium,* the severity of disease can vary immensely in different mouse strains, ranging from a mild self-resolving form to a lethal infection (Vallance et al., 2003). This variation has been exploited to map genetic loci (Cri1) and even single genes (R-spondon 2) that result in disease susceptibility (Diez et al., 2011; Papapietro et al., 2013). To determine whether the Cri1 locus is involved in the susceptibility of mice to *Shigella,* congenic mice that possess an allele of a resistant or susceptible Cri locus were infected with *Shigella*. There was no significant change in mortality between the two strains, suggesting while this locus controls susceptibility to *Citrobacter* infection, it is not involved in *Shigella* infection. . The difference seen could be due to difference between the bacteria, *Shigella* is an intracellular pathogen while *Citrobacter* is an extracellular pathogen, because of this difference in niche how these pathogens interact with the environment and modulate the immune response is different. (Ashida et al., 2015; Bhinder et al., 2014). However,

because there is variation in disease severity for *Shigella* infection, a similar mapping method could be preformed to identify genes responsible for *Shigella* susceptibility

4.4 Potential role of the microbiome during *Shigella* infection

The AKR/J strain of mouse was found to have a large variance in susceptibility depending on the facility and origin of the mouse. An established breeding colony at McGill University was the original group to be infected with WT *Shigella,* all mice reached an experimental morbidity endpoint by day 3. This phenotype was not observed in new AKR/J mice that were ordered from Jackson labs, regardless of whether they were infected at Dalhousie or at McGill. This suggested that either there was a genetic mutation present in the breeding colony, or that environmental factors such as the microbiome could mediate the difference in susceptibility.

To investigate the potential role of differences in the microbiome, 16S profiling on DNA extracted from the fecal pellets of mice from each group was performed. These data showed that many of the genera were the same between the groups, although the proportions varied. However, there were some unique genera identified in each group and it is known that single species of bacteria can have important effects of susceptibility. In the case of *Vibrio cholera* a group was able to identify that colonization with *Ruminococcus obeum* that was able to restrict expression of quorm sensing by the pathogen (Hsiao et al., 2014). This shows that low abundance species cannot be discounted.

4.5 Host factors that might be involved in susceptibility

There was a large variation in disease severity observed between different mouse strains infected with wild-type *Shigella,* suggesting that host genetics could also play a role in *Shigella* susceptibility. One thing that the more susceptible strains of mice had in common was a defect in complement component 5 (C5). A/J, AKR/J and FVB mice all have a mutation in the Hc gene causing a deficiency in C5 (Ooi and Colten, 1979). To directly test the role of the complement system in *Shigella* infection, I depleted complement through hyperactivation, from *Shigella*-resistant BALB/c mice using CVF *(Shapiro et al., 2002)*. In mice pretreated with CVF, increased mortality was observed. C5 is an important protein in the complement pathway that is cleaved into C5a and C5b, a potent anaphylatoxin and the first component of the membrane attack complex, respectively (Carroll, 2004).

The complement system involves more than 30 components found soluble in the blood and on cells, and is activated through a cascade of proteolytic cleavage steps that stem from three separate activation pathways. These are: the classical pathway which is activated by antigen-antibody binding, the lectin pathway that recognizes the bacterial carbohydrate mannose; and the alternative pathway, which is activated upon recognition of microbial surface markers by low level of spontaneous activation of C3 (Carroll, 2004). The complement system represents an important component of the innate immune system and has a role in regulating the adaptive immune response by enhancing B cell immunity via complement receptor CD21 and CD35 found on B cells as well as follicular dendritic cells (Carroll, 2004).

Complement has been shown to play a role in the control and killing of several bacterial species that infect the respiratory tract, such as *Pseudomonas aeruginosa* (Younger et al., 2003), and *Mycobacterium tuberculosis* (Daniel et al., 2006). The role of complement in gut health is not well understood; however, it has been shown that receptors of complement are present on colonic epithelial cells grown in tissue culture (Cao et al., 2012), suggesting that complement could be important in the immunity of the gut. Complement has also been shown to play an important role in boosting the innate immune system by enhancing the response to intracellular pathogens (Tam et al., 2014). My findings strongly suggest that the complement system is important in controlling *Shigella* infection. However, the pleiotropic nature of the complement system makes the identification of any single molecule during *Shigella* infection a challenging problem. By using reagents and knock out mice that exclude certain pathways may allow the role of complement during *Shigella* infection to become more well defined.

4.6 Multiple factors influence *Shigella s*usceptibility

In this thesis, I have shown that different *Shigella* mutants alter the severity of disease in the streptomycin mouse model. Other students in our lab have also observed differences in disease severity with other effector knock out strains of *Shigella*, such as IpaH 9.8. I have also shown that there is a difference in susceptibility dependent of the strain of mouse infected, and even within the same strain there are host and environmental factors that can affect susceptibility.

Although a specific cause underlying differences in susceptibility was not identified, I was able to demonstrate that host factors, bacteria effectors and colony differences play a role in regulating susceptibility to *Shigella* infection. In order to fully understand *Shigella*-host interactions we must consider host factors, bacterial factors, environmental factors, and the microbiome since all influence shigellosis. I was successful in expanding our knowledge of the streptomycin mouse model, and though I did not isolate a single host factor responsible for the differences between these strains I have opened up new areas to research for future students in the Rohde lab. Based on my data, I propose a two-part model of infection where streptomycin is essential to overcome colonization resistance before disease can progress. The severity of disease varies and is impacted by both host and bacterial factors (Figure 16).

Figure 15. Model for *Shigella* infection and variation in disease severity. Mice must be pretreated with streptomycin before colonization by *Shigella* can be successful. Once the colonization resistance is overcome, there is a range in disease severity from colonization with no clinical illness to severe clinical illness with mortality. The range in disease severity is affected by bacterial factors, host factors and the probably the microbiome

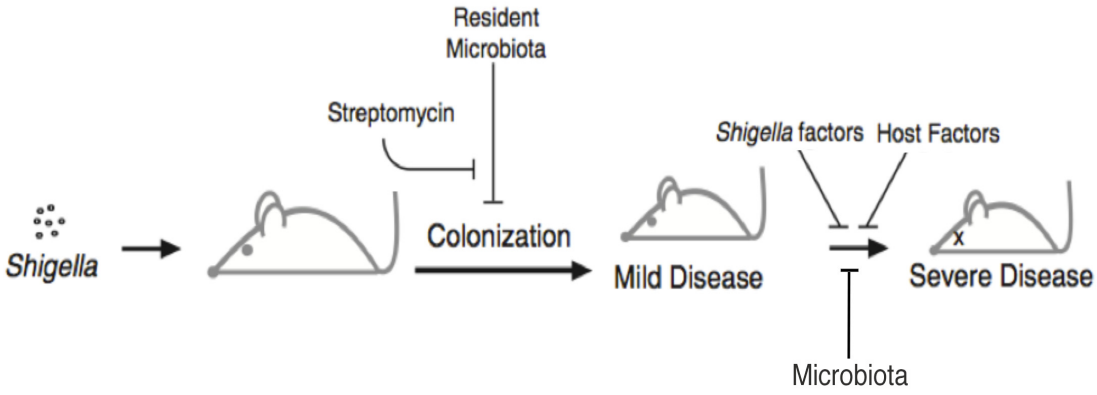
Resident
Microbiota
Streptomycin
Shigella factors
Host Factors
Shigella
Colonization
Mild Disease
x
Severe Disease
Microbiota

References

Allaoui, A., Sansonetti, P.J., and Parsot, C. (1993). MxiD, an outer membrane protein necessary for the secretion of the Shigella flexneri lpa invasins. Mol Microbiol *7*, 59-68.

Anderson, D.M., Schmalzer, K.M., Sato, H., Casey, M., Terhune, S.S., Haas, A.L., Feix, J.B., and Frank, D.W. (2011). Ubiquitin and ubiquitin-modified proteins activate the Pseudomonas aeruginosa T3SS cytotoxin, ExoU. Mol Microbiol *82*, 1454-1467.

Ashida, H., Kim, M., and Sasakawa, C. (2014). Manipulation of the host cell death pathway by Shigella. Cell Microbiol *16*, 1757-1766.

Ashida, H., Mimuro, H., and Sasakawa, C. (2015). Shigella manipulates host immune responses by delivering effector proteins with specific roles. Front Immunol *6*, 219.

Ashida, H., Nakano, H., and Sasakawa, C. (2013). Shigella IpaH0722 E3 ubiquitin ligase effector targets TRAF2 to inhibit PKC-NF-kappaB activity in invaded epithelial cells. PLoS Pathog *9*, e1003409.

Ashida, H., Toyotome, T., Nagai, T., and Sasakawa, C. (2007). Shigella chromosomal IpaH proteins are secreted via the type III secretion system and act as effectors. Mol Microbiol *63*, 680-693.

Barthel, M., Hapfelmeier, S., Quintanilla-Martinez, L., Kremer, M., Rohde, M., Hogardt, M., Pfeffer, K., Russmann, H., and Hardt, W.D. (2003). Pretreatment of mice with streptomycin provides a Salmonella enterica serovar Typhimurium colitis model that allows analysis of both pathogen and host. Infect Immun *71*, 2839-2858.

Bernardini, M.L., Mounier, J., d'Hauteville, H., Coquis-Rondon, M., and Sansonetti, P.J. (1989). Identification of icsA, a plasmid locus of Shigella flexneri that governs bacterial intra- and intercellular spread through interaction with F-actin. Proc Natl Acad Sci U S A *86*, 3867-3871.

Bhinder, G., Stahl, M., Sham, H.P., Crowley, S.M., Morampudi, V., Dalwadi, U., Ma, C., Jacobson, K., and Vallance, B.A. (2014). Intestinal epithelium-specific MyD88 signaling impacts host susceptibility to infectious colitis by promoting protective goblet cell and antimicrobial responses. Infect Immun *82*, 3753-3763.

Blocker, A., Jouihri, N., Larquet, E., Gounon, P., Ebel, F., Parsot, C., Sansonetti, P., and Allaoui, A. (2001). Structure and composition of the Shigella flexneri "needle complex", a part of its type III secreton. Mol Microbiol *39*, 652-663.

Bradbury, P., Bach, C.T., Paul, A., and O'Neill, G.M. (2014). Src Kinase Determines the Dynamic Exchange of the Docking Protein NEDD9 (Neural Precursor Cell Expressed Developmentally Down-regulated Gene 9) at Focal Adhesions. Journal of Biological Chemistry *289*, 24792-24800.

Buchrieser, C., Glaser, P., Rusniok, C., Nedjari, H., D'Hauteville, H., Kunst, F., Sansonetti, P., and Parsot, C. (2000). The virulence plasmid pWR100 and the repertoire of proteins secreted by the type III secretion apparatus of Shigella flexneri. Mol Microbiol *38*, 760-771.

Cao, Q., McIsaac, S.M., and Stadnyk, A.W. (2012). Human colonic epithelial cells detect and respond to C5a via apically expressed C5aR through the ERK pathway. Am J Physiol Cell Physiol *302*, C1731-1740.

Carroll, M.C. (2004). The complement system in regulation of adaptive immunity. Nat Immunol *5*, 981-986.

Cersini, A., Martino, M.C., Martini, I., Rossi, G., and Bernardini, M.L. (2003). Analysis of virulence and inflammatory potential of Shigella flexneri purine biosynthesis mutants. Infect Immun *71*, 7002-7013.

Chen, Z.J. (2012). Ubiquitination in signaling to and activation of IKK. Immunol Rev *246*, 95-106.

Costabile, M. (2010). Measuring the 50% haemolytic complement (CH50) activity of serum. J Vis Exp.

Daniel, D.S., Dai, G., Singh, C.R., Lindsey, D.R., Smith, A.K., Dhandayuthapani, S., Hunter, R.L., Jr., and Jagannath, C. (2006). The reduced bactericidal function of complement C5-deficient murine macrophages is associated with defects in the synthesis and delivery of reactive oxygen radicals to mycobacterial phagosomes. J Immunol *177*, 4688-4698.

Demers, B., Sansonetti, P.J., and Parsot, C. (1998). Induction of type III secretion in Shigella flexneri is associated with differential control of transcription of genes encoding secreted proteins. EMBO J *17*, 2894-2903.

Diez, E., Zhu, L., Teatero, S.A., Paquet, M., Roy, M.F., Loredo-Osti, J.C., Malo, D., and Gruenheid, S. (2011). Identification and characterization of Cri1, a locus controlling mortality during Citrobacter rodentium infection in mice. Genes Immun *12*, 280-290.

Etheridge, M.E., Hoque, A.T., and Sack, D.A. (1996). Pathologic study of a rabbit model for shigellosis. Lab Anim Sci *46*, 61-66.

Fernandez, M.I., Regnault, B., Mulet, C., Tanguy, M., Jay, P., Sansonetti, P.J., and Pedron, T. (2008). Maturation of paneth cells induces the refractory state of newborn mice to Shigella infection. J Immunol *180*, 4924-4930.

Feuerbacher, L.A., and Hardwidge, P.R. (2014). Influence of NleH effector expression, host genetics, and inflammation on Citrobacter rodentium colonization of mice. Microbes Infect *16*, 429-433.

Fontaine, A., Arondel, J., and Sansonetti, P.J. (1988). Role of Shiga toxin in the pathogenesis of bacillary dysentery, studied by using a Tox- mutant of Shigella dysenteriae 1. Infect Immun *56*, 3099-3109.

Formal, S.B., Oaks, E.V., Olsen, R.E., Wingfieldeggleston, M., Snoy, P.J., and Cogan, J.P. (1991). Effect of Prior Infection with Virulent Shigella-Flexneri 2a on the Resistance of Monkeys to Subsequent Infection with Shigella-Sonnei. Journal of Infectious Diseases *164*, 533-537.

Gates-Foundation (2014). What We Do Enteric and Diarrheal Disease Stratey Overview (http://www.gatesfoundation.org/What-We-Do/Global-Health/Enteric-and-Diarrheal-Diseases - bodyregion_0_interiorarticle_0_strategysections_2_strategysubsectionsbcc3b6c670134a2994f387c1b627c00d_0_lnkHeader: Bill & Melinda Gates Foundation).

Girardin, S.E., Boneca, I.G., Carneiro, L.A., Antignac, A., Jehanno, M., Viala, J., Tedin, K., Taha, M.K., Labigne, A., Zahringer, U.*, et al.* (2003). Nod1 detects a unique muropeptide from gram-negative bacterial peptidoglycan. Science *300*, 1584-1587.

Grishin, A.M., Condos, T.E., Barber, K.R., Campbell-Valois, F.X., Parsot, C., Shaw, G.S., and Cygler, M. (2014). Structural basis for the inhibition of host protein ubiquitination by Shigella effector kinase OspG. Structure *22*, 878-888.

Haraga, A., and Miller, S.I. (2006). A Salmonella type III secretion effector interacts with the mammalian serine/threonine protein kinase PKN1. Cell Microbiol *8*, 837-846.

Hershko, A. (1988). Ubiquitin-mediated protein degradation. J Biol Chem *263*, 15237-15240.

Hershko, A., and Ciechanover, A. (1998). The ubiquitin system. Annu Rev Biochem *67*, 425-479.

Hicke, L., and Dunn, R. (2003). Regulation of membrane protein transport by ubiquitin and ubiquitin-binding proteins. Annu Rev Cell Dev Bi *19*, 141-172.

High, N., Mounier, J., Prevost, M.C., and Sansonetti, P.J. (1992). IpaB of Shigella flexneri causes entry into epithelial cells and escape from the phagocytic vacuole. EMBO J *11*, 1991-1999.

Hsiao, A., Ahmed, A.M., Subramanian, S., Griffin, N.W., Drewry, L.L., Petri, W.A., Jr., Haque, R., Ahmed, T., and Gordon, J.I. (2014). Members of the human gut microbiota involved in recovery from Vibrio cholerae infection. Nature *515*, 423-426.

Huang, L., Kinnucan, E., Wang, G., Beaudenon, S., Howley, P.M., Huibregtse, J.M., and Pavletich, N.P. (1999). Structure of an E6AP-UbcH7 complex: insights into ubiquitination by the E2-E3 enzyme cascade. Science *286*, 1321-1326.

Hueck, C.J. (1998). Type III protein secretion systems in bacterial pathogens of animals and plants. Microbiol Mol Biol Rev *62*, 379-433.

Huibregtse, J., and Rohde, J.R. (2014). Hell's BELs: bacterial E3 ligases that exploit the eukaryotic ubiquitin machinery. PLoS Pathog *10*, e1004255.

Jain, U., Cao, Q., Thomas, N.A., Woodruff, T.M., Schwaeble, W.J., Stover, C.M., and Stadnyk, A.W. (2015). Properdin provides protection from Citrobacter rodentium-induced intestinal inflammation in a C5a/IL-6-dependent manner. J Immunol *194*, 3414-3421.

Jehl, S.P., Doling, A.M., Giddings, K.S., Phalipon, A., Sansonetti, P.J., Goldberg, M.B., and Starnbach, M.N. (2011). Antigen-specific CD8(+) T cells fail to respond to Shigella flexneri. Infect Immun *79*, 2021-2030.

Juris, S.J., Rudolph, A.E., Huddler, D., Orth, K., and Dixon, J.E. (2000). A distinctive role for the Yersinia protein kinase: actin binding, kinase activation, and cytoskeleton disruption. Proc Natl Acad Sci U S A *97*, 9431-9436.

Kayagaki, N., Warming, S., Lamkanfi, M., Vande Walle, L., Louie, S., Dong, J., Newton, K., Qu, Y., Liu, J., Heldens, S.*, et al.* (2011). Non-canonical inflammasome activation targets caspase-11. Nature *479*, 117-121.

Kayagaki, N., Wong, M.T., Stowe, I.B., Ramani, S.R., Gonzalez, L.C., Akashi-Takamura, S., Miyake, K., Zhang, J., Lee, W.P., Muszynski, A.*, et al.* (2013). Noncanonical inflammasome activation by intracellular LPS independent of TLR4. Science *341*, 1246-1249.

Kim, D.W., Lenzen, G., Page, A.L., Legrain, P., Sansonetti, P.J., and Parsot, C. (2005). The Shigella flexneri effector OspG interferes with innate immune responses by targeting ubiquitin-conjugating enzymes. Proc Natl Acad Sci U S A *102*, 14046-14051.

Konradt, C., Frigimelica, E., Nothelfer, K., Puhar, A., Salgado-Pabon, W., di Bartolo, V., Scott-Algara, D., Rodrigues, C.D., Sansonetti, P.J., and Phalipon, A. (2011). The Shigella flexneri type three secretion system effector IpgD inhibits T cell migration by manipulating host phosphoinositide metabolism. Cell Host Microbe *9*, 263-272.

Kotloff, K.L., Winickoff, J.P., Ivanoff, B., Clemens, J.D., Swerdlow, D.L., Sansonetti, P.J., Adak, G.K., and Levine, M.M. (1999). Global burden of Shigella infections: implications for vaccine development and implementation of control strategies. Bull World Health Organ *77*, 651-666.

Lawley, T.D., and Walker, A.W. (2013). Intestinal colonization resistance. Immunology *138*, 1-11.

Le-Barillec, K., Magalhaes, J.G., Corcuff, E., Thuizat, A., Sansonetti, P.J., Phalipon, A., and Di Santo, J.P. (2005). Roles for T and NK cells in the innate immune response to Shigella flexneri. J Immunol *175*, 1735-1740.

Levine, M.M. (2011). "IDEAL" vaccines for resource poor settings. Vaccine *29 Suppl 4*, D116-125.

Levine, M.M., Kotloff, K.L., Barry, E.M., Pasetti, M.F., and Sztein, M.B. (2007). Clinical trials of Shigella vaccines: two steps forward and one step back on a long, hard road. Nat Rev Microbiol *5*, 540-553.

Lima, C.D. (2007). Protein modification by SUMO, a small ubiquitin-like modifier. Faseb J *21*, A207-A207.

Lindberg, A.A., Karnell, A., and Weintraub, A. (1991). The lipopolysaccharide of Shigella bacteria as a virulence factor. Rev Infect Dis *13 Suppl 4*, S279-284.

Marlovits, T.C., and Stebbins, C.E. (2010). Type III secretion systems shape up as they ship out. Curr Opin Microbiol *13*, 47-52.

Marteyn, B., Gazi, A., and Sansonetti, P. (2012). Shigella: a model of virulence regulation in vivo. Gut Microbes *3*, 104-120.

Martino, M.C., Rossi, G., Martini, I., Tattoli, I., Chiavolini, D., Phalipon, A., Sansonetti, P.J., and Bernardini, M.L. (2005). Mucosal lymphoid infiltrate dominates colonic pathological changes in murine experimental shigellosis. J Infect Dis *192*, 136-148.

Martz, S.L., McDonald, J.A., Sun, J., Zhang, Y.G., Gloor, G.B., Noordhof, C., He, S.M., Gerbaba, T.K., Blennerhassett, M., Hurlbut, D.J.*, et al.* (2015). Administration of defined microbiota is protective in a murine Salmonella infection model. Sci Rep *5*, 16094.

Mavris, M., Page, A.L., Tournebize, R., Demers, B., Sansonetti, P., and Parsot, C. (2002). Regulation of transcription by the activity of the Shigella flexneri type III secretion apparatus. Molecular Microbiology *43*, 1543-1553.

Mellouk, N., Weiner, A., Aulner, N., Schmitt, C., Elbaum, M., Shorte, S.L., Danckaert, A., and Enninga, J. (2014). Shigella subverts the host recycling compartment to rupture its vacuole. Cell Host Microbe *16*, 517-530.

Menard, R., Sansonetti, P.J., and Parsot, C. (1993). Nonpolar mutagenesis of the ipa genes defines IpaB, IpaC, and IpaD as effectors of Shigella flexneri entry into epithelial cells. J Bacteriol *175*, 5899-5906.

Mounier, J., Boncompain, G., Senerovic, L., Lagache, T., Chretien, F., Perez, F., Kolbe, M., Olivo-Marin, J.C., Sansonetti, P.J., and Sauvonnet, N. (2012). Shigella effector IpaB-induced cholesterol relocation disrupts the Golgi complex and recycling network to inhibit host cell secretion. Cell Host Microbe *12*, 381-389.

Mounier, J., Vasselon, T., Hellio, R., Lesourd, M., and Sansonetti, P.J. (1992). Shigella flexneri enters human colonic Caco-2 epithelial cells through the basolateral pole. Infect Immun *60*, 237-248.

Nataro, J.P., Seriwatana, J., Fasano, A., Maneval, D.R., Guers, L.D., Noriega, F., Dubovsky, F., Levine, M.M., and Morris, J.G., Jr. (1995). Identification and cloning of a novel plasmid-encoded enterotoxin of enteroinvasive Escherichia coli and Shigella strains. Infect Immun *63*, 4721-4728.

Nothelfer, K., Arena, E.T., Pinaud, L., Neunlist, M., Mozeleski, B., Belotserkovsky, I., Parsot, C., Dinadayala, P., Burger-Kentischer, A., Raqib, R.*, et al.* (2014). B lymphocytes undergo TLR2-dependent apoptosis upon Shigella infection. J Exp Med *211*, 1215-1229.

Okuda, J., Toyotome, T., Kataoka, N., Ohno, M., Abe, H., Shimura, Y., Seyedarabi, A., Pickersgill, R., and Sasakawa, C. (2005). Shigella effector IpaH9.8 binds to a splicing factor U2AF(35) to modulate host immune responses. Biochem Biophys Res Commun *333*, 531-539.

Ooi, Y.M., and Colten, H.R. (1979). Genetic defect in secretion of complement C5 in mice. Nature *282*, 207-208.

Page, A.L., Ohayon, H., Sansonetti, P.J., and Parsot, C. (1999). The secreted IpaB and IpaC invasins and their cytoplasmic chaperone IpgC are required for intercellular dissemination of Shigella flexneri. Cellular Microbiology *1*, 183-193.

Papapietro, O., Teatero, S., Thanabalasuriar, A., Yuki, K.E., Diez, E., Zhu, L., Kang, E., Dhillon, S., Muise, A.M., Durocher, Y.*, et al.* (2013). R-spondin 2 signalling mediates susceptibility to fatal infectious diarrhoea. Nat Commun *4*, 1898.

Parsot, C., Menard, R., Gounon, P., and Sansonetti, P.J. (1995). Enhanced secretion through the Shigella flexneri Mxi-Spa translocon leads to assembly of extracellular proteins into macromolecular structures. Mol Microbiol *16*, 291-300.

Perdomo, J.J., Gounon, P., and Sansonetti, P.J. (1994a). Polymorphonuclear leukocyte transmigration promotes invasion of colonic epithelial monolayer by Shigella flexneri. J Clin Invest *93*, 633-643.

Perdomo, O.J., Cavaillon, J.M., Huerre, M., Ohayon, H., Gounon, P., and Sansonetti, P.J. (1994b). Acute inflammation causes epithelial invasion and mucosal destruction in experimental shigellosis. J Exp Med *180*, 1307-1319.

Petroski, M.D., and Deshaies, R.J. (2005). Mechanism of lysine 48-linked ubiquitin-chain synthesis by the cullin-RING ubiquitin-ligase complex SCF-Cdc34. Cell *123*, 1107-1120.

Phalipon, A., Kaufmann, M., Michetti, P., Cavaillon, J.M., Huerre, M., Sansonetti, P., and Kraehenbuhl, J.P. (1995). Monoclonal immunoglobulin A antibody directed against serotype-specific epitope of Shigella flexneri lipopolysaccharide protects against murine experimental shigellosis. J Exp Med *182*, 769-778.

Phalipon, A., and Sansonetti, P.J. (2007). Shigella's ways of manipulating the host intestinal innate and adaptive immune system: a tool box for survival? Immunol Cell Biol *85*, 119-129.

Pires, S.M., Fischer-Walker, C.L., Lanata, C.F., Devleesschauwer, B., Hall, A.J., Kirk, M.D., Duarte, A.S., Black, R.E., and Angulo, F.J. (2015). Aetiology-Specific Estimates of the Global and Regional Incidence and Mortality of Diarrhoeal Diseases Commonly Transmitted through Food. PLoS One *10*, e0142927.

Pruneda, J.N., Smith, F.D., Daurie, A., Swaney, D.L., Villen, J., Scott, J.D., Stadnyk, A.W., Le Trong, I., Stenkamp, R.E., Klevit, R.E*., et al.* (2014). E2~Ub conjugates regulate the kinase activity of Shigella effector OspG during pathogenesis. EMBO J *33*, 437-449.

Puhar, A., Tronchere, H., Payrastre, B., Nhieu, G.T., and Sansonetti, P.J. (2013). A Shigella effector dampens inflammation by regulating epithelial release of danger signal ATP through production of the lipid mediator PtdIns5P. Immunity *39*, 1121-1131.

Quandt, J., and Hynes, M.F. (1993). Versatile suicide vectors which allow direct selection for gene replacement in gram-negative bacteria. Gene *127*, 15-21.

Quezada, C.M., Hicks, S.W., Galan, J.E., and Stebbins, C.E. (2009). A family of Salmonella virulence factors functions as a distinct class of autoregulated E3 ubiquitin ligases. Proc Natl Acad Sci U S A *106*, 4864-4869.

Rohde, J.R., Breitkreutz, A., Chenal, A., Sansonetti, P.J., and Parsot, C. (2007). Type III secretion effectors of the IpaH family are E3 ubiquitin ligases. Cell Host Microbe *1*, 77-83.

Royan, S.V., Jones, R.M., Koutsouris, A., Roxas, J.L., Falzari, K., Weflen, A.W., Kim, A., Bellmeyer, A., Turner, J.R., Neish, A.S.*, et al.* (2010). Enteropathogenic E. coli non-LEE encoded effectors NleH1 and NleH2 attenuate NF-kappaB activation. Mol Microbiol *78*, 1232-1245.

Salgado-Pabon, W., Celli, S., Arena, E.T., Nothelfer, K., Roux, P., Sellge, G., Frigimelica, E., Bousso, P., Sansonetti, P.J., and Phalipon, A. (2013). Shigella impairs T lymphocyte dynamics in vivo. Proc Natl Acad Sci U S A *110*, 4458-4463.

Sanada, T., Kim, M., Mimuro, H., Suzuki, M., Ogawa, M., Oyama, A., Ashida, H., Kobayashi, T., Koyama, T., Nagai, S.*, et al.* (2012). The Shigella flexneri effector OspI deamidates UBC13 to dampen the inflammatory response. Nature *483*, 623-626.

Sansonetti, P.J. (2001). Microbes and microbial toxins: paradigms for microbial-mucosal interactions III. Shigellosis: from symptoms to molecular pathogenesis. Am J Physiol Gastrointest Liver Physiol *280*, G319-323.

Sansonetti, P.J. (2004). War and peace at mucosal surfaces. Nat Rev Immunol *4*, 953-964.

Sansonetti, P.J. (2006). Shigellosis: an old disease in new clothes? PLoS Med *3*, e354.

Sansonetti, P.J., Kopecko, D.J., and Formal, S.B. (1982). Involvement of a plasmid in the invasive ability of Shigella flexneri. Infect Immun *35*, 852-860.

Sansonetti, P.J., and Phalipon, A. (1999). M cells as ports of entry for enteroinvasive pathogens: mechanisms of interaction, consequences for the disease process. Semin Immunol *11*, 193-203.

Schuch, R., and Maurelli, A.T. (2001). MxiM and MxiJ, base elements of the Mxi-Spa type III secretion system of Shigella, interact with and stabilize the MxiD secretin in the cell envelope. J Bacteriol *183*, 6991-6998.

Sellge, G., Magalhaes, J.G., Konradt, C., Fritz, J.H., Salgado-Pabon, W., Eberl, G., Bandeira, A., Di Santo, J.P., Sansonetti, P.J., and Phalipon, A. (2010). Th17 cells are the dominant T cell subtype primed by Shigella flexneri mediating protective immunity. J Immunol *184*, 2076-2085.

Senerovic, L., Tsunoda, S.P., Goosmann, C., Brinkmann, V., Zychlinsky, A., Meissner, F., and Kolbe, M. (2012). Spontaneous formation of IpaB ion channels in host cell membranes reveals how Shigella induces pyroptosis in macrophages. Cell Death Dis *3*, e384.

Seydel, K.B., Li, E., Swanson, P.E., and Stanley, S.L., Jr. (1997). Human intestinal epithelial cells produce proinflammatory cytokines in response to infection in a SCID mouse-human intestinal xenograft model of amebiasis. Infect Immun *65*, 1631-1639.

Shapiro, S., Beenhouwer, D.O., Feldmesser, M., Taborda, C., Carroll, M.C., Casadevall, A., and Scharff, M.D. (2002). Immunoglobulin G monoclonal antibodies to Cryptococcus neoformans protect mice deficient in complement component C3. Infect Immun *70*, 2598-2604.

Shim, D.H., Suzuki, T., Chang, S.Y., Park, S.M., Sansonetti, P.J., Sasakawa, C., and Kweon, M.N. (2007). New animal model of shigellosis in the Guinea pig: its usefulness for protective efficacy studies. J Immunol *178*, 2476-2482.

Sidik, S., Kottwitz, H., Benjamin, J., Ryu, J., Jarrar, A., Garduno, R., and Rohde, J.R. (2014). A Shigella flexneri virulence plasmid encoded factor controls production of outer membrane vesicles. G3 (Bethesda) *4*, 2493-2503.

Singer, A.U., Rohde, J.R., Lam, R., Skarina, T., Kagan, O., Dileo, R., Chirgadze, N.Y., Cuff, M.E., Joachimiak, A., Tyers, M.*, et al.* (2008). Structure of the Shigella T3SS effector IpaH defines a new class of E3 ubiquitin ligases. Nat Struct Mol Biol *15*, 1293-1301.

Stenmark, H. (2009). Rab GTPases as coordinators of vesicle traffic. Nat Rev Mol Cell Biol *10*, 513-525.

Stillie, R., and Stadnyk, A.W. (2009). Role of TNF receptors, TNFR1 and TNFR2, in dextran sodium sulfate-induced colitis. Inflamm Bowel Dis *15*, 1515-1525.

Su, H., Joho, S., Huang, Y., Barcena, A., Arakawa-Hoyt, J., Grossman, W., and Kan, Y.W. (2004). Adeno-associated viral vector delivers cardiac-specific and hypoxia-inducible VEGF expression in ischemic mouse hearts. Proc Natl Acad Sci U S A *101*, 16280-16285.

Suzuki, S., Mimuro, H., Kim, M., Ogawa, M., Ashida, H., Toyotome, T., Franchi, L., Suzuki, M., Sanada, T., Suzuki, T.*, et al.* (2014). Shigella IpaH7.8 E3 ubiquitin ligase targets glomulin and activates inflammasomes to demolish macrophages. Proc Natl Acad Sci U S A *111*, E4254-4263.

Suzuki, T., Franchi, L., Toma, C., Ashida, H., Ogawa, M., Yoshikawa, Y., Mimuro, H., Inohara, N., Sasakawa, C., and Nunez, G. (2007). Differential regulation of caspase-1 activation, pyroptosis, and autophagy via Ipaf and ASC in Shigella-infected macrophages. PLoS Pathog *3*, e111.

Tam, J.C., Bidgood, S.R., McEwan, W.A., and James, L.C. (2014). Intracellular sensing of complement C3 activates cell autonomous immunity. Science *345*, 1256070.

Vallance, B.A., Deng, W., Jacobson, K., and Finlay, B.B. (2003). Host susceptibility to the attaching and effacing bacterial pathogen Citrobacter rodentium. Infect Immun *71*, 3443-3453.

von Seidlein, L., Kim, D.R., Ali, M., Lee, H., Wang, X., Thiem, V.D., Canh do, G., Chaicumpa, W., Agtini, M.D., Hossain, A.*, et al.* (2006). A multicentre study of Shigella diarrhoea in six Asian countries: disease burden, clinical manifestations, and microbiology. PLoS Med *3*, e353.

Wang, F., Jiang, Z., Li, Y., He, X., Zhao, J., Yang, X., Zhu, L., Yin, Z., Li, X., Wang, X.*, et al.* (2013). Shigella flexneri T3SS effector IpaH4.5 modulates the host inflammatory response via interaction with NF-kappaB p65 protein. Cell Microbiol *15*, 474-485.

Wassef, J.S., Keren, D.F., and Mailloux, J.L. (1989). Role of M cells in initial antigen uptake and in ulcer formation in the rabbit intestinal loop model of shigellosis. Infect Immun *57*, 858-863.

WHO (2005). Guidelines for the control of shigellosis, including epidemics due to Shigella dysenteriae I, D.N.F. Pierce, ed. (
Geneva, Switzerland: World Health Organization Press), pp. 1-64.

Xu, P., Duong, D.M., Seyfried, N.T., Cheng, D., Xie, Y., Robert, J., Rush, J., Hochstrasser, M., Finley, D., and Peng, J. (2009). Quantitative proteomics reveals the function of unconventional ubiquitin chains in proteasomal degradation. Cell *137*, 133-145.

Younger, J.G., Shankar-Sinha, S., Mickiewicz, M., Brinkman, A.S., Valencia, G.A., Sarma, J.V., Younkin, E.M., Standiford, T.J., Zetoune, F.S., and Ward, P.A. (2003). Murine complement interactions with Pseudomonas aeruginosa and their consequences during pneumonia. Am J Respir Cell Mol Biol *29*, 432-438.

Zhang, Z., Jin, L., Champion, G., Seydel, K.B., and Stanley, S.L., Jr. (2001). Shigella infection in a SCID mouse-human intestinal xenograft model: role for neutrophils in containing bacterial dissemination in human intestine. Infect Immun *69*, 3240-3247.

Zheng, L., Baumann, U., and Reymond, J.L. (2004). An efficient one-step site-directed and site-saturation mutagenesis protocol. Nucleic Acids Res *32*, e115.

Zhou, Y., Dong, N., Hu, L., and Shao, F. (2013). The Shigella type three secretion system effector OspG directly and specifically binds to host ubiquitin for activation. PLoS One *8*, e57558.

Zhu, Y., Li, H., Hu, L., Wang, J., Zhou, Y., Pang, Z., Liu, L., and Shao, F. (2008). Structure of a Shigella effector reveals a new class of ubiquitin ligases. Nat Struct Mol Biol *15*, 1302-1308.

Zychlinsky, A., Prevost, M.C., and Sansonetti, P.J. (1992). Shigella flexneri induces apoptosis in infected macrophages. Nature *358*, 167-169.

Appendix: Copyright Permissions

JOHN WILEY AND SONS LICENSE TERMS AND CONDITIONS

Jul 24, 2016

This Agreement between Angela V Daurie ("You") and John Wiley and Sons ("John Wiley and Sons") consists of your license details and the terms and conditions provided by John Wiley and Sons and Copyright Clearance Center.

License Number	3847861454653
License date	Apr 14, 2016
Licensed Content Publisher	John Wiley and Sons
Licensed Content Publication	The EMBO Journal
Licensed Content Title	E2~Ub conjugates regulate the kinase activity of Shigella effector OspG during pathogenesis
Licensed Content Author	Jonathan N Pruneda,F Donelson Smith,Angela Daurie,Danielle L Swaney,Judit Villén,John D Scott,Andrew W Stadnyk,Isolde Le Trong,Ronald E Stenkamp,Rachel E Klevit,John R Rohde,Peter S Brzovic
Licensed Content Date	Jan 20, 2014
Licensed Content Pages	13
Type of Use	Dissertation/Thesis
Requestor type	Author of this Wiley article
Format	Print and electronic
Portion	Figure/table
Number of figures/tables	1
Original Wiley figure/table number(s)	Figure 6
Will you be translating?	No
Title of your thesis / dissertation	Applications and characterization of a streptomycin mouse model for shigellosis
Expected completion date	May 2016
Expected size (number of pages)	110
Requestor Location	Angela V Daurie 5850 collage st Dalhousie university, microbiology and Immunology rm 7G HAlifax, NS B3H4R2 Canada Attn: Angela V Daurie
Publisher Tax ID	EU826007151
Billing Type	Invoice
Billing Address	Angela V Daurie 5850 collage st Dalhousie university, microbiology and Immunology rm 7G